

**INFLUENCE OF POLYMERS ON SUPERSATURATION OF
IBUPROFEN SODIUM *IN VITRO* AND *IN VIVO*:
A MECHANISTIC EVALUATION**

By

JENNA LESCHEK TEREKETSKI

A Dissertation submitted to the
Graduate School-New Brunswick
Rutgers, The State University of New Jersey
in partial fulfillment of the requirements

for the degree of

Doctor of Philosophy

Graduate Program in Pharmaceutical Science

written under the direction of

Professor Bozena Michniak-Kohn, Ph.D.

and approved by

New Brunswick, New Jersey

May 2014

ABSTRACT OF THE DISSERTATION

Influence of Polymers on Supersaturation of Ibuprofen Sodium *In Vitro* and *In Vivo*:

A Mechanistic Evaluation

by JENNA LESCHEK TEREKETSKI

Dissertation Director:
Professor Bozena Michniak-Kohn, Ph.D.

To maximize the pharmacological effect of a pain reliever such as ibuprofen, early onset of action is critical. Unfortunately, the acidic nature of ibuprofen minimizes the amount of drug that can be solubilized in the stomach and would be available for immediate absorption upon entry into the intestine. Although the sodium salt of ibuprofen has high aqueous solubility, rapid conversion from the salt to the poorly soluble free acid phase occurs under gastric conditions. In order to prolong the solubility enhancement initially afforded by the salt, the impact of polymers on ibuprofen supersaturation was evaluated *in vitro* and *in vivo*, with a focus on establishing a mechanistic understanding for how polymers enabled supersaturation.

For this research, dissolution profiles of ibuprofen sodium in the presence of polymers were examined in order to assess degree and duration of supersaturation. In addition, the roles that polymers played in altering drug solubility, pKa, physical form, particle morphology, solution speciation, and media viscosity were probed. Finally *in vivo* studies were conducted in order to understand the influence of supersaturation on pharmacokinetic parameters.

Supersaturation of ibuprofen was effectively prolonged in the presence of a variety of polymers. This was the first example of work that demonstrated prolonged supersaturation when combining a salt form of a drug with a polymeric precipitation inhibitor in the absence of surfactant. Characterization during dissolution demonstrated that mechanism of supersaturation was dependent on specific drug-polymer interactions. *In situ* formation of stabilized amorphous colloids enabled supersaturation in the presence of PVP-VA64. Intermolecular hydrogen bonding was driving supersaturation in the presence of HPMC by inhibiting nucleation and altering crystal growth. Alternatively, increased media viscosity effectively prolonged supersaturation of ibuprofen when combined with MC.

In vitro supersaturation observed with these ibuprofen-polymer formulations translated to an increase in C_{\max} and an earlier T_{\max} for the PVP-VA64, MC, and HPC formulations relative to ibuprofen only controls when administered orally to rats. Based on these observations, combining ibuprofen sodium with polymers is a viable formulation approach to prolong supersaturation in the stomach and enable an optimized pharmacokinetic profile *in vivo* where rapid onset of action is desired.

DEDICATION

I lovingly dedicate this dissertation to my husband, Rob, and our family who have encouraged me throughout this journey.

ACKNOWLEDGEMENTS

The completion of this dissertation would not be possible without the support of numerous people. I would like to thank everyone who has played a part in my graduate school education especially all of the professors in the Department of Pharmaceutics at the Ernest Mario School of Pharmacy, my managers and colleagues at Merck, and all of my family and friends that have supported and encouraged me.

I would like to express my gratitude to my advisor, Dr. Bozena Michniak-Kohn, who has guided me through this endeavor and supported me with continuous encouragement. I would also like to thank Dr. Arash Hatefi, Dr. Dennis Leung, Dr. Sachin Lohani, and Dr. Tamara Minko, members of my dissertation committee, for taking the time out of their schedules to guide me through this process. Your critiques, comments, and guidance have truly been appreciated.

I would also like to thank my DPS and PSCS managers and colleagues at Merck for your continued support throughout this endeavor. The financial support from Greg Szpunar, Mike Kress, Allen Templeton, and Caroline McGregor has enabled me to conduct quality research while still developing professionally at Merck. The scientific guidance and encouragement from my manager, Annette Bak, and my scientific mentors, Sachin Lohani and Dennis Leung, have been tremendously valuable and have enhanced my growth as a scientist.

Most importantly, this dissertation would not have been possible without the patience, encouragement, love, and support of my family and friends. Their confidence in me gave me the strength and resilience to complete this journey. My parents, Joe and

Joan Leschek, have supported me throughout my academic career. I thank you both for your continued love and encouragement. Thank you to my sister, Jessica Capone; my in-laws, Bob and Kathy Terebetski; and the rest of my family who have been a motivating cheering squad throughout my graduate school tenure. Finally, I need to thank my best friend and husband, Rob Terebetski. Rob, your encouragement, patience, and love have been unwavering. Thank you for being my rock throughout this process. I could not have done this without you. Thank you!

TABLE OF CONTENTS

Abstract of the Dissertation	ii
Dedication	iv
Acknowledgements	v
Table of Contents	vii
List of Tables	xv
List of Figures	xxi
Abbreviations	xxiv
Chapter 1. Introduction and Specific Aims	1
1.1. Introduction	1
1.2. Specific Aims	3
Chapter 2. Background and Significance	6
2.1. Oral Drug Delivery Challenges	6
2.2. Approaches to Enhance Dissolution	7
2.3. Fundamentals of Salts During Oral Administration	8
2.4. The Supersaturation Phenomenon	12
2.5. Polymeric Precipitation Inhibitors	14
2.6. Supersaturating Systems <i>In Vivo</i>	17
2.7. Combining Salt Forms of Drugs with Precipitation Inhibitors	17

2.8. References	18
Chapter 3. Influence of Structurally Diverse Polymers on Supersaturation of Ibuprofen Sodium in Aqueous Media	23
3.1. Introduction	23
3.2. Materials and Methods	25
3.2.1. Materials	25
3.2.2. Methods	26
3.2.2.1. pH Solubility Profile of Ibuprofen	26
3.2.2.2. Preparation of Ibuprofen:Polymer Blends	27
3.2.2.3. Characterization of Blends by X-Ray Powder Diffraction (XRPD).....	27
3.2.2.4. <i>In Vitro</i> Dissolution Testing and Equilibrium Solubility Assessment.....	28
3.2.2.5. High Performance Liquid Chromatography (HPLC) Analysis	29
3.2.2.6. XRPD Analysis of Slurries	29
3.2.2.7. Light Microscopy of Precipitate	30
3.2.2.8. Viscosity	30
3.2.2.9. Dynamic Light Scattering (DLS) to Assess Solution Interactions	30
3.3. Results and Discussion.....	31
3.3.1. pH Solubility Profile of Ibuprofen	31
3.3.2. Characterization of Ibuprofen:Polymer Blends by XRPD	34
3.3.3. <i>In Vitro</i> Dissolution Testing	36

3.3.4. Influence of Polymers on Equilibrium Solubility of Ibuprofen	43
3.3.5. Evaluation of Ibuprofen Polymorphism Following Dissolution	47
3.3.6. Microscopy of Precipitate.....	49
3.3.7. Influence of Polymers on Media Viscosity	53
3.3.8. Dynamic Light Scattering of Filtrate to Assess Solution Behavior	54
3.4. Conclusions	60
3.5. References	60
 Chapter 4. Combined Use of Crystalline Sodium Salt and Polymeric Precipitation	
Inhibitors to Improve Pharmacokinetic Profile of Ibuprofen Through	
Supersaturation.....	63
4.1. Introduction	63
4.2. Materials and Methods	65
4.2.1. Materials	65
4.2.2. Methods	66
4.2.2.1. Supersaturation Screening of Ibuprofen in the Presence of Polymers.....	66
4.2.2.2. Two-Stage Dissolution of Drug-Polymer Formulations.....	67
4.2.2.3. High Performance Liquid Chromatography (HPLC) Analysis	68
4.2.2.4. <i>In Vivo</i> Studies	69
4.2.2.5. Plasma Extraction and Chromatographic Analysis.....	69
4.2.2.6. Pharmacokinetic Analysis.....	70

4.3. Results and Discussion.....	71
4.3.1. Supersaturation Screening.....	71
4.3.2. Two-Stage Dissolution.....	78
4.3.3. <i>In Vivo</i> Studies.....	83
4.4. Conclusions.....	90
4.5. References.....	91
 Chapter 5. Combining Ibuprofen Sodium with Cellulosic Polymers: Assessing Impact of Hydrogen Bonding Potential on Degree and Duration of Supersaturation.....	 93
5.1. Introduction.....	93
5.2. Materials and Methods.....	97
5.2.1. Materials.....	97
5.2.2. Methods.....	98
5.2.2.1. <i>In Vitro</i> Supersaturation Testing and Equilibrium Solubility Assessment.....	98
5.2.2.2. High Performance Liquid Chromatography (HPLC) Analysis.....	100
5.2.2.3. Viscosity.....	101
5.2.2.4. Light Microscopy of Precipitate.....	101
5.2.2.5. X-ray Powder Diffraction (XRPD).....	101
5.2.2.6. Fourier Transfer Infrared Spectroscopy (FTIR).....	101

5.3. Results and Discussion.....	102
5.3.1. Supersaturation Profiles of Ibuprofen in the Presence of HPMC.....	102
5.3.2. Phase Characterization of Ibuprofen Following Dissolution	108
5.3.3. Evaluation of Ibuprofen and HPMC by FTIR Spectroscopy	111
5.3.4. Role of Other Cellulosic Polymers on Supersaturation of Ibuprofen.....	114
5.4. Conclusions	119
5.5. References	121
Chapter 6. Probing the Speciation of Ibuprofen in the Presence of Polymers during In Vitro Supersaturation.....	124
6.1. Introduction	124
6.2. Materials and Methods	125
6.2.1. Materials and Sample Preparation.....	125
6.2.2. Methods	126
6.2.2.1. Speciation of Ibuprofen Sodium in Aqueous Media.....	126
6.2.2.2. Dissolution of Drug-Polymer Formulations	127
6.2.2.3. High Performance Liquid Chromatography (HPLC) Analysis	128
6.2.2.4. Dynamic Light Scattering (DLS) Studies	129
6.2.2.5. Optical Microscopy Studies	129
6.2.2.6. X-ray Powder Diffraction (XRPD) Analysis	130
6.2.2.7. pKa Determination.....	130

6.3. Results and Discussion.....	131
6.3.1. Evaluating Speciation of Ibuprofen Sodium in Aqueous Media.....	131
6.3.2. Characterization of Drug-Polymer Formulations during Dissolution.....	134
6.3.3. pKa Determination	151
6.4. Conclusions	151
6.5. References	152

Appendix A. Physical Characterization of Ibuprofen Free Acid and Sodium

Salt.....	154
A.1. Physical Characterization of Ibuprofen.....	154
A.1.1. Materials	154
A.1.2. Methods	155
A.1.2.1. X-ray Powder Diffraction (XRPD).....	155
A.1.2.2. Light Microscopy	155
A.1.2.3. Differential Scanning Calorimetry (DSC)	155
A.1.2.4. Thermal Gravimetric Analysis (TGA).....	155
A.1.2.5. Microtrac Assessment of Particle Size.....	155
A.1.3. Results of Ibuprofen Free Acid Characterization	156
A.1.4. Results of Ibuprofen Sodium Characterization	157
A.2. pKa Titration for Ibuprofen Sodium	160
A.2.1. Methods	160

A.2.1.1. pKa Determination.....	160
A.2.2. Results of pKa Determination of Ibuprofen Sodium.....	161
A.3. pH-Dependent Solubility Profile of Ibuprofen Sodium	161
A.3.1. Methods	161
A.3.1.1. Equilibrium Solubility as a Function of pH.....	161
A.3.1.2. High Performance Liquid Chromatography (HPLC) Analysis.....	162
A.3.2. Results of pH-Dependent Solubility Assessment.....	162
A.4. References	163
Appendix B. HPLC Method Validation of Ibuprofen	164
B.1. HPLC Method Validation.....	164
B.1.1. Materials	164
B.1.2. Methods	164
B.1.3. Standard Preparation.....	164
B.1.4. Method Validation	165
B.1.5. Specificity	167
B.1.5.1. Filter Validation	167
B.1.5.2. Solution Stability.....	168
Appendix C. Polymer Summary.....	170
C.1. Description of Polymers Evaluated	170
C.2. Particle Size Distribution of Polymers Evaluated	173

C.2.1. Methods	173
C.2.1.1. Microtrac Assessment of Particle Size.....	173
C.2.2. Results of Polymer Particle Size Assessment.....	173
C.3. Viscosity Assessment of Polymers in Dissolution Media	174
C.3.1. Methods	174
C.3.1.1. Media Preparation	174
C.3.1.2. Viscosity Measurements	175
C.3.2. Results of Viscosity Measurements for Pre-Dissolved Polymer in Dissolution Media.....	175
C.4. Solubility of Evaluated Polymers in Dissolution Media	177
C.4.1. Methods	177
C.4.1.1. Visual Assessment of Polymer Solubility.....	177
C.4.2. Results of Polymer Threshold Solubility Assessment in Dissolution Media.....	178
C.5. References	179
Appendix D. Influence of Polymers on pKa of Ibuprofen	180
D.1. Influence of Polymers on pKa of Ibuprofen.....	180
D.1.1. Methods for pKa Determination.....	180
D.1.2. Results for Ibuprofen pKa Determination in Presence of Polymers	181

LIST OF FIGURES

Figure 2.1. The pH dependence of the gastrointestinal tract	9
Figure 2.2. Schematic representation of pH-solubility profiles for (a) basic and (b) acidic drugs.....	9-10
Figure 2.3. Schematic representation of the Gibbs free energy of molecules present in a supersaturation solution.	13
Figure 3.1. pH solubility profile of ibuprofen following 24 hours of shaking at 37°C. ...	31
Figure 3.2. XRPD traces of ibuprofen isolated following 24 hours of shaking across the biorelevant pH range at 37°C, with representative patterns color codes for (A) questionable traces in grey, (B) amorphous material in light green, (C) ibuprofen free acid in orange, and (D) ibuprofen sodium in dark green.	32
Figure 3.3. XRPD traces of 1:1 ibuprofen (sodium salt or free acid):polymer following blending. XRPD patterns matching ibuprofen sodium are highlighted in green and ibuprofen free acid are highlighted in orange while blends with only amorphous halos are purple.	36
Figure 3.4. XRPD overlays of 1:1 blends of ibuprofen sodium with PAA, Carbopol 974, and Carbopol 934 compared to control samples of ibuprofen sodium and ibuprofen free acid.....	36
Figure 3.5. Dissolution profiles of 1:1 ibuprofen sodium:polymer in SGF at 37 °C.....	37
Figure 3.6. Dissolution profiles of 1:1 ibuprofen sodium:polymer in pH 5 buffer at 37 °C.	38

Figure 3.7. Dissolution profiles of 1:1 ibuprofen sodium:pre-dissolved polymer in SGF at 37 °C.	40
Figure 3.8. Dissolution profiles of 1:1 ibuprofen sodium:pre-dissolved polymer in pH 5 buffer at 37 °C.....	41
Figure 3.9. XRPD patterns comparing solid isolated from slurry of ibuprofen sodium in pH 5 buffer to control spectra of racemic ibuprofen free acid and ibuprofen sodium dihydrate..	47
Figure 3.10. XRPD overlays comparing solid isolated from slurries of ibuprofen sodium in pH 5 buffer without any polymer (light green) or with HPMC (pink), PVP-VA64 (brown), HPMCAS-HF (navy), Soluplus (dark green), or HPC (orange) to control spectra of racemic ibuprofen free acid (red) and ibuprofen sodium dihydrate (blue).....	48-49
Figure 3.11. Microscopy following dissolution of (a) ibuprofen sodium alone or with (b) HPMC, (c) PVP-VA64, (d) PAA, (e) Carbopol 974P, (f) Plasdane K12, (g) HPMCAS-HF, (h) CMC Na, (i) HPC-SL, (j) MC, (k) Kollidon 25, (l) Carbopol 934P, (m) Soluplus, (n) HPMCP, and (o) HPC in pH 5.0 buffer at 100x magnification..	50
Figure 3.12. Microscopy following dissolution of ibuprofen sodium with HPMCAS-HF at 100x magnification..	52
Figure 3.13. DLS plots of ibuprofen sodium slurried in (a) SGF or (b) pH 5 buffer for 20 minutes.....	55
Figure 3.14. DLS of ibuprofen with polymers in pH 5 buffer at 20 minutes (pink), 40 minutes (blue), 60 minutes (green), 120 minutes (yellow), and with polymer only (grey).....	56

Figure 3.15. DLS overlays comparing ibuprofen sodium with (a) PVP-VA64 and (b) HPC in combination and against control samples of ibuprofen sodium and polymer alone.....	58-59
Figure 4.1. Dissolution profiles of 1:1 ibuprofen sodium: pre-dissolved polymer in SGF at 37 °C during supersaturation screen.	72
Figure 4.2. Microscopy following dissolution of ibuprofen sodium in SGF (a) without polymer or (b) with HPMCAS-HF at 100x magnification.	76
Figure 4.3. Dissolution of ibuprofen free acid and ibuprofen sodium salt with the presence or absence of polymer in SGF at 37 °C.	80
Figure 4.4. Two-stage dissolution profile of ibuprofen with the presence or absence of polymer in SGF for 60 minutes followed by pH adjustment to pH 6.8 at 37 °C.	82
Figure 4.5. Mean plasma concentration of ibuprofen following oral administration in Wistar Han rats (n=6) under fasted conditions at a dose of 25 mpk. Ibuprofen free acid (◆), ibuprofen sodium salt (■), 1:1 ibuprofen sodium:HPMC (▲), 1:1 ibuprofen sodium:PVP-VA64 (□), 1:1 ibuprofen sodium:MC (△), 1:1 ibuprofen sodium:HPC (●), and 1:1 ibuprofen sodium:Soluplus (○).....	84
Figure 4.6. Mean (± SD) plasma concentration of ibuprofen following oral administration in Wistar Han rats (n=6) under fasted conditions at a dose of 25 mpk. Figures compare the ibuprofen sodium salt (■) profile to (a) ibuprofen free acid (◆), (b) 1:1 ibuprofen sodium:PVP-VA64 (□), (c) 1:1 ibuprofen sodium:MC (△), (d) 1:1 ibuprofen sodium:HPC (●), and (e) 1:1 ibuprofen sodium:Soluplus (○)..	86-87
Figure 5.1. Dissolution profile of ibuprofen sodium in SGF at 37 °C without polymer (●) and with pre-dissolved HPMC (▲). Error bars represent the standard deviation	103

Figure 5.2. Dissolution profile of ibuprofen sodium in pH 5.0 buffer at 37 °C without HPMC (●), with solid HPMC (△), and with pre-dissolved HPMC (▲). Error bars represent the standard deviation, n = 3.	104
Figure 5.3. Dissolution profile of ibuprofen sodium in pH 5.0 buffer at 25 °C without HPMC (●), with pre-dissolved HPMC void of seed (△), and with pre-dissolved HPMC with seed added (▲). Error bars represent the standard deviation, n = 3.	107
Figure 5.4. Microscopic images at 200x magnification of precipitate following dissolution of ibuprofen sodium in pH 5 buffer for (A) Type A, (B) Type B, and (C) Type C.	109
Figure 5.5. XRPD patterns comparing (a) ibuprofen free acid as received to (b) Type A and (c) Type B isolated following dissolution in pH 5 buffer	110
Figure 5.6. XRPD trace of Type C.....	111
Figure 5.7. FTIR spectra comparing (A) ibuprofen free acid, (B) Type B, (C) Type C, and (D) HPMC.....	112
Figure 5.8. FTIR spectra comparing (A) Type C, (B) ibuprofen free acid, and (c) HPMC in the carbonyl region.	113
Figure 5.9. Kinetic solubility of ibuprofen sodium in pH 5 buffer at 25 °C with pre-dissolved polymer in the absence of seed. Error bars represent the standard deviation, n = 3.....	116
Figure 5.10. Dissolution profile of ibuprofen sodium in pH 5.0 buffer at 25 °C without polymer (●) and with pre-dissolved HPMC (■), HPC (◆), and MC (▲) with seed added. Error bars represent the standard deviation, n = 3.	117

Figure 5.11. Microscopic images at 200x magnification following loss of supersaturation of ibuprofen sodium in pH 5 buffer (A) with pre-dissolved MC and (B) with pre-dissolved HPC in systems void of seed.	118
Figure 6.1. Normalized intensity (◆) or hydrodynamic radius (■) as a function of ibuprofen sodium concentration in water at 25 °C.	132
Figure 6.2. Supersaturation profiles of ibuprofen following addition of ibuprofen sodium formulations to SGF. Ibuprofen concentration was determination by (a) filtration or (b) ultracentrifugation.	135-136
Figure 6.3. Ibuprofen solubility profiles in SGF at 37 °C for (a) ibuprofen sodium alone or ibuprofen sodium with (b) MC, (c) PVP-VA64, or (d) HPMC. Ibuprofen concentrations were determined following filtration (open symbols) and ultracentrifugation (closed symbols). The <i>dashed line</i> represents the 24 hour solubility of ibuprofen with polymer in SGF.	137-139
Figure 6.4. Particle size distribution by dynamic light scattering of ibuprofen with (a) MC, (b) PVP-VA64, and (c) HPMC in SGF at 10 minutes following filtration.	141-142
Figure 6.5. Comparison of ibuprofen supersaturation to particle size of filtrate as a function of time during dissolution in SGF of ibuprofen sodium with (a) MC, (b) PVP-VA64, or (c) HPMC. The bars represent the supersaturation of ibuprofen determined in triplicate and the error bars indicate standard deviation. The solid line represents average particle size data determined by DLS. The dashed line represents the particle size of polymer alone in SGF determined by DLS.	143-144

Figure 6.6. Polarized optical microscopy of pellets isolated via ultracentrifugation of filtrate following 10 minutes of ibuprofen sodium dissolution with (a) MC, (b) PVP-VA64, or (c) HPMC, at 100x magnification.....	147
Figure 6.7. Optical microscopy following isolation of slurries from dissolution baths at 100x magnification.	149
Figure 6.8. XRPD patterns comparing (a) ibuprofen free acid as a reference to ibuprofen sodium slurried in SGF at 37°C for 2 hours (b) alone, or with (c) PVP-VA64, (d) HPMC, or (e) MC.....	150
Figure A.1. Structure of ibuprofen free acid.....	154
Figure A.2. Structure of ibuprofen sodium.....	154
Figure A.3. XRPD of ibuprofen free acid.....	156
Figure A.4. Microscopy of ibuprofen free acid at 200x magnification.	157
Figure A.5. DSC trace of ibuprofen free acid.....	157
Figure A.6. XRPD of ibuprofen sodium dihydrate.....	158
Figure A.7. Microscopy of ibuprofen sodium dihydrate at 200x magnification.	158
Figure A.8. Overlay of DSC and TGA of ibuprofen sodium dihydrate.....	159
Figure A.9. Summary of particle size data for ibuprofen sodium dihydrate.	160
Figure A.10. pKa determination of ibuprofen sodium in ISA water (unionized species in blue and ionized species in red)	161
Figure A.11. pH solubility profile of ibuprofen sodium dihydrate at 37 °C.....	163
Figure B.1. Average ibuprofen standard curve, with standard concentrations ranging from 1.0 – 178.5 µg/mL.....	166

LIST OF TABLES

Table 3.1. Influence of various polymers on maximum degree of supersaturation of ibuprofen following dissolution of ibuprofen sodium in the presence of solid or pre-dissolved polymer at 37 °C.....	43
Table 3.2. Influence of various polymers on solubility of ibuprofen following dissolution of 1:1 ibuprofen:polymer in SGF at 37 °C.	45
Table 3.3. Influence of various polymers on solubility of ibuprofen following dissolution of 1:1 ibuprofen:polymer in pH 5 buffer at 37 °C.	46
Table 3.4. Summary of viscosity data in SGF and pH 5 buffer at 37 °C, n=3.....	54
Table 4.1. Influence of various polymers on maximum degree of supersaturation of ibuprofen following dissolution of ibuprofen sodium in the presence of pre-dissolved polymer in SGF at 37° C.	73
Table 4.2. Influence of various polymers on solubility of ibuprofen following equilibration in SGF containing 1 mg/mL polymer at 37 °C.	77
Table 4.3. Ibuprofen pharmacokinetic parameters following oral administration to Wistar Han rats at a dose of 25 mpk.....	88
Table 4.4. Comparison of degree of ibuprofen supersaturation achieved during SGF dissolution of solid drug-polymer blends to pharmacokinetic parameters following oral administration to Wistar Han rats at a dose of 25 mpk.....	89
Table 5.1. Summary of polymer structure and substitution based on manufacturer information.....	98
Table 5.2. Impact of HPMC on solubility of ibuprofen in SGF and pH 5 buffer at	

37 °C.	106
Table 5.3. Precipitate classification for solids isolated following dissolution of ibuprofen sodium in pH 5.0 buffer.	107
Table 6.1. Solubility of ibuprofen sodium following 24 hours in SGF with and without 1 mg/mL polymer at 37 °C.	129
Table 6.2. Measured drug concentration and DLS evaluation of ibuprofen sodium in water at 25 °C following 0.45 µm filtration or ultracentrifugation.....	134
Table 6.3. Particle size data during dissolution of ibuprofen sodium in SGF in the presence and absence of polymer following filtration.	140
Table 6.4. DLS data during dissolution of ibuprofen sodium in SGF in the presence and absence of polymer following ultracentrifugation.	145
Table 6.5. pKa values for ibuprofen in ISA water obtained by spectrophotometric titration in the absence and presence of polymer.	151
Table A.1. Particle size distribution data for ibuprofen sodium dihydrate.	160
Table B.1. Ibuprofen standard concentrations with average chromatogram peak area, standard deviation, and relative standard deviation of three separate runs.....	165
Table B.2. Filter validation set for centrifuge filtration.	168
Table B.3. Filter validation set for syringe filtration.....	168
Table B.4. Filter validation set for syringe filtration (with 2 mL discarded prior to analysis)	168
Table B.5. Solution stability of 50.0 µg/mL standard following 22 hours of storage at ambient conditions.	169
Table C.1. Summary of polymer structure and property information.	170-173

Table C.2. Average particle size of each polymer evaluated.....	174
Table C.3. Influence of polymer on media viscosity at 1 mg/mL in SGF at 37 °C.....	176
Table C.4. Influence of polymer on media viscosity at 1 mg/mL in pH 5 buffer at 37 °C.	177
Table C.5. Threshold solubility of polymers in SGF following 2 hours of equilibration at 37 °C.	179
Table D.1. pKa of ibuprofen in the presence of polymers using spectrophotometric titration (n=3)	181

ABBREVIATIONS

API: Active Pharmaceutical Ingredient

AUC: Area Under the Curve

BCS: Biopharmaceutical Classification System

CAC: Critical Aggregate Concentration

CMC: Critical Micelle Concentration

DLS: Dynamic Light Scattering

DSC: Differential Scanning Calorimetry

FA: Free Acid

FTIR: Fourier-Transfer Infrared Spectroscopy

GI: Gastrointestinal

HPC: Hydroxypropyl Cellulose

HPLC: High Performance Liquid Chromatography

HPMC: Hydroxypropyl Methylcellulose; Pharmacout 603

ISA: Ionic Strength Adjusted

IVIVC: *In Vitro-In Vivo* Correlation

LOD: Limit of Detection

LOQ: Limit of Quantitation

MC: Methylcellulose

Na: Sodium

NSAID: Non-Steroidal Anti-Inflammatory Drug

PD: Pharmacodynamics

PK: Pharmacokinetics

PSD: Particle Size Distribution

PVP: Polyvinyl Pyrrolidone

PVP-VA64: Polyvinyl Pyrrolidone-Vinyl Acetate Copolymer

QC: Quality Control

RT: Room Temperature

SGF: Simulated Gastric Fluid

TGA: Thermal Gravimetric Analysis

XRPD: X-Ray Powder Diffraction

CHAPTER 1

Introduction and Specific Aims

1.1. Introduction

The most convenient way to deliver pharmaceutical agents to patients is via the oral route (tablets, capsules, etc.). However, if the compound has poor solubility, insufficient absorption across the gastrointestinal membrane could limit the systemic exposure required to induce a pharmacologic effect. Although chemical modification of the API may circumvent these issues, formulation optimization is the preferred strategy to mitigate dissolution-limited absorption associated with poorly soluble compounds that have already progressed into the drug development stage. Supersaturation in the gastrointestinal tract was the focused formulation strategy to enhance the intestinal absorption of the poorly water-soluble model drug. The salt form of the drug was used to generate supersaturation relative to the poorly soluble neutral phase and polymers were added to the system in order to maintain the compound in the supersaturated state.

The objective of this work was to establish a mechanistic understanding for how polymers can influence the supersaturation of a pharmaceutical salt of the active compound during the *in vitro* dissolution process. In addition, it was investigated whether specific mechanisms of supersaturation correlated with enhanced exposure when the dosage form was administered orally *in vivo*. In oral drug delivery, pharmaceutical salts are commonly used to increase the exposure of poorly soluble compounds. However, salts of acidic drugs undergo disproportionation to neutral species during dissolution in the stomach due to the low pH. This phase conversion from a salt to the thermodynamically stable neutral phase generally corresponds to a reduction in drug

solubility which in turn limits the amount of drug in solution that is available for absorption. In the case of a non-steroidal anti-inflammatory drug (NSAID), the low solubility of the neutral phase can be a challenge since rapid absorption of the drug is critical for immediate pain relief. It was hypothesized that the addition of polymeric precipitation inhibitors would prolong the solubility enhancement afforded by the salt form of the drug via various mechanisms of supersaturation. Therefore, the goal of the present research was to perform a comparative evaluation of drug: polymer combinations in order to understand how mechanisms of supersaturation could prolong *in vitro* dissolution and enhance *in vivo* exposure more effectively than standard oral dosage formulations thereby reducing the required dose and optimizing the pharmacokinetic (PK) profile for enhanced pharmacodynamic (PD) effect.

Ibuprofen was used as the model NSAID for this work since the well-characterized sodium salt has much higher solubility than the unionized free acid phase. The sodium salt of ibuprofen, which undergoes disproportionation to the poorly soluble neutral phase during dissolution in biorelevant gastric media, was used as the supersaturating system while an assortment of structurally diverse polymers were evaluated based on their potential to prolong supersaturation via various mechanisms in order to probe degree and duration of supersaturation. A deep dive into the mechanisms of supersaturation was conducted in order to understand how specific polymers interact with ibuprofen when in the supersaturated state and whether specific physicochemical properties of polymers could be used to empirically predict degree and duration of supersaturation. Animal studies were also run as a means to probe whether specific mechanisms of supersaturation were linked to enhanced *in vivo* exposure.

1.2. Specific Aims

The primary objective of this research was to inform on the design of solid dosage formulations of pharmaceutical salts that risk disproportionation during oral administration as a means to optimize exposure without relying on enabled formulation development, such as amorphous solid dispersions. Towards this goal, the research was divided into five aims.

Specific Aim 1: To identify polymers which prolong the supersaturation of ibuprofen during *in vitro* dissolution.

Small-scale dissolution of ibuprofen sodium in the presence of structurally diverse polymers was conducted in biorelevant media in order to identify polymers that were most effective in prolonging degree and duration of supersaturation. Cellulosic, vinyl-based, and acrylate-based polymers with varying functionality were included in the preliminary screen. The impact of polymers on viscosity, pH, equilibrium solubility of ibuprofen, polymorphism of final form and crystal morphology following loss of supersaturation was evaluated as a means to initially probe mechanisms of supersaturation.

Specific Aim 2: To investigate the hydrogen bonding potential of cellulosic polymers on degree and duration of ibuprofen supersaturation.

Dissolution of ibuprofen sodium with various cellulosic polymers, including HPMC, MC and HPC, was conducted in the presence and absence of ibuprofen free acid seed in order to evaluate the role that these polymers played in nucleation inhibition and crystal growth modulation of ibuprofen during supersaturation. Detailed characterization,

including microscopy and FTIR spectroscopy, of isolated solids was also conducted in order to probe hydrogen bonding potential. The impact of these polymers on degree and duration of supersaturation as well as effect on crystal growth was monitored as a means to assess whether the varying degree of polymer hydrophobicity played a role in the mechanism of supersaturation of ibuprofen.

Specific Aim 3: To assess the role of solution-mediated interactions between ibuprofen and polymers on salt disproportionation and supersaturation.

In order to probe the potential for solution-mediated interactions between ibuprofen and various polymers, dynamic light scattering was conducted on ibuprofen with and without polymers. The presence of aggregate or micelle formation was monitored in parallel to dissolution experiments as a means to correlate solution speciation to supersaturation. In addition, the influence of polymers on ibuprofen pKa was evaluated.

Specific Aim 4: To assess whether specific physicochemical properties of polymers can be used to predict degree and duration of supersaturation.

Polymer properties were compared to experimental dissolution data in order to assess feasibility of empirically predicting degree and duration of supersaturation. The properties of polymers that were considered include functionality, ionization state in biorelevant media, potential for charge interactions, molecular weight, degree of water solubility, and viscosity in biorelevant media.

Specific Aim 5: To explore the impact of mechanism of supersaturation on *in vivo* exposure in preclinical pharmacokinetic studies.

Combinations of drugs with polymers that prolong supersaturation via different mechanisms, including viscosity enhancement, hydrogen bonding and solution-mediated interactions, were explored in greater detail. Two-stage dissolution was conducted with the formulations of interest. This was followed by *in vivo* rat PK studies in order to determine whether an *in vitro* – *in vivo* correlation could be drawn among these supersaturating systems.

CHAPTER 2

Background and Significance

2.1. Oral Drug Delivery Challenges

An increase in the number of Class II and IV compounds in the drug development pipeline is trending with more design challenges for oral drug delivery formulations. Based on the Biopharmaceutical Classification System (BCS), Class II and IV compounds are categorized as such based on poor solubility and high or low permeability, respectively (1). A recent compilation of solubility and permeability data comparing marketed drugs to compounds in the development pipeline illustrates this shift toward decreased solubility and increased permeability (2, 3). This trend in physicochemical properties can largely be attributed to an industry-wide shift from manual to high-throughput *in vitro* potency assays utilized to prioritize molecules in the discovery space. Under this paradigm, compounds are solubilized in DMSO stock solutions, and this has resulted in a de-emphasis of sufficient aqueous solubility to probe efficacy at the receptor. The general practice of progressing compounds based on potency alone has therefore resulted in satisfactory physicochemical properties being overlooked (4, 5).

The challenge that this presents from a drug delivery perspective is that physical properties of the drug substance play a significant role in the absorption of the drug during oral administration. This is clearly depicted in Fick's First law:

$$J = PC$$

where flux (J) of a drug through the gastrointestinal membrane is dependent on the permeability coefficient (P) and the drug concentration (C) in the gastrointestinal lumen when sink conditions are assumed. Therefore, in the case of poorly soluble compounds, absorption can be limited by the maximum amount of drug that can dissolve (1).

2.2. Approaches to Enhance Dissolution

In order to overcome dissolution-limited absorption, a number of approaches to enhance drug dissolution have been successfully applied to the delivery of poorly water soluble compounds. The Noyes-Whitney equation describes the factors that contribute the rate of drug dissolution (dC/dt):

$$dC / dt = [AD(C_s - C)] / h$$

Based on the above equation, dissolution is impacted by the surface area (A) of the compound that is available for dissolution, the diffusion coefficient (D) of the compound, the solubility (C_s) of the compound in media, the total concentration (C) of the drug in the dosage form, and the thickness (h) of the diffusion boundary layer. In order to enhance dissolution, compound physicochemical properties including solubility and surface area can be modified (6). In order to circumvent dissolution-limited absorption issues, both physical and chemical modification can be made to the drug substance and drug product. Examples of physical modifications include particle size reduction through micronization or nano-milling (7, 8), modification of crystal habit (9), polymorph or amorphous phase selection for a higher energy form (10, 11), complexation or solubilization through the use of surfactants or cyclodextrins (12, 13), or drug dispersions in stabilizing carriers (14). Alternatively, chemical modification of the compound can

include the introduction of a soluble prodrug moiety (15) or compound ionization through salt formation (16).

The challenge with prioritizing a dissolution-enhancing approach is that most modifications to the API or formulation carry added risk. For example, selection of a metastable polymorph may result in phase conversion upon storage (10, 17) while development of a prodrug presents additional regulatory challenges (18). Alternatively, controlled processing conditions and the need for added stabilizers increases the complexity of preparing nanoparticles (7). Stabilized amorphous dispersions provide an additional case study for formulation limitations, including increased risk of chemical and physical instability during storage as well as large-scale manufacturing challenges (19-21). Therefore it is desirable to focus on compound ionization as a mechanism to overcome dissolution-limited absorption since salts are stable solid phases that can be included in preclinical and clinical formulations for drug candidates with poor solubility (16, 22).

2.3. Fundamentals of Salts During Oral Administration

Salt forms of drugs are often utilized in development because of stable physical properties, purity upgrades, and enhanced solubility over the neutral form (16, 22). However, the challenges with salts are that they often exhibit pH-dependent solubility (23, 24) that impacts the concentration in solution at a given region in the gastrointestinal (GI) tract (Figure 2.1).

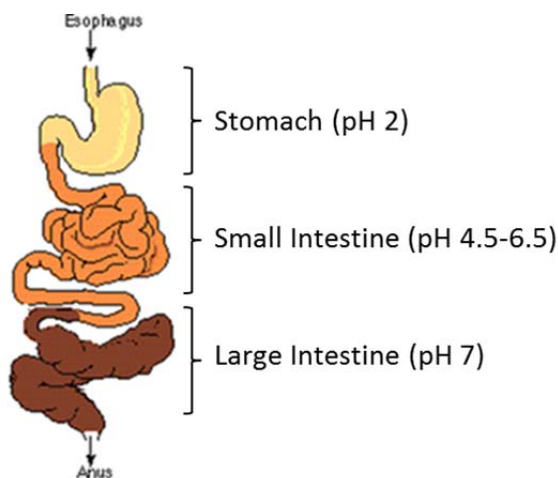
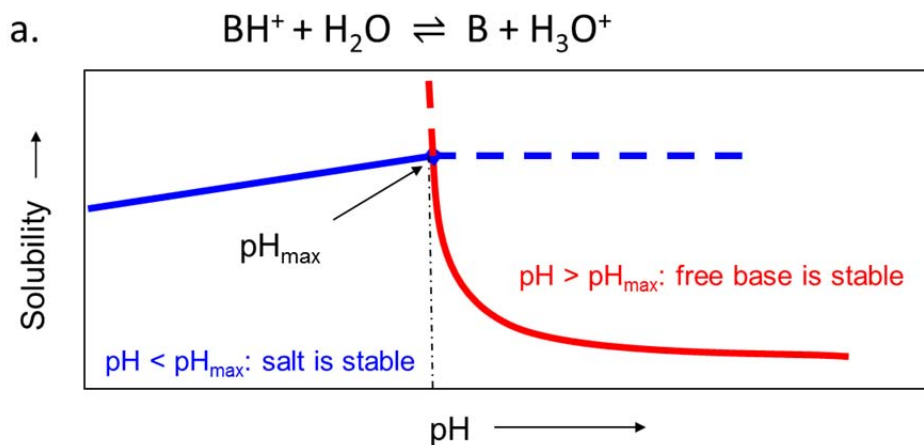


Figure 2.1. The pH dependence of the gastrointestinal tract.

Since compound ionization is driven by pH, disproportionation of salts can occur at varying regions of the GI tract (23). Basic, ionized species will maintain solubility enhancement in the stomach, but may disproportionate as the pH increases above the pH_{max} and the compound converts to the free base form as illustrated in Figure 2.2a.

Alternatively, acidic compounds will become protonated immediately after entering the stomach due to the acidic pH, resulting in disproportionation of the starting salt form followed by ionization as the acid transits through the intestine and the pH shifts above the pH_{max} (Figure 2.2b).



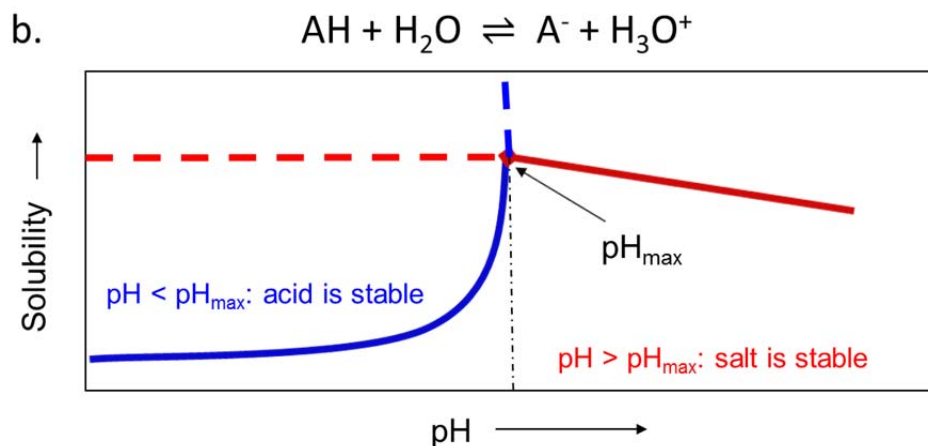


Figure 2.2. Schematic representation of pH-solubility profiles for (a) basic and (b) acidic drugs.

The disproportionation phenomenon can have complicating effects on drug exposure due to uncontrolled precipitation of the lower solubility free form or variable disproportionation depending on localized pH of the GI from patient to patient which would result in decreased or highly variable PK. Therefore, it is desirable to maintain the solubility enhancement that is afforded by the salt or at least control the loss in solubility that occurs following disproportionation in order to limit absorption issues. Two possible approaches to maintain this solubility enhancement include (1) delaying disproportionation and (2) artificially maintaining supersaturation even after change in ionization state has occurred.

Since disproportionation is driven by the pH_{max} of the compound, it is important to know what pH_{max} is in order to identify approaches that can be taken to avoid or delay this behavior. The pH_{max} for a given compound is the critical point at which the solution is saturated with respect to the free form and the salt (23). In the case of a base, the salt will convert to the free base at all pH values above the pH_{max} (Figure 2.2a). This value will be different for each phase of a given compound, as shown in the equation:

$$\text{pH}_{\text{max}} = \text{pK}_a + \log [\text{B}] / \sqrt{\text{K}_{\text{sp}}}$$

Based on this equation, the pH_{max} is dependent on the pK_a of the compound, the intrinsic solubility of the free base ($[\text{B}]$), and the solubility of the salt ($\sqrt{\text{K}_{\text{sp}}}$). Therefore, there may be opportunities to alter any of these parameters in order to shift the pH_{max} to a range that delays or prevents disproportionation of a desirable salt. For example, an order of magnitude decrease in the solubility of the selected salt would shift the pH_{max} by one unit, meaning that a more stable and less soluble polymorph of a salt would be less likely to convert to the free acid (25). This was demonstrated with prolonged supersaturation and delayed conversion of the less soluble siramesine-HCl monohydrate when compared to the more soluble anhydrous HCl salt which precipitated as the free acid due to its low pH_{max} (26).

Alternatively, excipients can be used to delay the disproportionation of salts by serving as pH modifiers during dissolution. In this role, formulation components possessing either acidic or basic functionality can impact the boundary diffusion layer of the solid dosage formulation by modifying the microenvironmental pH (27, 28). Depending on the properties of the drug substance and selected excipients, the kinetics of disproportionation can be delayed in both the solid-state and during dissolution (29, 30). While there has been a historic focus on delaying salt disproportionation through phase selection of the most stable salt form and altering the microenvironmental pH with the use of excipients, minimal work has been conducted to date to explore the viability of combining salts with polymeric precipitation inhibitors to prolong supersaturation even after disproportionation.

2.4. The Supersaturation Phenomenon

Supersaturation occurs when the concentration of drug in solution is above the equilibrium solubility of the thermodynamically stable crystal phase. This is the scenario that occurs when a soluble salt of an acidic compound first encounters a region in the GI that is below its pH_{max} (Figure 2.2b). The dissolution of the salt will exceed the solubility limit of the thermodynamically stable free acid initially and may promote increased absorption (11, 16). Unfortunately, thermodynamics will drive the compound to the most stable and often least soluble form. Therefore, the extent of supersaturation may be insufficient to substantially enhance oral exposure unless formulation optimization is conducted to stabilize the supersaturated phase. The same behavior holds true for basic compounds that are solubilized in the stomach due to ionization in the acidic media, but convert to the less soluble free base form following transition into the intestine when the local pH is above their pH_{max} (Figure 2.2a). For example, incomplete absorption of the basic compound L-735,524 occurred when administered as a sulfate salt solution due to the impact of intestinal pH on compound solubilization. Alternatively, if the animals were pre-treated with citric acid in order to acidify the gastrointestinal environment, then significant enhancement in exposure was observed (31).

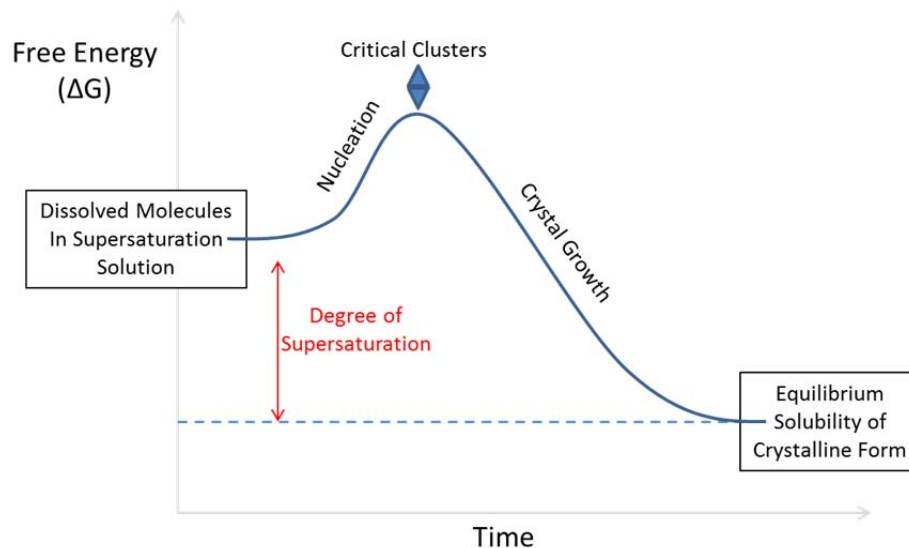


Figure 2.3. Schematic representation of the Gibbs free energy of molecules present in a supersaturation solution; modified from (32)

The mechanisms that factor into loss of supersaturation are illustrated in Figure 2.3, with nucleation and crystal growth being the two essential processes for drug precipitation. In general, the driving force for nucleation is dependent on the maximum feasible degree of supersaturation that could be achieved in the system. In other words, the difference in chemical potential ($\Delta\mu$) of a supersaturated solution (μ_1) versus a saturated solution (μ_{eq}) is the driver for crystallization of the thermodynamically stable crystalline phase. The definition of chemical potential is:

$$\Delta\mu = \mu_1 - \mu_{eq} = RT \ln(a_1 / a_{eq})$$

where R is the gas constant, T is the temperature and a_1 and a_{eq} are the activity of the solute in a supersaturated and saturated state, respectively. If no difference in the activity coefficients are assumed, then:

$$\Delta\mu = RT \ln(C_1 / C_{eq}) = RT \ln(S)$$

where C_1 and C_{eq} are the drug concentration during supersaturation and equilibrium, respectively, and S is the supersaturation ratio. This equation therefore correlates a

reduction in chemical potential with a reduction in supersaturation. In order to correlate supersaturation ratio to nucleation, the nucleation rate equation can be modified assuming homogeneous nucleation as follows:

$$J_n = N_0 v \exp (-\Delta G^* / k_b T) = N_0 v \exp (-16\pi v^2 \gamma_{ns}^3 / 3(k_b T)^3 (\ln (S))^2)$$

where the nucleation rate is J_n , N_0 is the number of molecules in a unit volume, v is the frequency of molecular transport at the nucleus-liquid interface, k_b is the Boltzmann's constant, ΔG^* is the Gibbs free energy change for the formation of critical clusters, v is the molecular volume of the crystallizing solute and γ_{ns} is the interfacial energy per unit area between the cluster and the surrounding solvent. This equation therefore illustrates that nucleation is inversely proportional to supersaturation (32-34). In other words, systems with higher levels of supersaturation will have faster nucleation rates.

Once the energy barrier for nucleation is overcome and sufficient pre-crystalline nuclei are present, the crystal growth process will initiate. This two-step process requires diffusion of the molecules in solution to the crystal interface followed by integration into the crystal lattice. The crystal growth rate (dr/dt) states that:

$$dr/dt = [DvN_A / (r + D/k_+)] * (C - C_{eq})$$

where D is the diffusion coefficient, k_+ is the surface integration factor, N_A is the Avogadro constant, and $(C - C_{eq})$ is the difference between the bulk concentration and the concentration in solution at the surface of the nuclei (32, 34). Based on this equation, crystal growth is influenced by both internal and external factors.

2.5. Polymeric Precipitation Inhibitors

Since supersaturating systems typically provide only transient increases in solubility, the addition of precipitation inhibitors can be used to prolong supersaturation by interfering in nucleation and/or crystal growth stages. Polymeric precipitation inhibitors can alter the bulk solution properties of the drug. For example, increasing surface tension can decelerate surface nucleation or increasing solubility relative at constant supersaturation can decrease the likelihood of nucleation (35). A change in the adsorption layer at the crystal-solution interface can potentially decrease the rate of diffusion of drug molecules to the crystal nuclei (36, 37) while polymer adsorbs to the crystal surface interface, growth terraces, and/or surface imperfections to block or disrupt crystal growth (36, 38). Alternatively, changes in the surface energy of the crystal face can potentially impact the level of solvation (20, 39).

Although mechanisms of prolonged supersaturation are not fully understood, the general thought is that precipitation inhibition occurs as a result of either chemical or physical interactions between the drug and polymer. And the factors that influence drug-polymer interactions (39) include:

- Temperature: binding will decrease between drug and polymer with increased temperature (40);
- Molecular weight: higher molecular weight polymers interact more strongly with drug molecules due to increased viscosity or availability of more functional groups (41-43);
- Viscosity: increased viscosity decreases the rate of drug diffusion from bulk solution, resulting in crystallization inhibition (36, 38, 44);

- Dielectric constant: decreased dielectric constant can increase drug solubility, resulting in decreased degree of interaction between the drug and polymer (41);
- Hydrogen bonding: increasing the number of hydrogen bonding sites may increase drug-polymer interactions. This could lead to delayed nucleation (37, 42) or crystal growth inhibition (45, 46).

Mechanisms of supersaturation are case specific, with the individual compound and excipient playing unique roles in prospective interactions. In one example, Raghavan *et al.* evaluated the morphology of hydrocortisone acetate following precipitation from supersaturated solutions in the presence of various polymers. Based on microscopy, the crystalline habit was modified when HPMC was present, but not when PVP or PEG400 was used. This suggested that HPMC contributed to growth inhibition and crystal habit modification, while PVP and PEG400 acted mainly as growth inhibitors. It was also suggested that hydrogen bonding between the drug molecule and the polymer may be used to explain the mechanism of nucleation inhibition. Since the polymer molecules are able to hydrogen bond to the hydrocortisone acetate molecules, the polymer molecules can adsorb onto the crystal surface and retard growth of the crystals. Also, the accumulation of polymer at the diffusion boundary layer may limit the diffusion of drug molecules through the barrier, thus inhibiting growth further. Since HPMC has a high level of hydroxyl groups available to form hydrogen bonds compared to PVP which only has one hydrogen bonding carbonyl group per monomer, it is suggested that the high level of hydrogen bonding can result in habit modification (37). The authors present

interesting proposals around mechanisms of supersaturation; however, this type of deep dive has not yet been extended to assess implications on salt disproportionation.

2.6. Supersaturating Systems *In Vivo*

Orolonged supersaturation has been shown to translate to extended dissolution and increased oral bioavailability (39, 47). The identification of suitable polymers that can inhibit crystallization and extend the dissolution profile of a supersaturated formulation *in vitro* has led to the identification of formulations that have also performed well *in vivo*. For example, a solid dispersion formulation of tacrolimus that demonstrates prolonged supersaturation *in vitro* has been shown to increase AUC and C_{\max} relative to crystalline tacrolimus when orally administered to dogs (48). Likewise, DiNunzio *et al.* have demonstrated that a more enhanced and prolonged supersaturation profile *in vitro* also provided a two-fold increase in rodent exposure, suggesting that the optimized intestinal targeting of the enteric polymer and its ability to increase the duration of supersaturation correlates to an improvement in bioavailability (49). In a final example, Gao *et al.* showed that a small amount of HPMC (2%) could maintain supersaturation of PNU-91325 in a cosolvent formulation and in a SEDDS formulation by retarding drug precipitation. The presence of HPMC also resulted in an increase in oral bioavailability of PNU-91325 (50). While these examples provide merit to utilizing supersaturating drug delivery systems as means to overcome dissolution-limited absorption, it is still unclear how mechanisms of supersaturation impact oral exposure.

2.7. Combining Salt Forms of Drugs with Precipitation Inhibitors

The utility of supersaturating systems in combination with precipitation inhibitors has been leveraged to extend dissolution and enhance bioavailability of orally administered BCS II drugs. Since many active pharmaceutical ingredients are ionizable, development of salts is often the first step in enhancing solubility and generating supersaturated systems. Unfortunately, disproportionation of salts can occur due to the pH gradient encountered during GI transit, and this may result in significant loss of solubility and uncontrolled precipitation of the drug. Since polymers have been shown to delay nucleation and crystal growth of drugs, the combination of salts with polymers offers an interesting formulation option to overcome dissolution-limited absorption associated with poorly soluble free forms of the drugs.

Guzmán et al. have demonstrated that specific combinations of crystalline salt forms of celecoxib with polymers and surfactants can provide both enhanced dissolution and high oral bioavailability; however a mechanistic understanding into how these excipients are interacting with celecoxib is not pursued (51). Since a combination of drug, polymer, and surfactant is required to maintain supersaturation in the case of celecoxib, it is desirable to evaluate an alternative drug substance in order to determine whether simple combinations of salts with polymers could prolong supersaturation during *in vitro* dissolution testing and enable optimized pharmacokinetic parameters *in vivo*. This is of particular interest for compounds that require rapid absorption for immediate onset of action.

2.8. References

1. G.L. Amidon, H. Lennernas, V.P. Shah, and J.R. Crison. A theoretical basis for a biopharmaceutic drug classification: the correlation of in vitro drug product dissolution and in vivo bioavailability. *Pharm Res.* 12:413-420 (1995).
2. T. Takagi, C. Ramachandran, M. Bermejo, S. Yamashita, L.X. Yu, and G.L. Amidon. A Provisional Biopharmaceutical Classification of the Top 200 Oral Drug Products in the United States, Great Britain, Spain, and Japan. *Mol Pharmaceutics.* 3:631-643 (2006).
3. C.-Y. Wu and L.Z. Benet. Predicting Drug Disposition via Application of BCS: Transport/Absorption/ Elimination Interplay and Development of a Biopharmaceutics Drug Disposition Classification System. *Pharm Res.* 22:11-23 (2005).
4. W. Curatolo. Physical chemical properties of oral drug candidates in the discovery and exploratory development settings. *Pharm Sci Technol Today.* 1:387-393 (1998).
5. G.M. Keseru and G.M. Makara. The influence of lead discovery strategies on the properties of drug candidates. *Nat Rev Drug Discovery.* 8:203-212 (2009).
6. D. Horter and J.B. Dressman. Influence of physicochemical properties on dissolution of drugs in the gastrointestinal tract. *Adv Drug Delivery Rev.* 46:75-87 (2001).
7. J. Hu, K.P. Johnston, and R.O. Williams III. Nanoparticle engineering processes for enhancing the dissolution rates of poorly water soluble drugs. *Drug Dev Ind Pharm.* 30:233-245 (2004).
8. N. Rasenack and B.W. Muller. Dissolution rate enhancement by in situ micronization of poorly water-soluble drugs. *Pharm Res.* 19:1894-1900 (2002).
9. N. Blagden, M. De Matas, P.T. Gavan, and P. York. Crystal engineering of active pharmaceutical ingredients to improve solubility and dissolution rates. *Adv Drug Delivery Rev.* 59:617-630 (2007).
10. D. Singhal and W. Curatolo. Drug polymorphism and dosage form design: a practical perspective. *Adv Drug Delivery Rev.* 56:335-347 (2004).
11. B. Hancock and M. Parks. What is the True Solubility Advantage for Amorphous Pharmaceuticals? *Pharm Res.* 17:397-404 (2000).
12. V. Shah, J. Konecny, R. Everett, B. McCullough, A.C. Noorizadeh, and J. Skelly. In Vitro Dissolution Profile of Water-Insoluble Drug Dosage Forms in the Presence of Surfactants. *Pharm Res.* 6:612-618 (1989).
13. V.J. Stella and R.A. Rajewski. Cyclodextrins: their future in drug formulation and delivery. *Pharm Res.* 14:556-567 (1997).
14. C. Leuner and J. Dressman. Improving drug solubility for oral delivery using solid dispersions. *Eur J Pharm Biopharm.* 50:47-60 (2000).
15. V.J. Stella and K.W. Nti-Addae. Prodrug strategies to overcome poor water solubility. *Adv Drug Delivery Rev.* 59:677-694 (2007).
16. S.M. Berge, L.D. Bighley, and D.C. Monkhouse. Pharmaceutical salts. *J Pharm Sci.* 66:1-19 (1977).
17. G.G.Z. Zhang, D. Law, E.A. Schmitt, and Y. Qiu. Phase transformation considerations during process development and manufacture of solid oral dosage forms. *Adv Drug Delivery Rev.* 56:371-390 (2004).

18. V.J. Stella. Prodrugs: Some thoughts and current issues. *J Pharm Sci.* 99:4755-4765 (2010).
19. F. Qian, J. Huang, and M.A. Hussain. Drug-polymer solubility and miscibility: Stability consideration and practical challenges in amorphous solid dispersion development. *J Pharm Sci.* 99:2941-2947 (2010).
20. T.f. Vasconcelos, B. Sarmiento, and P. Costa. Solid dispersions as strategy to improve oral bioavailability of poor water soluble drugs. *Drug Discovery Today.* 12:1068-1075 (2007).
21. A. Serajuddin. Solid dispersion of poorly water-soluble drugs: early promises, subsequent problems, and recent breakthroughs. *J Pharm Sci.* 88:1058-1066 (1999).
22. R.J. Bastin, M.J. Bowker, and B.J. Slater. Salt selection and optimisation procedures for pharmaceutical new chemical entities. *Org Process Res Dev.* 4:427-435 (2000).
23. A. Serajuddin. Salt formation to improve drug solubility. *Adv Drug Delivery Rev.* 59:603-616 (2007).
24. A. Avdeef. Solubility of sparingly-soluble ionizable drugs. *Adv Drug Delivery Rev.* 59:568-590 (2007).
25. M. Pudipeddi, A.T.M. Serajuddin, D.J.W. Grant, and P.H. Stahl. Solubility and dissolution of weak acids, bases, and salts. In P.H. Stahland C.G. Wermuth (eds.), *Handbook of pharmaceutical salts: properties, selection, and use*, Wiley-VCH, Weinheim, 2002, pp. 19-39.
26. A. Zimmermann, F. Tian, H. Lopez de Diego, M. Ringkjøbing Elema, J. Rantanen, A. Müllertz, and L. Hovgaard. Influence of the solid form of siramesine hydrochloride on its behavior in aqueous environments. *Pharm Res.* 26:846-854 (2009).
27. M.C. Adeyeye. *Preformulation in solid dosage form development*, Informa Healthcare, 2008.
28. P. Guerrieri and L.S. Taylor. Role of salt and excipient properties on disproportionation in the solid-state. *Pharm Res.* 26:2015-2026 (2009).
29. E.A. Zannou, Q. Ji, Y.M. Joshi, and A. Serajuddin. Stabilization of the maleate salt of a basic drug by adjustment of microenvironmental pH in solid dosage form. *Int J Pharm.* 337:210-218 (2007).
30. M. Hawley and W. Morozowich. Modifying the diffusion layer of soluble salts of poorly soluble basic drugs to improve dissolution performance. *Mol Pharmaceutics.* 7:1441-1449 (2010).
31. G. Kwei, L. Novak, L. Hettrick, E. Reiss, D. Ostovic, A. Loper, C. Lui, R. Higgins, I.W. Chen, and J. Lin. Regiospecific Intestinal Absorption of the HIV Protease Inhibitor L-735,524 in Beagle Dogs. *Pharm Res.* 12:884-888 (1995).
32. J. Brouwers, M.E. Brewster, and P. Augustijns. Supersaturating drug delivery systems: The answer to solubility limited oral bioavailability? *J Pharm Sci.* 98:2549-2572 (2009).
33. D. Kashchiev and G.M. Van Rosmalen. Review: Nucleation in solutions revisited. *Cryst Res Technol.* 38:555-574 (2003).

34. N. Rodríguez-Hornedo and D. Murphy. Significance of controlling crystallization mechanisms and kinetics in pharmaceutical systems. *J Pharm Sci.* 88:651-660 (1999).
35. T. Loftsson, H.n. Friariksdatir, and T.r.K. Guamundsdattir. The effect of water-soluble polymers on aqueous solubility of drugs. *Int J Pharm.* 127:293-296 (1996).
36. P. Gao, A. Akrami, F. Alvarez, J. Hu, L. Li, C. Ma, and S. Surapaneni. Characterization and optimization of AMG 517 supersaturatable self-emulsifying drug delivery system (S-SEDDS) for improved oral absorption. *J Pharm Sci.* 98:516-528 (2009).
37. S. Raghavan, A. Trividic, A. Davis, and J. Hadgraft. Crystallization of hydrocortisone acetate: influence of polymers. *Int J Pharm.* 212:213-221 (2001).
38. J.C. DiNunzio, D.A. Miller, W. Yang, J.W. McGinity, and R.O. Williams III. Amorphous compositions using concentration enhancing polymers for improved bioavailability of itraconazole. *Mol Pharmaceutics.* 5:968-980 (2008).
39. D.B. Warren, H. Benameur, C.J.H. Porter, and C.W. Pouton. Using polymeric precipitation inhibitors to improve the absorption of poorly water-soluble drugs: A mechanistic basis for utility. *J Drug Targeting*:1-28 (2010).
40. J.A. Plaizier-Vercammen and R.E. De Neve. Interaction of povidone with aromatic compounds II: evaluation of ionic strength, buffer concentration, temperature, and pH by factorial analysis. *J Pharm Sci.* 70:1252-1256 (1981).
41. J.A. Plaizier-Vercammen. Interaction of povidone with aromatic compounds IV: effects of macromolecule molecular weight, solvent dielectric constant, and ligand solubility on complex formation. *J Pharm Sci.* 72:1042-1044 (1983).
42. D.A. Miller, J.C. DiNunzio, W. Yang, J.W. McGinity, and R.O. Williams III. Enhanced in vivo absorption of itraconazole via stabilization of supersaturation following acidic-to-neutral pH transition. *Drug Dev Ind Pharm.* 34:890-902 (2008).
43. U.S. Kestur, H. Lee, D. Santiago, C. Rinaldi, Y.-Y. Won, and L.S. Taylor. Effects of the molecular weight and concentration of polymer additives, and temperature on the melt crystallization kinetics of a small drug molecule. *Cryst Growth Des.* 10:3585-3595 (2010).
44. F. Usui, K. Maeda, A. Kusai, and K. Nishimura. Inhibitory effects of water-soluble polymers on precipitation of RS-8359. *Int J Pharm.* 154:59-66 (1997).
45. P.N. Balani, S.Y. Wong, W.K. Ng, E. Widjaja, R.B.H. Tan, and S.Y. Chan. Influence of polymer content on stabilizing milled amorphous salbutamol sulphate. *Int J Pharm.* 391:125-136 (2010).
46. S. Xie, S.K. Poornachary, P.S. Chow, and R.B.H. Tan. Direct precipitation of micron-size salbutamol sulfate: new insights into the action of surfactants and polymeric additives. *Cryst Growth Des.* 10:3363-3371 (2010).
47. P. Gao and Y. Shi. Characterization of supersaturatable formulations for improved absorption of poorly soluble drugs. *AAPS J.* 14:703-713 (2012).
48. K. Yamashita, T. Nakate, K. Okimoto, A. Ohike, Y. Tokunaga, R. Ibuki, K. Higaki, and T. Kimura. Establishment of new preparation method for solid dispersion formulation of tacrolimus. *Int J Pharm.* 267:79-91 (2003).

49. J. DiNunzio, D. Miller, W. Yang, J. McGinity, and R. Williams. Amorphous Compositions Using Concentration Enhancing Polymers for Improved Bioavailability of Itraconazole. *Mol Pharmaceutics*, under review (2008).
50. P. Gao, M. Guyton, T. Huang, J. Bauer, K. Stefanski, and Q. Lu. Enhanced Oral Bioavailability of a Poorly Water Soluble Drug PNU-91325 by Supersaturatable Formulations. *Drug Dev Ind Pharm*. 30:221-229 (2004).
51. H.R. Guzmán, M. Tawa, Z. Zhang, P. Ratanabanangkoon, P. Shaw, C.R. Gardner, H. Chen, J.P. Moreau, Ö. Almarsson, and J.F. Remenar. Combined use of crystalline salt forms and precipitation inhibitors to improve oral absorption of celecoxib from solid oral formulations. *J Pharm Sci*. 96:2686-2702 (2007).
52. K. Rainsford. Ibuprofen: pharmacology, efficacy and safety. *Inflammopharmacology*. 17:275-342 (2009).

CHAPTER 3

Influence of Structurally Diverse Polymers on Supersaturation of Ibuprofen Sodium in Aqueous Media

3.1. Introduction

Ibuprofen is a well-known non-steroidal anti-inflammatory drug (NSAID) that is widely used for its analgesic, antipyretic, and anti-inflammatory effects (1). The commercial form of ibuprofen is the racemic free acid; however, this neutral phase of the drug is practically insoluble (2). Although ibuprofen has high membrane permeability, the low aqueous solubility of the free acid causes rate-limited dissolution that results in slow absorption of the drug following oral administration (3). Since ibuprofen has a pKa of 4.5-4.6 associated with its carboxylic acid (4), salt formation is feasible.

The use of a salt form of a drug can be leveraged to circumvent the dissolution-limited absorption of the free acid by selecting a highly soluble salt over the less soluble free form of the drug. However, since compound ionization is driven by pH, disproportionation of salts can occur at varying regions of the GI tract (5). In the case of an acidic compound, such as ibuprofen, disproportionation will occur in the stomach if the pH_{max} of the compound is above the pH in that region of the GI. Therefore, the dissolution enhancement afforded by the salt is quickly lost as the drug disproportionates and precipitates as the less soluble free acid. The disproportionation phenomenon can have complicating effects on exposure due to uncontrolled precipitation of the less solubility free form. Alternatively, variable disproportionation could occur from patient to patient due to differences in localized pH of the GI and this could result in decreased

or highly variable PK. Therefore, it is desirable to maintain the solubility enhancement that is afforded by the salt or at least control the loss in solubility that occurs following disproportionation.

Excipients have been shown to delay the disproportionation of salts by serving as pH modifiers during dissolution. In this role, formulation components possessing either acidic or basic functionality will impact the boundary diffusion layer of the solid dosage formulation by modifying the microenvironmental pH (6, 7). Depending on the properties of the drug substance, the kinetics of disproportionation can be modified based on the selected excipients (8). However, this approach can have limited success if immediate release of the drug is required for rapid absorption, which is the case with pain relief therapies such as ibuprofen.

Alternatively, if disproportionation cannot be avoided, then it is desirable to prolong the solubility enhancement afforded by the salt over the equilibrium solubility of the thermodynamically stable free acid in the stomach by maintaining supersaturation of ibuprofen. In order to prolong supersaturation achieved by higher energy phases, precipitation inhibitors have been shown to interfere in the nucleation and/or crystal growth stages of the more thermodynamically stable phase (9). Warren et al. (2010) presents a thorough review of polymeric precipitation inhibitors and summarizes proposed mechanisms of supersaturation previously presented in the literature. In general, prolonged supersaturation is due to physical or chemical interactions that take place between the drug and excipient which can be influenced by pH, temperature, molecular weight of excipients, viscosity, and the potential for hydrogen bonding. However, the

majority of mechanistic evaluations have typically been conducted on solid dispersions, lipid formulations, and solvent-solubilized solutions.

Guzmán *et al.* have demonstrated that specific combinations of crystalline salt forms of celecoxib with polymers and surfactants can provide both enhanced dissolution and high oral bioavailability; however a mechanistic understanding into how these excipients are interacting with celecoxib is not pursued (10). Since a combination of drug, polymer, and surfactant is required to maintain supersaturation in the case of celecoxib, it is desirable to evaluate an alternative drug substance in order to determine whether simple combinations of salts with polymers could prolong supersaturation during *in vitro* dissolution testing. It is proposed that a variety of mechanisms could contribute to prolonged supersaturation depending on the drug-excipient combinations. Therefore, the primary objective of this chapter was to identify polymers that effectively prolonged the supersaturation of ibuprofen. And the second objective was to begin a mechanistic evaluation into how ibuprofen interacted with the specific polymers that maintained supersaturation for an extended period of time.

3.2. Materials and Methods

3.2.1. Materials

(*R/S*)-(\pm)-ibuprofen (free acid) was purchased from Sigma (Sigma-Aldrich, St. Louis, MO, USA) and the (*R/S*)-ibuprofen sodium dihydrate was prepared from the free acid and 1.006 molar equivalents of sodium hydroxide. The crystallization for ibuprofen sodium dihydrate was based on the procedures outlined by Lee and Wang (11), but without the need for cosolvent to facilitate precipitation. The final form of ibuprofen

sodium dihydrate was confirmed to be the racemic conglomerate (12). Pharmacoat 603 (hydroxypropyl methylcellulose, HPMC, Shin-Etsu, JAPAN), Kollidon VA64 (polyvinyl pyrrolidone-vinyl acetate copolymer, PVP-VA, BASF), Poly(acrylic acid) (PAA, Aldrich), Carbopol 974P (Lubrizol), Plasdane K12 (polyvinyl pyrrolidone, Ashland), hydroxypropyl methylcellulose acetate succinate (HPMCAS, HF grade, Shin-Etsu), carboxymethylcellulose sodium salt (CMC Na, Sigma), hydroxypropyl cellulose (HPC, SL grade), methylcellulose (MC, 400 cPs, Sigma-Aldrich), Kollidon 25 (polyvinyl pyrrolidone, Sigma), Carbopol 934P (Lubrizol), Soluplus (BASF), HPMCP 50 (hydroxypropyl methylcellulose phthalate, Acros), and Klucel EXF (hydroxypropyl cellulose, HPC, Ashland) were used as polymeric excipients.

Sodium chloride, hydrochloric acid, and sodium acetate purchased from Fisher, USA and glacial acetic acid (Mallinckrodt, USA) were used in the preparation of the dissolution buffers. HPLC grade acetonitrile and 85% phosphoric acid were purchased from Sigma-Aldrich (St. Louis, MO, USA). Deionized water from the house line was used for all aqueous solutions and these were prepared as needed for each experiment.

3.2.2. Methods

3.2.2.1. pH Solubility Profile of Ibuprofen

The pH solubility profile of ibuprofen was evaluated with excess free acid or sodium salt slurried in water and pH adjusted with hydrochloric acid or sodium hydroxide in the biorelevant pH range of 1.5 to 7. For these studies, the sample plate was controlled at 37 °C and allowed to shake at 500 rpm. Following 24 hours of equilibration, measurements of pH were made using an Accumet pH meter and it was noted that excess solid remained in each well. Therefore, aliquots of filtrate were diluted following

centrifugation through a MultiScreen_{HTS}-PCF filter plate (Millipore, Billerica, MA, USA) and assayed using high performance liquid chromatography (HPLC) to determine ibuprofen concentration. The excess solid remaining on the filter plate were also analyzed on a D8 Discover X-ray diffractometer (Bruker AXS, Madison, WI, USA) in transmission scan mode programmed with a 600 second acquisition time and oscillation amplitude of 0.5. Data were collected using Symyx Epoch and viewed using Spectra Studio (Accelrys, Inc., San Diego, CA, USA).

3.2.2.2. Preparation of Ibuprofen: Polymer Blends

For the initial set of dissolution experiments, ibuprofen sodium or ibuprofen free acid was blended with each polymer at a weight ratio of 1:1. For the SGF experiments, 1 mg of each component was added to round bottom HPLC vials while 2 mg of each component was added to vials for the dissolution experiments in pH 5.0 buffer. In order to blend the components, the vials were placed on a LabRAM (Resodyn Acoustic Mixers, Inc., Butte, MT, USA) and mixed at an intensity of 30% for 120 minutes to ensure uniform blending. These samples were then directly used for dissolution testing. For all other dissolution experiments, only ibuprofen sodium was added to each vial and then media with and without pre-dissolved polymer was added at the initiation of the dissolution study.

3.2.2.3. Characterization of Blends by X-ray Powder Diffraction (XRPD)

X-ray powder diffractograms of 1:1 ibuprofen sodium:polymer blends were measured on a D8 Discover X-ray diffractometer (Bruker AXS, Madison, WI, USA). Samples were prepared on a 20 mg scale and mixed at an intensity of 30% for 120 minutes prior to being analyzed in transmission scan mode with a 600 second acquisition

time and oscillation amplitude of 0.5. Data were collected using Symyx Epoch and viewed using Spectra Studio (Accelrys, Inc., San Diego, CA, USA).

3.2.2.4. *In Vitro* Dissolution Testing and Equilibrium Solubility Assessment

Dissolution experiments were performed at 37 °C in simulated gastric fluid (SGF) and 50 mM acetate buffer at pH 5.0. The recipe for SGF was 2 g/L sodium chloride and 1.4 mL/L of 12N hydrochloric acid in deionized water for a final pH of 1.8. In order to fully evaluate potential mechanisms of supersaturation, 50 mM acetate buffer at a pH of 5.0 was also used as dissolution media since it falls between the pK_a of ibuprofen and the pH_{max} of the ibuprofen sodium salt. The intent was to avoid immediate neutralization of the ibuprofen sodium in the media by selecting a condition that could have slower kinetics of disproportionation and would have a lower degree of supersaturation from the starting concentration to the equilibrium solubility of ibuprofen in the selected media. For experiments where polymer was pre-dissolved in media, polymer solutions were prepared at 1 mg/mL in SGF and 2 mg/mL in pH 5 buffer.

Dissolution screening was conducted in round bottom HPLC vials on a 1 mL scale, with an ibuprofen sodium concentration of 1 mg/mL for SGF studies and 2 mg/mL for dissolution in pH 5 buffer. Samples were shaken at 500 rpm on a temperature controlled shaker programmed at 37 °C to enable uniform mixing. At various time points, aliquots of slurries were centrifuge filtered through a MultiScreen_{HTS}-PCF filter plate (Millipore, Billerica, MA, USA) and the filtrate was diluted and assayed using high performance liquid chromatography (HPLC) to determine ibuprofen concentration.

Since excess solid remained in the media, dissolution samples were allowed to equilibrate for 24 hours in order to determine equilibrium solubility of ibuprofen in the

presence and absence of polymer. In order to confirm that equilibrium was achieved, slurries of ibuprofen free acid were also evaluated with the same amount of polymer present following 24 hours. The degree of supersaturation was calculated by dividing the actual concentration of the drug in the solution by its equilibrium solubility determined following 24 hours in the system of interest. Measurements of pH were also made using an Accumet pH meter.

All dissolution experiments were conducted in triplicate and data is reported as average concentration of free acid in solution \pm standard deviation.

3.2.2.5. High Performance Liquid Chromatography (HPLC) Analysis

Sample concentrations for the dissolution test and equilibrium solubility studies were determined using an Agilent 1100 series HPLC instrument. The HPLC method used an Ascentis Express C18 column (2.7 μ m fused-core particle size, 4.6 mm i.d. \times 100 mm length) at 40 °C with a 3-minute linear gradient from 10% to 95% mobile phase A (acetonitrile) and 90% to 5% of mobile phase B (0.1% phosphoric acid) followed by a 1-minute hold at 95% A. The flow rate was 1.8 mL/min and the injection volume was 5 μ L. The samples were analyzed with UV detection at 210 nm. Calibration curves were constructed from peak area measurements using standard solutions of ibuprofen free acid at known concentrations. The retention time of ibuprofen was approximately 3.1 minutes. Linearity was demonstrated from 0.01 to 0.27 mg/mL ($r^2 \geq 0.999$) and the relative standard deviation of six injections was less than 0.5%. All solubility values will be reported in free acid equivalents.

3.2.2.6. XRPD Analysis of Slurries

In order to assess the final crystal forms of the solids isolated following dissolution experiments, slurries were centrifuged and wet cakes were analyzed by XRPD. X-ray powder diffractograms were measured on a PANalytical X'Pert PRO X-ray diffractometer (Almelo, The Netherlands). The voltage and current were 45 kV and 40 mA, respectively. Samples were measured in reflection mode in the 2θ -range from 4-40° using an X'celerator detector. Data were collected using X'Pert Data Collector and viewed using X'Pert HighScore (PANalytical B.V., The Netherlands).

3.2.2.7. Light Microscopy of Precipitate

The morphology of crystals produced following dissolution were observed using a Zeiss Axiovert 200M polarizing microscope at a magnification of 100x and recorded using an Axiocam HRC digital camera (Carl Zeiss, Inc., Beograd, Austria).

3.2.2.8. Viscosity

The viscosity of dissolution media with and without polymer was measured on 1 mL samples at 37 °C using a viscometer (Viscolab 3000, Cambridge Viscosity, Medford, MA, USA). A 0.310" piston was selected based on its suitability for low viscosity (0.25-5 cP) measurements.

3.2.2.9. Dynamic Light Scattering (DLS) to Assess Solution Interactions

Solution interactions of ibuprofen with polymers were interrogated by using the DynaPro Plate Reader (Wyatt Technology, Santa Barbara, CA, USA). During dissolution of 1:1 blends of ibuprofen sodium with polymer in SGF and pH 5 buffer, aliquots were filtered and transferred to a 386 well assay plate for DLS analysis at various time points. Each sample was analyzed 10 times with a single acquisition lasting 3 seconds. Data was analyzed using Dyanmics 7.0 (Wyatt Technology, Santa Barbara, CA, USA).

3.3. Results and Discussion

3.3.1. pH Solubility Profile of Ibuprofen

The solubility of ibuprofen was evaluated across the biorelevant pH range of 1.5 to 7 following 24 hours of shaking at 37 °C. The pH solubility profile (Figure 3.1) illustrates low solubility of ibuprofen from pH 1.5 to 4.4, followed by an increase in solubility with increased pH at and above pH 4.5. This increase in solubility corresponds to the published pKa of ibuprofen, which ranges from pH 4.5-4.6 (4).

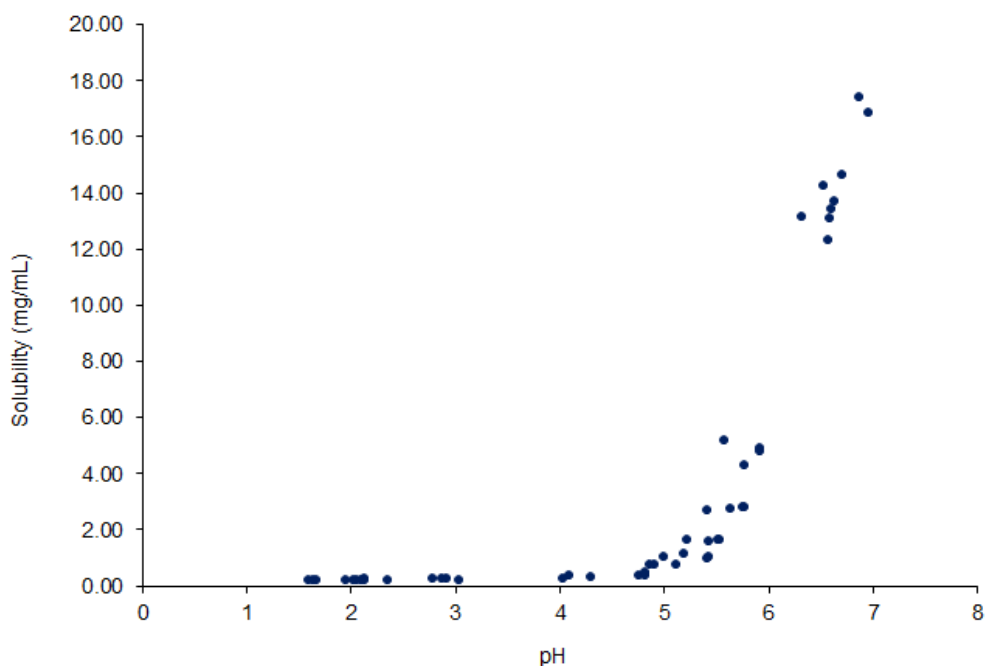


Figure 3.1. pH solubility profile of ibuprofen following 24 hours of shaking at 37 °C.

XRPD analysis (Figure 3.2) was also conducted to confirm that across the pH range of 1.5 to 5.8, ibuprofen was only present in the free acid form. Within the pH of 5.9 to 6.9, insufficient material was recovered and phase confirmation could not be obtained. However, since a plateauing of solubility was not observed below pH 6.9, it is anticipated that the pH_{max} was not yet reached. Therefore only ibuprofen free acid should be present

in the solid state throughout the evaluated pH ranges if equilibration has been achieved as per the pH-solubility interrelationship of a free acid and its salt (5).

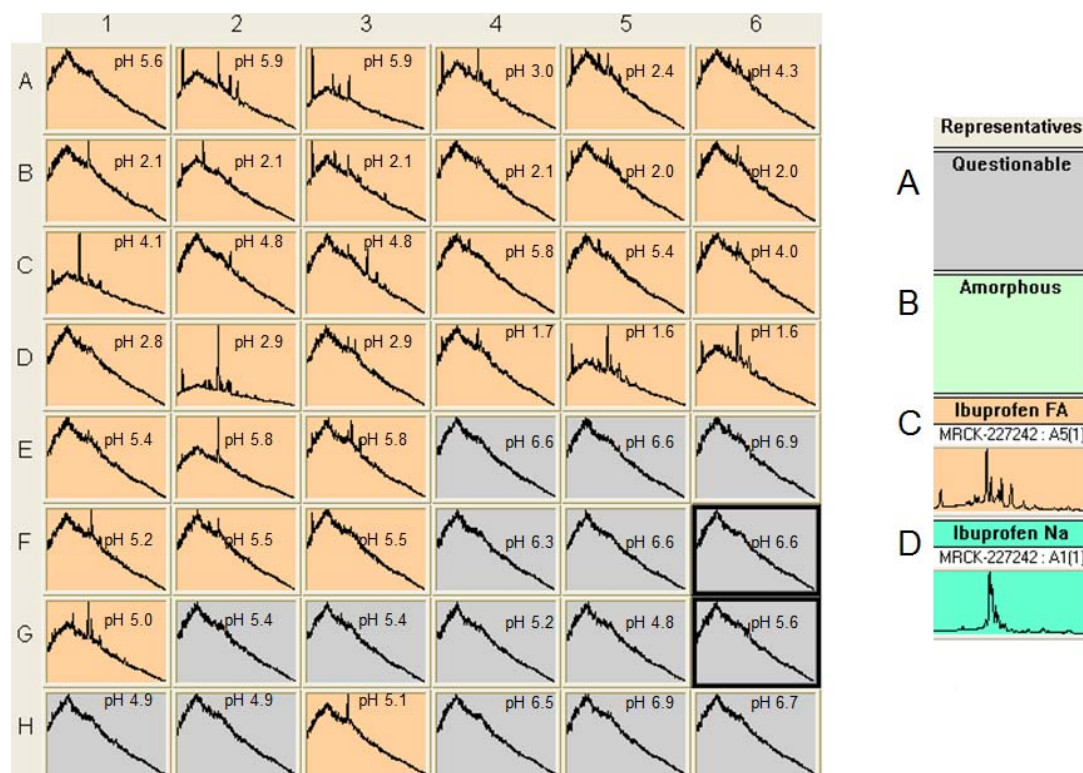


Figure 3.2. XRPD traces of ibuprofen isolated following 24 hours of shaking across the biorelevant pH range at 37 °C, with representative patterns color codes for (A) questionable traces in grey, (B) amorphous material in light green, (C) ibuprofen free acid in orange, and (D) ibuprofen sodium in dark green.

Based on this pH solubility profile, dissolution experiments were conducted in simulated gastric fluid (SGF) at pH 1.8 to evaluate supersaturation potential under the biorelevant conditions of the stomach. However, rapid neutralization of ibuprofen sodium was anticipated in SGF since the pH of the media was significantly below the pKa of ibuprofen. Therefore, a second media was also evaluated in order to increase feasibility of elucidating mechanisms of supersaturation by increasing potential for prolonged duration of supersaturation. In order to improve the likelihood of probing mechanisms of supersaturation, media selection required that two criteria be met:

1. The sodium salt needed to disproportionate in the solid-state at the selected pH in order to evaluate equilibration kinetics of the crystalline free acid under thermodynamically stable conditions.
2. The driving force for nucleation needed to be reduced by lowering the maximum feasible degree of supersaturation that could be achieved in the selected system. In other words, there needed to be a reduced difference in chemical potential of ibuprofen in a supersaturated solution (μ_1) versus a saturated solution (μ_{eq}). This is because the difference in chemical potential ($\Delta\mu$) is the driver for crystallization of ibuprofen free acid as the thermodynamically stable crystalline phase in the selected media, where:

$$\Delta\mu = \mu_1 - \mu_{eq}$$

The definition of chemical potential is:

$$\Delta\mu = RT \ln (a_1 / a_{eq})$$

where R is the gas constant, T is the temperature and a_1 and a_{eq} are the activity of the solute in a supersaturated and saturated state, respectively. If no difference in the activity coefficients are assumed, then:

$$\Delta\mu = RT \ln (C_1 / C_{eq}) = RT \ln (S)$$

where C_1 and C_{eq} are the drug concentration during supersaturation and equilibrium, respectively, and S is the supersaturation ratio. This equation therefore correlates a reduction in chemical potential with a reduction in supersaturation. In order to correlate supersaturation ratio to nucleation, the nucleation rate equation can be modified assuming homogeneous nucleation as follows:

$$J_n = N_0 v \exp (-\Delta G^* / k_b T) = N_0 v \exp (-16\pi v^2 \gamma_{ns}^3 / 3(k_b T)^3 (\ln (S))^2)$$

where the nucleation rate J_n , N_0 is the number of molecules in a unit volume, v is the frequency of molecular transport at the nucleus-liquid interface, k_b is the Boltzmann's constant, ΔG^* is the Gibbs free energy change for the formation of critical clusters, v is the molecular volume of the crystallizing solute and γ_{ns} is the interfacial energy per unit area between the cluster and the surrounding solvent. This equation therefore illustrates that nucleation is inversely proportional to supersaturation (9, 13, 14).

Therefore, 50 mM acetate buffer at a pH of 5.0 was selected as the second dissolution media since it fell between the pKa of ibuprofen and the anticipated pH_{max} of the ibuprofen sodium salt. Under these conditions, ibuprofen sodium still converted to ibuprofen free acid as illustrated in Figure 3.2, demonstrating that the free acid is the thermodynamically stable phase at the selected pH. In addition, there is a reduction in the maximum degree of supersaturation that could be achieved in pH 5 buffer since ibuprofen had a higher equilibrium solubility at pH 5 than it did in SGF. Although maximum solubilization of ibuprofen was increased 2 fold from SGF to pH 5 based on the starting concentration, the solubility difference from pH 1.8 to 5.0 was greater than 10 fold. This translated to a reduction in the maximum degree of supersaturation that could be achieved in pH 5 media. Since reduction in supersaturation could slow nucleation kinetics, dissolution in pH 5 buffer was conducted in order to probe mechanisms of drug-polymer interactions.

3.3.2. Characterization of Ibuprofen: Polymer Blends by XRPD

Prior to dissolution studies, physical stability of ibuprofen sodium and free acid following blending with a 1:1 weight ratio of various polymers for 120 minutes at 30% intensity was assessed by x-ray diffraction. Based on an initial evaluation of diffractograms illustrated in Figure 3.3, phase conversion of the ibuprofen sodium salt to the free acid was not observed following blending with any polymer evaluated. However, upon closer evaluation (Figure 3.4), presence of some ibuprofen free acid was observed when the sodium salt was blended with PAA, Carbopol 974P and Carbopol 934P. Since each of these polymers contained carboxylic acids, this moiety was likely driving disproportionation of the sodium salt of ibuprofen. These acidic polymers were serving as pH modifiers and lowering the microenvironmental pH of the system toward a region below the pH_{max} of the sodium salt. This type of behavior has previously been reported in other work that evaluated solid-state stability of salts in the presence of acidic or basic excipients (7, 15-17). Alternatively, no disproportionation of the sodium salt of ibuprofen was detected in the presence of CMC Na since CMC is already ionized and had a higher microenvironmental pH than the unionized free acid polymers. Based on this initial physical stability assessment, polymers containing unionized carboxylic acids should not be paired with ibuprofen sodium as a means to prolong supersaturation due to their ability to expedite disproportionation of the sodium salt in the solid-state.

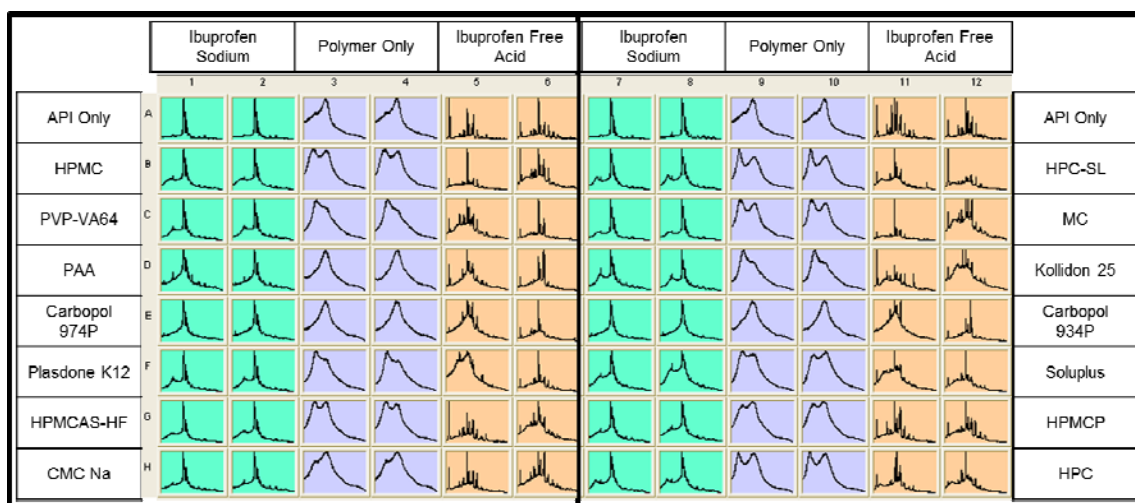


Figure 3.3. XRPD traces of 1:1 ibuprofen (sodium salt or free acid):polymer following blending. XRPD patterns matching ibuprofen sodium are highlighted in green and ibuprofen free acid are highlighted in orange while blends with only amorphous halos are purple.

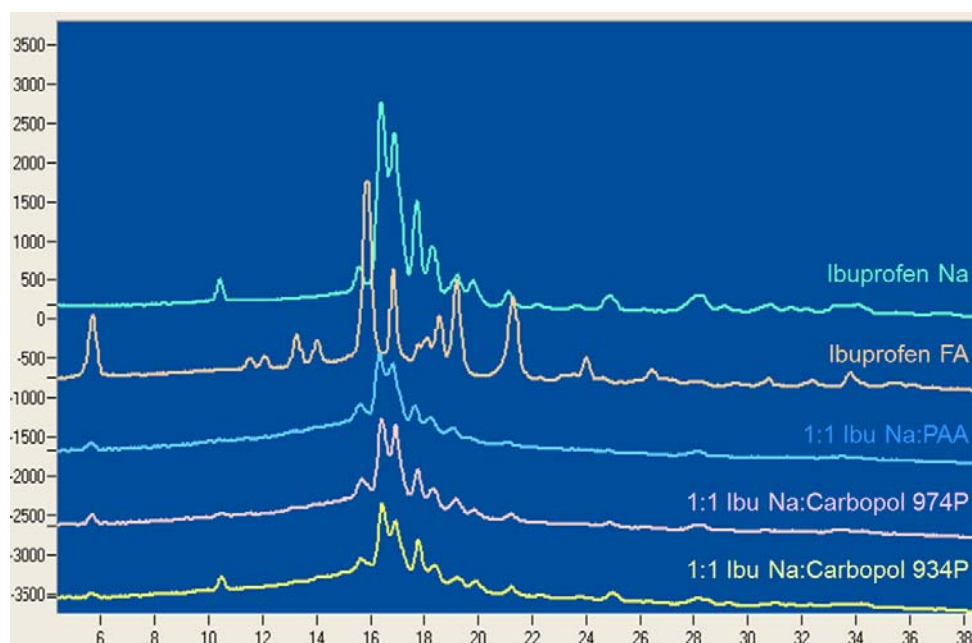


Figure 3.4. XRPD overlays of 1:1 blends of ibuprofen sodium with PAA, Carbopol 974, and Carbopol 934 compared to control samples of ibuprofen sodium and ibuprofen free acid.

3.3.3. *In Vitro* Dissolution Testing

Initial dissolution screening was conducted in SGF and pH 5 buffer with 1:1 solid blends of ibuprofen sodium and a diverse set of polymers. The intent of this work was to identify polymers that could interact with ibuprofen to prolong supersaturation prior to

reaching equilibrium as the free acid. The kinetic dissolution profiles of ibuprofen sodium with polymers in SGF (Figure 3.5) illustrated that supersaturation was achieved in the presence of PVP-VA64 and HPC for 20-40 minutes while supersaturation was further prolonged in the presence of HPC-SL, MC and Soluplus. When evaluating the dissolution profiles in pH 5 buffer (Figure 3.6), 20-40 minutes of prolonged supersaturation was obtained with HPMC and HPC while 60-120 minutes of supersaturation was achieved with PVP-VA64. Although initial supersaturation was not observed with HPMCAS-HF or Soluplus, an increase in solubility relative the ibuprofen control was noted.

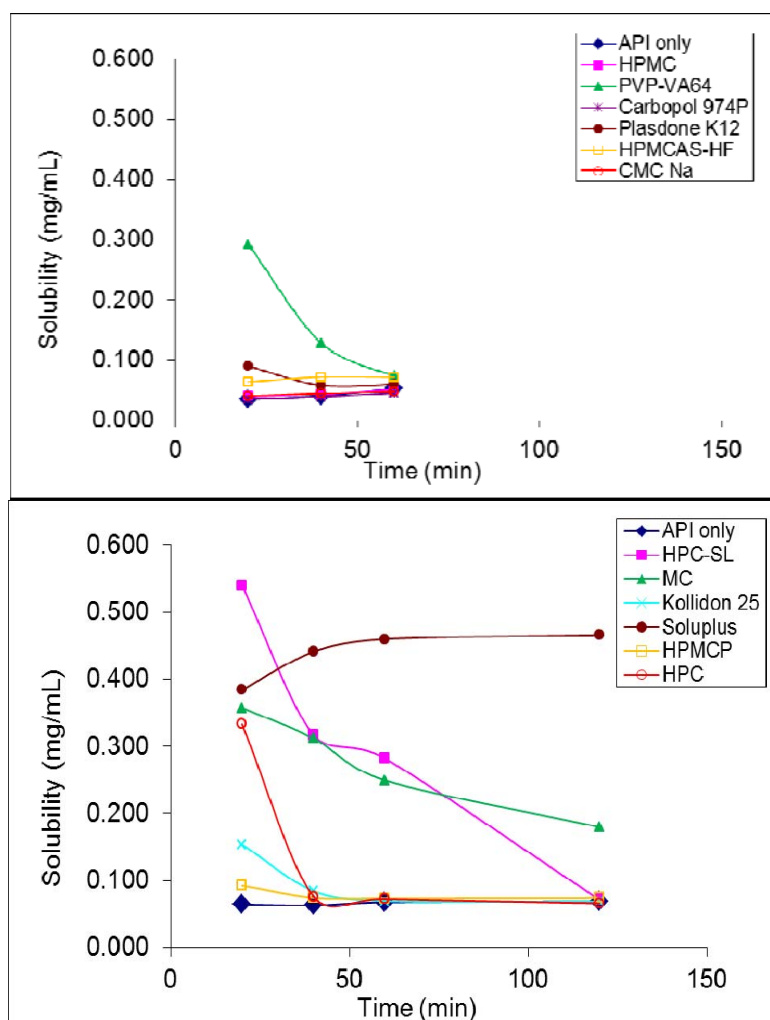


Figure 3.5. Dissolution profiles of 1:1 ibuprofen sodium:polymer in SGF at 37 °C.

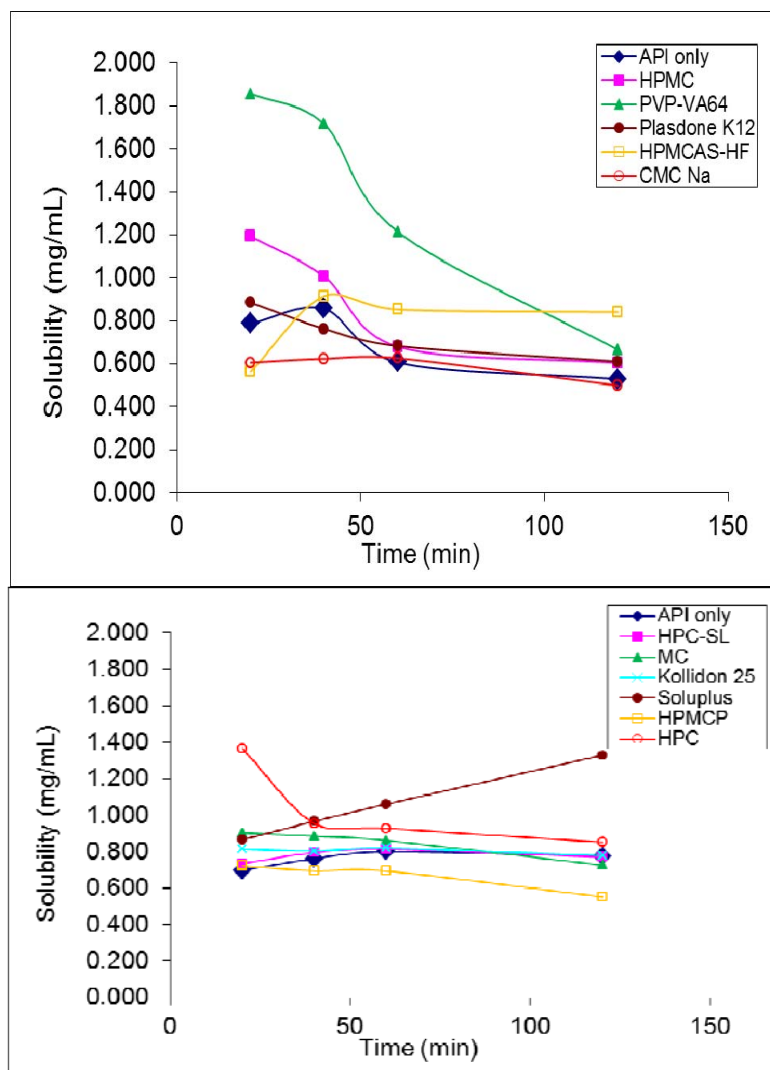


Figure 3.6. Dissolution profiles of 1:1 ibuprofen sodium:polymer in pH 5 buffer at 37 °C.

When comparing the dissolution profiles of ibuprofen sodium with polymers in SGF (Figure 3.5) to profiles in pH 5 buffer (Figure 3.6), a similar duration of supersaturation was observed with HPC and an increase in solubility was obtained with Soluplus over the duration of the dissolution experiment. Alternatively, an increase in duration of supersaturation was observed with PVP-VA64 while duration of supersaturation was reduced with HPC-SL and MC in pH 5 buffer when compared to the dissolution profiles in SGF. In addition significant supersaturation was observed with HPMC in pH 5 buffer, but not in SGF.

Prior to probing mechanisms of supersaturation and exploring whether interactions between ibuprofen and polymers could be media-dependent, additional dissolution studies were conducted. It was hypothesized that the degree and/or duration of supersaturation of ibuprofen in the co-blended formulations could be rate-limited by the dissolution of polymer. Differences in polymer dissolution in SGF versus pH 5 buffer could account for the differences in supersaturation observed with the different media noted above. Therefore, in order to eliminate the variable of polymer dissolution kinetics, dissolution of ibuprofen sodium was also conducted in the presence of pre-dissolved polymers while maintaining the same 1:1 ratio of drug: polymer at the same concentrations. In the presence of pre-dissolved polymers in SGF (Figure 3.7), prolonged supersaturation was observed for 20 minutes with MC, 90 minutes with HPMC and HPC-SL, and >120 minutes with PVP-VA64 and HPC. In addition, an increase in solubility was observed and maintained for 120 minutes with HPMCAS-HF and Soluplus.

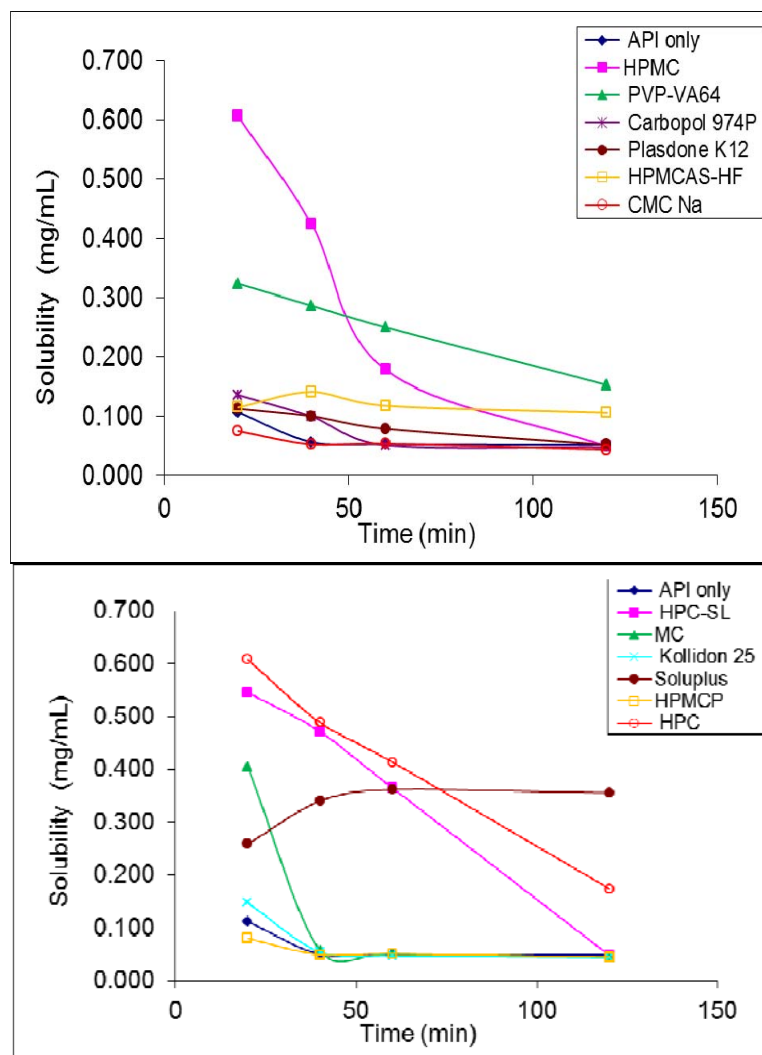


Figure 3.7. Dissolution profiles of 1:1 ibuprofen sodium:pre-dissolved polymer in SGF at 37 °C.

The same durations of supersaturation observed in SGF with pre-dissolved polymers (Figure 3.7) were also maintained with pre-dissolved polymers in pH 5 buffer (Figure 3.8), with the exception of MC. In the case of pre-dissolved MC, the maximum degree of supersaturation achieved in pH buffer was lower than in SGF. However, the duration of supersaturation in the presence of MC was maintained for an extended period of time in pH 5 buffer when compared to the profile in SGF.

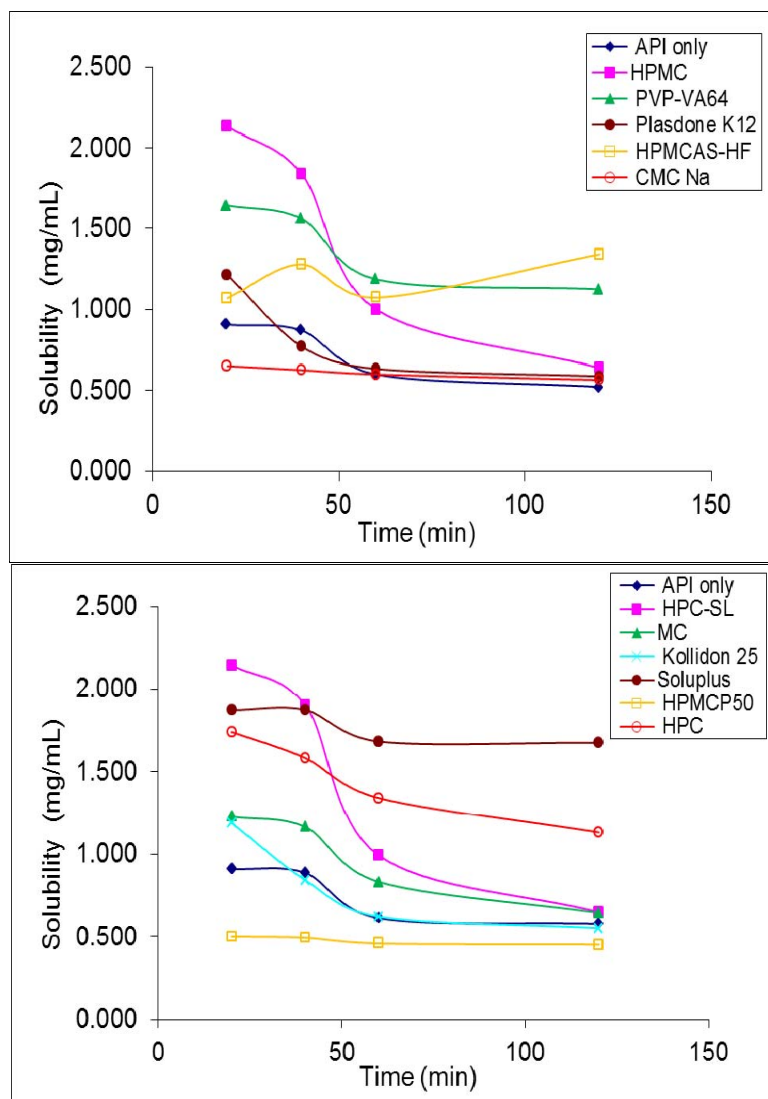


Figure 3.8. Dissolution profiles of 1:1 ibuprofen sodium:pre-dissolved polymer in pH 5 buffer at 37 °C.

A comparison of ibuprofen dissolution profiles with pre-dissolved versus solid polymers in SGF and pH 5 buffer suggest that the kinetics of polymer dissolution contributed to the durations of supersaturation achieved with various polymers. Differences in duration of supersaturation with pre-dissolved versus solid polymers were noteworthy with HPMC, PVP-VA64, HPC, and MC in SGF. In these systems, duration of supersaturation was prolonged further when the polymers were pre-dissolved; however, MC was the exception, with duration of supersaturation prolonged with solid

polymer rather than pre-dissolved polymer. The same trend with extended duration of supersaturation with pre-dissolved polymers was also observed with HPMC, PVP-VA64, and HPC in pH 5 buffer, as well as with HPC-SL and MC. While this observation could have significant implications for the design of solid dosage formulations, prioritization of polymers for mechanistic assessments were focused on dissolution data generated in the presence of pre-dissolved polymers for the purpose of this work. These polymers included HPC, HPC-SL, HPMC, HPMCAS-HF, MC, PVP-VA64 and Soluplus.

In order to assess the influence of polymer starting-state and media composition on degree of maximum supersaturation, Table 3.1 compared degree of ibuprofen supersaturation achieved with solid versus pre-dissolved polymers in both SGF and pH 5 buffer. In SGF, the only significant enhancement in degree of supersaturation with solid versus pre-dissolved polymer was observed with HPMC. This increase in degree of supersaturation also occurred in pH 5 buffer with pre-dissolved HPMC, suggesting that HPMC had a slow rate of dissolution in both media. Since supersaturation was observed and maintained for an extended period of time with pre-dissolved polymer when compared to solid polymer, it may be concluded that the process for supersaturation in the presence of HPMC was solution-mediated since polymer needed to be dissolved in order to impact precipitation of ibuprofen. HPMC was the only example where the presence of pre-dissolved polymer changed the degree of supersaturation in either SGF or pH 5 buffer when compared to the solid polymer used during the dissolution experiment. This suggested that all other polymers either quickly dissolved in order to interact with ibuprofen or were able to interact with ibuprofen in the solid state because they did not have sufficient solubility for complete dissolution, which was the case for Carbopol 934,

Carbopol 974, HPMCAS-HF, HPMCP, and PAA. When comparing the role of media only to degree of supersaturation, significant increases in degree of supersaturation were observed in SGF with HPMC, PVP-VA64, HPC-SL,MC, and HPC when compared to the same polymers in pH 5 buffer which was anticipated since ibuprofen has much lower equilibrium solubility in SGF than pH 5 buffer. Based on these observations, media pH had a significant impact on degree of supersaturation while the starting state of the polymer during the dissolution experiment was only relevant in the case of HPMC.

Table 3.1. Influence of various polymers on maximum degree of supersaturation of ibuprofen following dissolution of ibuprofen sodium in the presence of solid or pre-dissolved polymer at 37 °C.

Polymer	Supersaturation in SGF (solid polymer)	Supersaturation in SGF (pre-dissolved polymer)	Supersaturation in pH5 Buffer (solid polymer)	Supersaturation in pH5 Buffer (pre-dissolved polymer)
API only ¹	1.2	3.8	1.5	1.7
HPMC ¹	1.2	18.5	2.2	4.0
PVP-VA64 ¹	7.3	8.0	3.1	2.7
PAA ¹	*	*	*	*
Carbopol 974P ¹	1.3	5.0	*	*
Plasdone K12 ¹	1.8	2.2	1.3	1.8
HPMCAS-HF ¹	0.9	1.7	0.9	1.7
CMC Na ¹	0.8	1.5	1.0	1.1
API only ²	1.4	2.4	0.6	0.8
HPC-SL ²	12.4	12.6	0.7	2.0
MC ²	9.9	11.2	0.8	1.1
Kollidon 25 ²	3.1	3.0	0.8	1.2
Carbopol 934P ²	*	*	*	*
Soluplus ²	2.1	1.4	0.5	1.1
HPMCP ²	1.6	1.4	0.7	0.5
HPC ²	7.0	12.7	1.4	1.8

¹ Experiment 1

² Experiment 2

* Insufficient filtration to prepare solubility samples

3.3.4. Influence of Polymers on Equilibrium Solubility of Ibuprofen

Tables 3.2 and 3.3 summarized the 24 hour solubility data for ibuprofen with and without polymers in SGF and pH 5 buffer, respectively. Since the SGF solubility of

ibuprofen in the presence of a specific polymer was the same regardless of starting with the free acid or the sodium salt, it was concluded that ibuprofen reached equilibrium within the 24 hour time period that was evaluated. Although a two-fold increase in solubility was observed with ibuprofen sodium slurried in pH 5 buffer when compared to ibuprofen free acid slurries, this correlated to a right shift in pH of the systems that started with the sodium salt. This increase in pH was due to the disproportionation of ibuprofen sodium at pH 5. While the same shift in pH was observed in SGF, this had a negligible effect on solubility because the final pH remained well below the pKa of ibuprofen where no ionizable ibuprofen would remain in solution. Alternatively, an increase in pH from 5.0 to 5.2 translated to a significant increase because it was between the pKa and the pH_{max} of ibuprofen on the pH-solubility curve (Figure 3.1). Due to the pH dependence in this region, a head-to-head comparison of ibuprofen sodium salt versus free acid with polymer in pH 5 buffer cannot be used to confirm that equilibrium was achieved in 24 hours. Therefore, solubility of ibuprofen sodium and free acid slurried with the various polymers was compared to the control samples without polymer to determine whether there were any significant differences at the 24 hour time point.

Table 3.2. Influence of various polymers on solubility of ibuprofen following dissolution of 1:1 ibuprofen:polymer in SGF at 37 °C.

Polymer	Ibuprofen Sodium Salt		Ibuprofen Free Acid	
	Solubility at 24 Hours (mg/mL \pm SD)	Final pH of Media	Solubility at 24 Hours (mg/mL \pm SD)	Final pH of Media
API only ¹	0.028 \pm 0.001	1.98	0.041 \pm 0.008	1.87
HPMC ¹	0.033 \pm 0.001	1.86	0.043 \pm 0.005	1.80
PVP-VA64 ¹	0.040 \pm 0.002	2.10	0.043 \pm 0.005	1.76
PAA ¹	*	1.81	*	1.79
Carbopol 974P ¹	0.027 \pm 0.006	1.89	0.036 \pm 0.004	1.76
Plasdone K12 ¹	0.051 \pm 0.004	2.13	0.049 \pm 0.001	1.72
HPMCAS-HF ¹	0.069 \pm 0.039	1.78	0.045 \pm 0.001	1.75
CMC Na ¹	0.049 \pm 0.002	2.14	0.042 \pm 0.012	1.81
API only ²	0.046 \pm 0.002	2.02	0.047 \pm 0.000	1.82
HPC-SL ²	0.043 \pm 0.001	2.20	0.048 \pm 0.001	1.85
MC ²	0.036 \pm 0.001	2.10	0.047 \pm 0.001	1.82
Kollidon 25 ²	0.050 \pm 0.005	2.13	0.049 \pm 0.002	1.85
Carbopol 934P ²	*	2.05	*	1.83
Soluplus ²	0.185 \pm 0.048	2.17	0.206 \pm 0.139	1.81
HPMCP ²	0.057 \pm 0.006	2.13	0.054 \pm 0.003	1.83
HPC ²	0.048 \pm 0.004	2.19	0.051 \pm 0.003	1.84

¹ Experiment 1² Experiment 2

* Insufficient filtration to prepare solubility samples

Table 3.3. Influence of various polymers on solubility of ibuprofen following dissolution of 1:1 ibuprofen:polymer in pH 5 buffer at 37 °C.

Polymer	Ibuprofen Sodium Salt		Ibuprofen Free Acid	
	Solubility at 24 Hours (mg/mL \pm SD)	Final pH of Media	Solubility at 24 Hours (mg/mL \pm SD)	Final pH of Media
API only ¹	0.542 \pm 0.027	5.36	0.262 \pm 0.020	5.12
HPMC ¹	0.532 \pm 0.005	5.39	0.262 \pm 0.024	5.07
PVP-VA64 ¹	0.608 \pm 0.023	5.43	0.304 \pm 0.008	5.03
PAA ¹	*	5.29	*	4.87
Carbopol 974P ¹	*	5.06	*	4.91
Plasdone K12 ¹	0.687 \pm 0.083	5.45	0.316 \pm 0.003	5.12
HPMCAS-HF ¹	0.646 \pm 0.100	5.37	0.272 \pm 0.056	5.11
CMC Na ¹	0.595 \pm 0.071	5.50	0.313 \pm 0.030	5.11
API only ²	1.213 \pm 0.056	5.40	0.586 \pm 0.061	4.98
HPC-SL ²	1.056 \pm 0.080	5.34	0.549 \pm 0.010	4.98
MC ²	1.153 \pm 0.054	5.33	0.560 \pm 0.016	4.98
Kollidon 25 ²	1.028 \pm 0.044	5.30	0.508 \pm 0.019	5.01
Carbopol 934P ²	*	5.00	*	4.77
Soluplus ²	1.701 \pm 0.415	5.37	1.873 \pm 0.209	4.95
HPMCP ²	1.028 \pm 0.021	5.36	0.491 \pm 0.018	5.08
HPC ²	0.949 \pm 0.057	5.36	0.501 \pm 0.036	5.07

¹ Experiment 1² Experiment 2

* Insufficient filtration to prepare solubility samples

No appreciable increase in solubility was observed in SGF or pH 5 buffer in the presence of any polymers, except Soluplus. Therefore the prolonged dissolution profile of ibuprofen in the presence of Soluplus (Figures 3.5-3.8) was associated with ibuprofen reaching a thermodynamically stable state rather than maintaining prolonged supersaturation. Since the solubility of ibuprofen free acid in the presence of Soluplus was in the same region as the ibuprofen sodium salt slurry with Soluplus, it was not believed that ibuprofen sodium was stabilized in this Soluplus system. The increase in ibuprofen solubility during dissolution with Soluplus was not related to supersaturation, but rather an increase in equilibrium solubility due to the polyethylene glycol

incorporated into the Soluplus copolymer graft. In order to confirm this conclusion, XRPD analysis was conducted and is discussed below.

3.3.5. Evaluation of Ibuprofen Polymorphism Following Dissolution

Solid isolated from a slurry of ibuprofen sodium in pH 5 buffer had the same XRPD pattern as the control sample of ibuprofen free acid rather than the starting sodium salt (Figure 3.9), providing evidence that the (*R/S*)-ibuprofen sodium salt disproportionated to the racemic free acid at these buffer conditions. Due to the limited amount of solid isolated following the slurry, the signal for this solid is not as intense as the control sample. However, there were key peaks present in the isolated slurry at 6 and 12.5°2 θ that were associated with the racemic free acid while the primary identifying peak for the sodium salt at 11°2 θ was absent. Since none of these peaks were also present in the other well characterized form of the free acid, the S(+)-enantiomer (18, 19), it was concluded that conversion from the sodium salt to the racemic ibuprofen free acid occurred in pH 5 buffer.

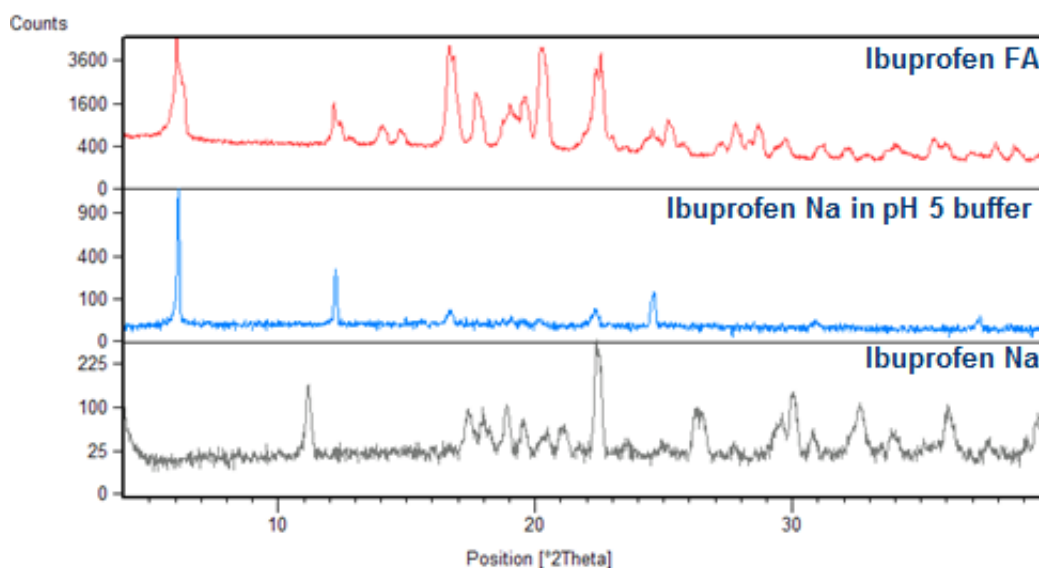


Figure 3.9. XRPD patterns comparing solid isolated from slurry of ibuprofen sodium in pH 5 buffer to control spectra of racemic ibuprofen free acid and ibuprofen sodium dihydrate.

The same characterizing peaks within the early region of $4-14^{\circ}2\theta$ were the focus of XRPD evaluation of solids isolated from slurries in the presence of various polymers. The intent of this experiment was to determine whether any polymers could alter the physical stability of ibuprofen in the pH 5 media. The XRPD overlays comparing control samples to solids isolated following 24 hours of equilibration (Figure 3.10) showed that in the presence of HPMC, PVP-VA64, HPMCAS-HF, Soluplus and HPC, ibuprofen sodium converted to racemic ibuprofen free acid within the 24 hour equilibration period in pH 5 buffer. This observation was especially relevant for the Soluplus slurry since Table 3.3 highlighted a significant increase in solubility of ibuprofen in the presence of this polymer. The conversion of the sodium salt to the free acid observed by XRPD confirmed that Soluplus had a solubility enhancing effect on ibuprofen free acid rather than had a role in altering polymorphism of ibuprofen free acid or stabilizing the sodium salt during dissolution.

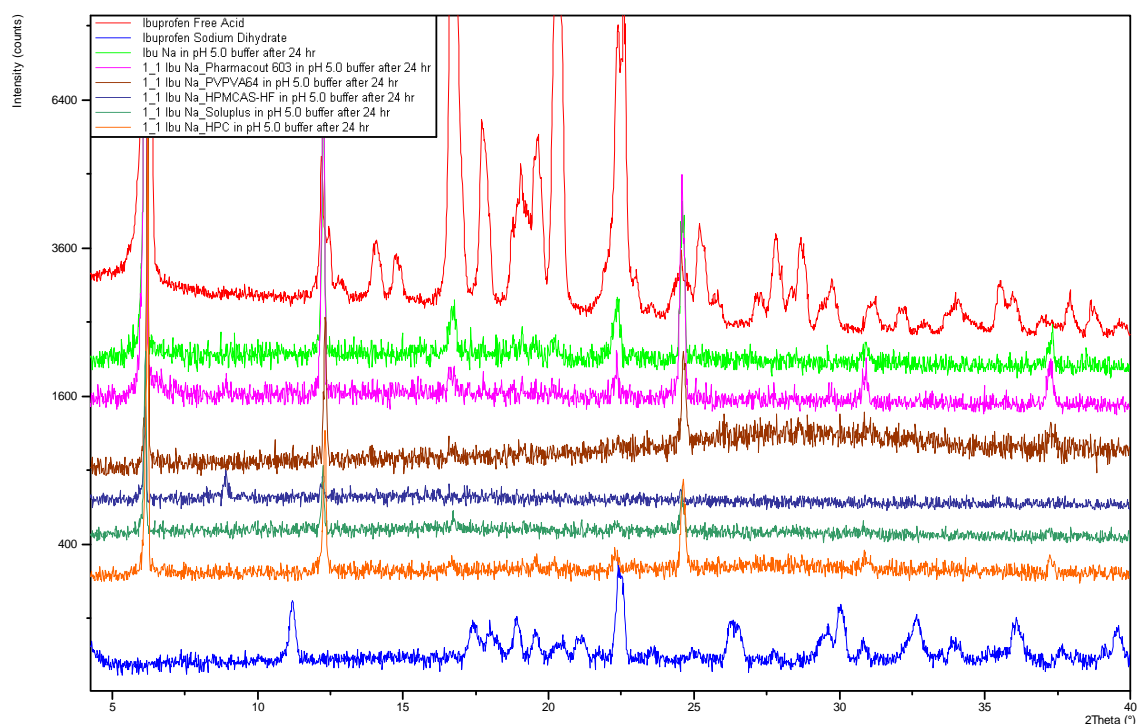


Figure 3.10. XRPD overlays comparing solid isolated from slurries of ibuprofen sodium in pH 5 buffer without any polymer (light green) or with HPMC (pink), PVP-VA64 (brown), HPMCAS-HF (navy), Soluplus (dark green), or HPC (orange) to control spectra of racemic ibuprofen free acid (red) and ibuprofen sodium dihydrate (blue).

3.3.6. Microscopy of Precipitate

Since loss of supersaturation could be attributed to either nucleation and/or crystal growth of the thermodynamically stable free acid, observations by optical microscopy were made in order to assess the role that the various polymers could play in the crystal growth stage (Figure 3.11). Crystals were observed in all samples; however, in the case of slurries with HPMCAS-HF and Soluplus, these insoluble polymers were detected by microscopy as large irregularly shaped agglomerates that lacked birefringence due to the amorphous nature of these polymers. Following disproportionation of ibuprofen sodium salt to the free acid in pH 5 buffer, the morphology of the free acid was determined to be needle to rod-like (Figure 3.11a). The same observations of crystal habit were observed in the presence of all polymers except HPMC and HPMCAS-HF.

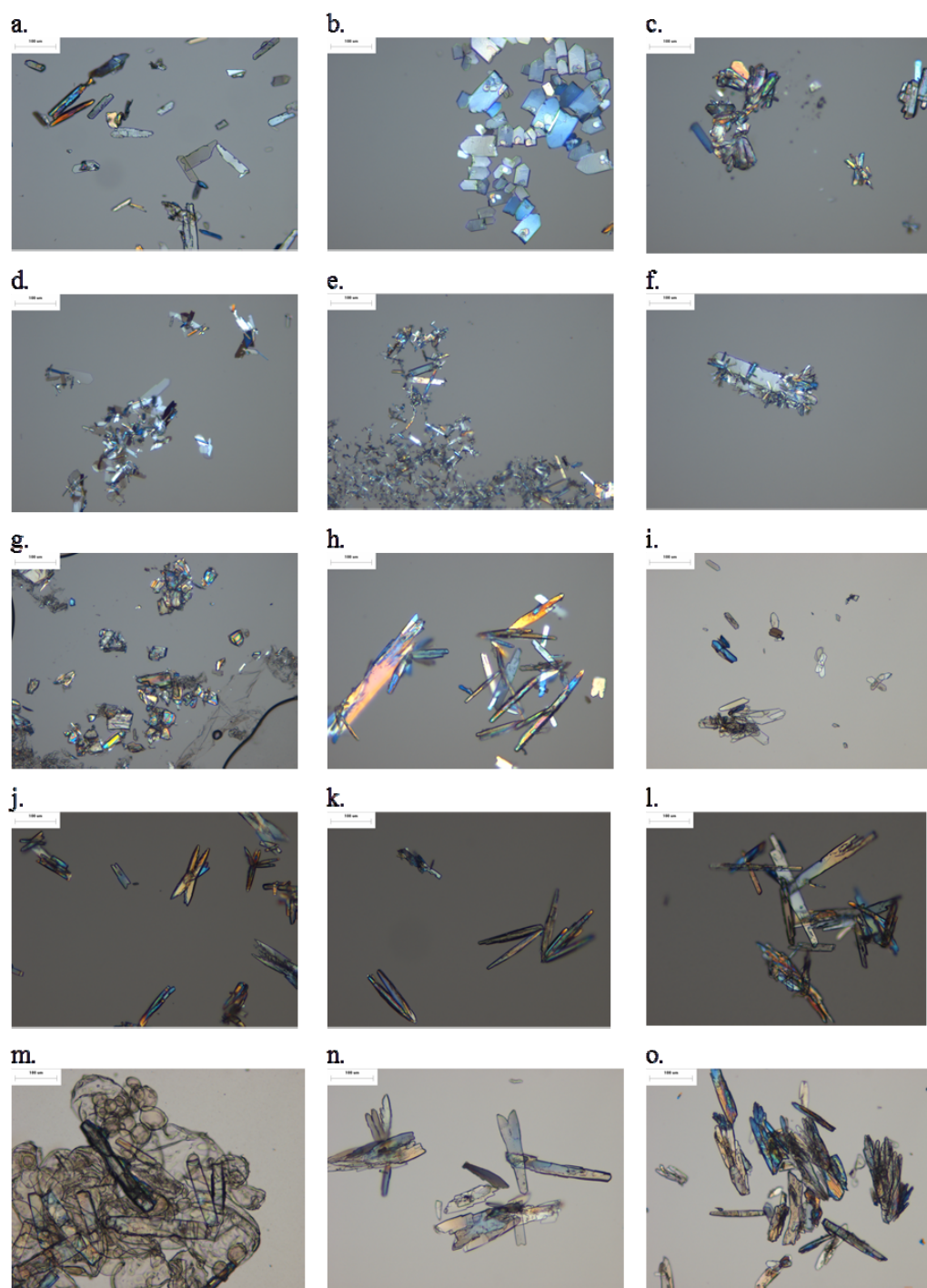


Figure 3.11. Microscopy following dissolution of (a) ibuprofen sodium alone or with (b) HPMC, (c) PVP-VA64, (d) PAA, (e) Carbopol 974P, (f) Plasdone K12, (g) HPMCAS-HF, (h) CMC Na, (i) HPC-SL, (j) MC, (k) Kollidon 25, (l) Carbopol 934P, (m) Soluplus, (n) HPMCP, and (o) HPC in pH 5.0 buffer at 100x magnification.

The lack of altered morphology of ibuprofen free acid crystals grown following loss of supersaturation in the presence of the majority of polymers suggested that these polymers did not interfere with the crystal growth process through adsorption onto the different faces of the crystal. Although the crystal habit was maintained for the majority of systems evaluated, there were some observations of decreased particle size in the presence of PAA and Carbopol 974P. These decreases in particle size could be attributed to either an inhibition in growth due to the presence of the polymer accumulated in the hydrodynamic boundary layer or adsorption of the polymer to the crystal surface (20). Since PAA and Carbopol 974P were not fully solubilized during these experiments, it was proposed that in the cases of these two systems, the polymer could be adsorbing to the crystal surface to reduce the particle size of the crystalline free acid. However, this was anticipated to only affect crystal growth since no supersaturation was observed kinetically when starting with the ibuprofen sodium salt in the presence of either of these polymers.

The two outstanding systems that exhibited significant differences in crystal morphology following loss of supersaturation included HPMCAS-HF and HPMC. Based on the XPRD data summarized in Figure 3.10, these changes in morphology were not associated with a crystalline form other than the racemic free acid. The solid isolated from the HPMCAS-HF slurry (Figure 3.11g) had irregular particle morphology. Since HPMCAS-HF was not fully dissolved in the pH 5 media, it was suggested that the habit modification could be due to different extents of adsorption of the polymer to the faces of the free acid crystal. This was nicely illustrated during a repeat dissolution experiment with HPMCAS-HF and ibuprofen sodium where solid polymer was visibly seen

surrounding the crystals of ibuprofen as shown in Figure 3.12. The ability of HPMCAS-HF to delay crystal growth could be one possible reason for prolonged supersaturation observed during dissolution in both pH 5 buffer and SGF. Alternatively, the observed adsorption of the HPMCAS-HF to the surface of the free acid crystals could have also occurred with the sodium salt. In this case, the solid HPMCAS-HF could have retarded the rate of water ingress to the ibuprofen sodium, which could explain why the maximum degree of supersaturation was not as high in the presence of HPMCAS-HF when compared to other polymer systems. In this scenario, there would have been a decrease in the apparent solubility of ibuprofen sodium which could have delayed the loss of supersaturation.

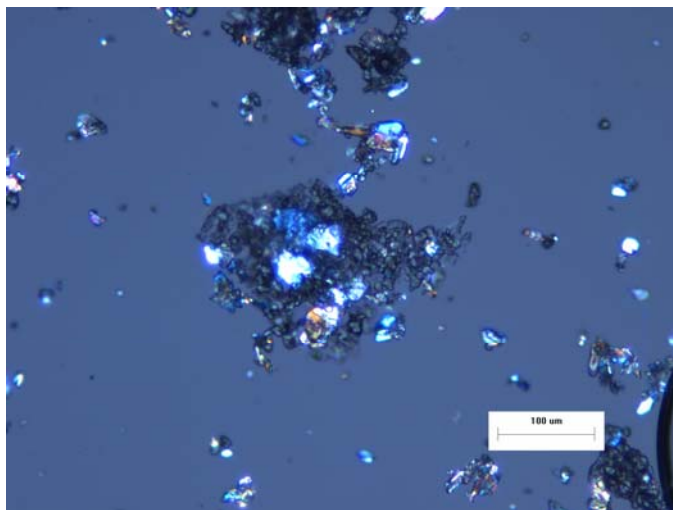


Figure 3.12. Microscopy following dissolution of ibuprofen sodium with HPMCAS-HF at 100x magnification.

Finally, significant changes in particle morphology and aspect ratio were observed in the presence of HPMC (Figure 3.11b) when compared to the control ibuprofen sodium sample without polymer (Figure 3.11a). The change in crystal habit suggested that an interaction between ibuprofen and HPMC could be occurring, and this interaction could provide an explanation for the prolonged supersaturation observed in

the presence of pre-dissolved polymer (Figures 7 and 8). Previous work by Gordon and Amin showed that differences in aspect ratios of ibuprofen crystals could be attributed to the ability of ibuprofen to interact with solvents of varying polarity (21). Specifically for ibuprofen, high aspect ratio needles were typically grown in non-polar solvents while increased polarity of solvents correlated with a decrease in the aspect ratios of the crystals (22). Based on these observations, it was hypothesized that the prolonged supersaturation of ibuprofen in the presence of HPMC was attributed to hydrogen bonding between the drug and polymer which in turn resulted in ibuprofen free acid crystals with reduced aspect ratio following loss of supersaturation. A more detailed assessment of interactions between ibuprofen and HPMC to probe hydrogen bonding potential was conducted and will be discussed in a later chapter.

3.3.7. Influence of Polymers on Media Viscosity

The viscosity of each formulation was measured in order to evaluate the influence of polymers on media viscosity and determine whether this physical change could contribute to prolonged supersaturation with any systems. The majority of polymers did not influence viscosity; however, there were a subset that did increase viscosity, including PAA, Carbopol 974P, CMC Na, MC, and Carbopol 934P (Table 3.4). Although prolonged supersaturation was not observed with PAA, Carbopol 974P, CMC Na or Carbopol 934P, there were observations of decreased particle size of ibuprofen free acid crystals grown following the dissolution of ibuprofen sodium in the presence of PAA and Carbopol 974P (Figure 3.11d and e). For these polymers, it was suggested that changes in particle size could be attributed to the polymer adsorbing to the crystal surface to reduce the particle size of the crystalline free acid. Alternatively, the reduction in particle size

could be associated with a decreased rate of drug diffusion from the bulk solution to the crystal surface due to solvent viscosity. The only polymer that increased media viscosity and also prolonged the supersaturation of ibuprofen was MC. The increase in media viscosity could be a contributing factor to the observation of supersaturation. When taking a closer look at the microscopy of solids isolated following loss of supersaturation in the presence of MC in Figure 3.11j, rough edges of the crystals were detected. This observation suggested that growth of the free acid could be taking place via a diffusion mechanism and the high viscosity of the MC system could play a role in this diffusion controlled growth.

Table 3.4. Summary of viscosity data in SGF and pH 5 buffer at 37 °C, n=3.

Polymer	Viscosity in SGF ¹ (cP ± SD)	Viscosity in pH 5 buffer ² (cP ± SD)
Media Only	0.64 ± 0.01	0.71 ± 0.03
HPMC	0.66 ± 0.01	0.82 ± 0.05
PVP-VA64	0.67 ± 0.01	0.71 ± 0.01
PAA	N.D.	4.69 ± 0.67
Carbopol 974P	0.89 ± 0.11	1.84 ± 0.13
Plasdone K12	0.63 ± 0.01	0.65 ± 0.00
HPMCAS-HF	0.64 ± 0.01	0.71 ± 0.05
CMC Na	0.70 ± 0.01	0.93 ± 0.02
HPC-SL	0.67 ± 0.02	0.69 ± 0.02
MC	0.89 ± 0.02	1.25 ± 0.17
Kollidon 25	0.66 ± 0.01	0.66 ± 0.01
Carbopol 934P	0.84 ± 0.08	1.50 ± 0.33
Soluplus	0.67 ± 0.00	0.68 ± 0.02
HPMCP	0.64 ± 0.00	0.71 ± 0.01
HPC	0.71 ± 0.02	0.78 ± 0.01

¹ Polymer concentration at 1 mg/mL

² Polymer concentration at 2 mg/mL

ND = Not Determined due to solid settling during experiment

3.3.8. Dynamic Light Scattering of Filtrate to Assess Solution Behavior

In order to conduct a preliminary assessment of speciation of ibuprofen in solution, dynamic light scattering of ibuprofen in solution was assessed. At the 20 minute

time point during the dissolution experiment, there was a lack of an intense signal due to ibuprofen in solution in SGF (Figure 3.13a) while a signal was detected in pH 5 buffer (Figure 3.13b). The signal detected in pH 5 buffer was associated with particles having an average radius of 75.5 nm suggesting that speciation of ibuprofen could be detected by DLS at pH 5 where partial ionization of ibuprofen was maintained based on the pH solubility profile (Figure 3.1). Although published data has determined that ibuprofen sodium forms micelles in aqueous conditions, the critical micelle concentration was cited as 180 mM which is significantly higher than the concentrations that were evaluated during these experiments (23). In addition, ibuprofen micelles were previously noted to have a radius of 1 nm (24), which was significantly larger than the observed particles in Figure 3.13b. This data suggested that either large aggregates or pre-crystalline nuclei could be detected by DLS.

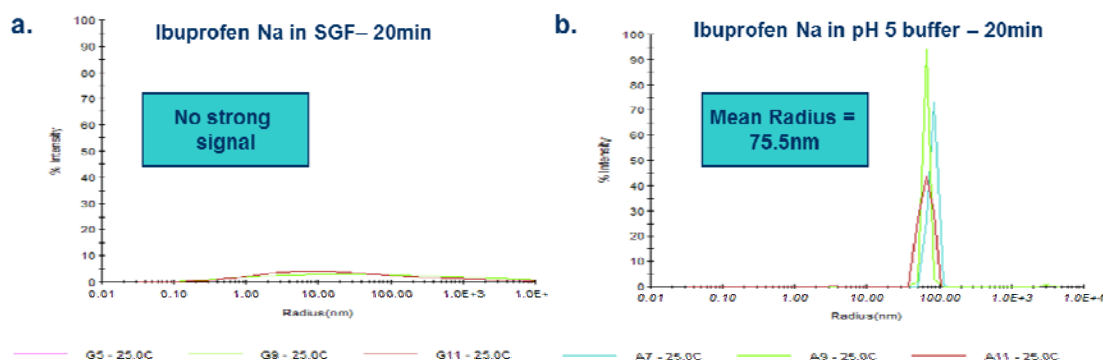


Figure 3.13. DLS plots of ibuprofen sodium slurried in (a) SGF or (b) pH 5 buffer for 20 minutes.

The kinetics of speciation was monitored by DLS analysis of ibuprofen sodium slurried in pH 5 buffer in the presence of various polymers (Figure 3.14) in order to highlight any solution-interactions that could be detected by dynamic light scattering. The two noteworthy systems where significant increases in particle size were observed in comparison to the ibuprofen sodium control were HPC and PVP-VA64. In these

scenarios, the polymer without API had significantly smaller particle size than the drug-polymer combinations. Since the particle size was reported in average radius, a reduction in particle size would have been anticipated if ibuprofen and polymer were not interacting. This increase in particle size suggests that ibuprofen and HPC or PVP-VA64 are interacting in solution.

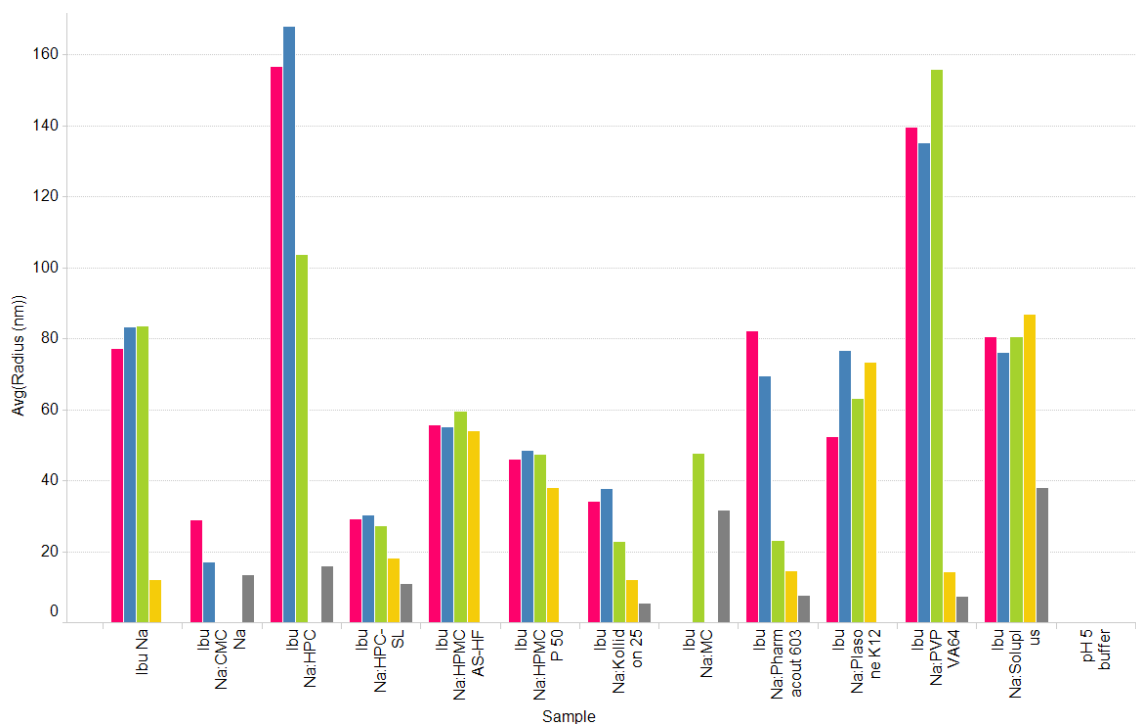
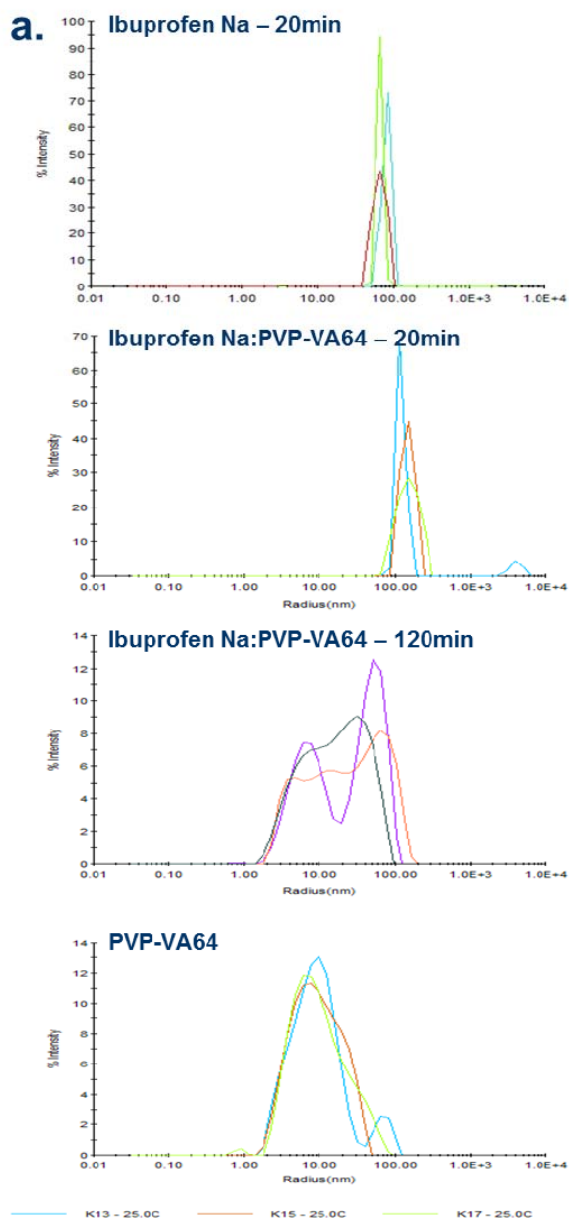


Figure 3.14. DLS of ibuprofen with polymers in pH 5 buffer at 20 minutes (pink), 40 minutes (blue), 60 minutes (green), 120 minutes (yellow), and with polymer only (grey).

In order to probe the potential interactions between ibuprofen and PVP-VA64 and HPC closer, the DLS overlays were shown in Figure 3.15. At the 20 minute time point, a single peak is observed within the region of 140 nm for ibuprofen sodium with PVP-VA64 and at 160 nm for ibuprofen sodium with HPC. When compared to the ibuprofen sodium sample without polymer at the same time point, there is a noticeable right shift in the peak which corresponds with the observed increase in particle size summarized for these two polymer systems in Figure 3.14. It was also noted that while PVP-VA64 and

HPC exhibit distinct peak intensity at the lower particle size regions of 7 and 16 nm respectively, these peaks were not detected with the combination slurries at the early time point. This data further supported the proposal that solution interactions were occurring between ibuprofen and these two polymers. The loss of the ibuprofen-polymer peaks at the 120 minute time point and increased intensity of the polymer peaks suggested that these interactions were kinetic. This trend in loss of aggregate presence also corresponded to loss of supersaturation of ibuprofen in the presence of both PVP-VA64 and HPC (Figures 6 and 8), providing evidence that the solution interactions between ibuprofen and PVP-VA64 or HPC was driving the supersaturation.



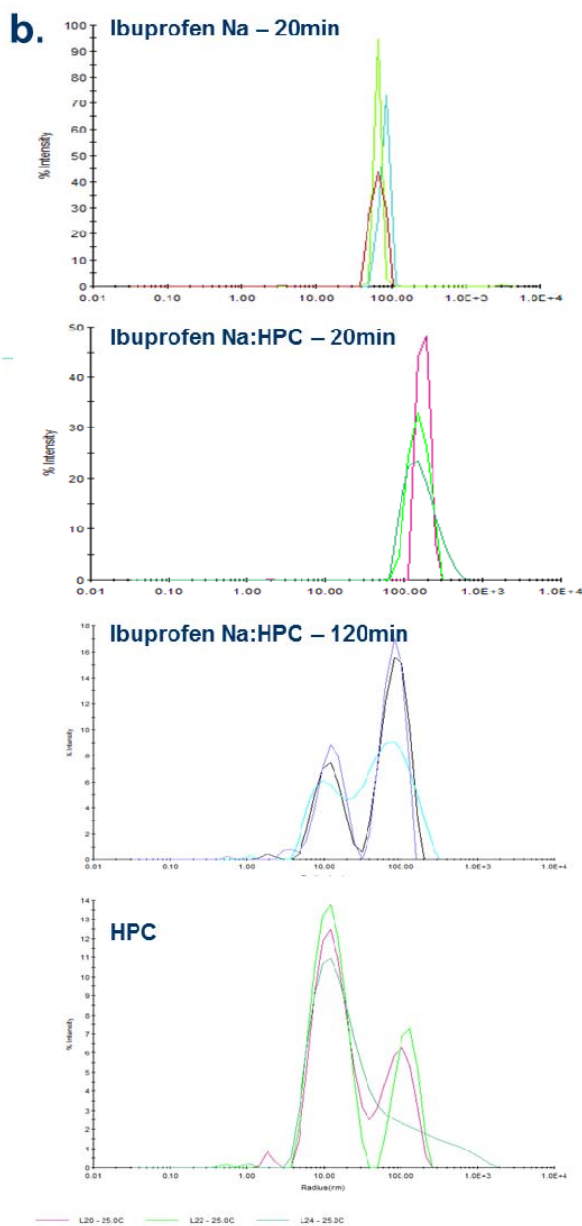


Figure 3.15. DLS overlays comparing ibuprofen sodium with (a) PVP-VA64 and (b) HPC in combination and against control samples of ibuprofen sodium and polymer alone.

In order to determine whether the prolonged supersaturation of ibuprofen in the presence of PVP-VA64 and HPC was due to delayed disproportionation of ibuprofen sodium in solution or due to a change in the critical cluster size required for nucleation, additional studies were conducted and will be discussed in Chapter 6.

3.4. Conclusions

Supersaturation of ibuprofen sodium was effectively prolonged in the presence of a variety of polymers including MC, HPMC, HPC, HPC-SL, and HPMCAS-HF. This was the first example of work that demonstrated prolonged supersaturation when combining a salt form of a drug with a polymeric precipitation inhibitor in the absence of surfactant. Characterization during supersaturation as well as after equilibration of ibuprofen in SGF and pH 5 buffer enabled preliminary conclusions to be drawn around mechanisms of supersaturation. The polymer-specific properties of MC prolonged supersaturation by increasing media viscosity while HPMCAS-HF had a solid-mediated effect on dissolution rate. In addition, ibuprofen-polymer interactions that occurred in solution were observed in the form of changes in particle morphology during crystal growth with HPMC and with aggregation formation observed in the presence of PVP-VA64 and HPC. In conclusion, these results emphasized that mechanisms of supersaturation could differ significantly depending on the specific drug-polymer combination.

3.5. References

1. K. Rainsford. Ibuprofen: pharmacology, efficacy and safety. *Inflammopharmacology*. 17:275-342 (2009).
2. N.A. Kasim, M. Whitehouse, C. Ramachandran, M. Bermejo, H. Lennernas, A.S. Hussain, H.E. Junginger, S.A. Stavchansky, K.K. Midha, and V.P. Shah. Molecular properties of WHO essential drugs and provisional biopharmaceutical classification. *Mol Pharmaceutics*. 1:85-96 (2004).
3. M. Newa, K.H. Bhandari, D.X. Lee, J.H. Sung, J.A. Kim, B.K. Yoo, J.S. Woo, H.G. Choi, and C.S. Yong. Enhanced Dissolution of Ibuprofen Using Solid Dispersion with Polyethylene Glycol 20000. *Drug Dev Ind Pharm*. 34:1013-1021 (2008).

4. H. Potthast, J.B. Dressman, H.E. Junginger, K.K. Midha, H. Oeser, V.P. Shah, H. Vogelpoel, and D.M. Barends. Biowaiver monographs for immediate release solid oral dosage forms: Ibuprofen. *J Pharm Sci.* 94:2121-2131 (2005).
5. A. Serajuddin. Salt formation to improve drug solubility. *Adv Drug Delivery Rev.* 59:603-616 (2007).
6. M.C. Adeyeye. Preformulation in solid dosage form development, Informa Healthcare, 2008.
7. P. Guerrier and L.S. Taylor. Role of salt and excipient properties on disproportionation in the solid-state. *Pharm Res.* 26:2015-2026 (2009).
8. M. Hawley and W. Morozowich. Modifying the diffusion layer of soluble salts of poorly soluble basic drugs to improve dissolution performance. *Mol Pharmaceutics.* 7:1441-1449 (2010).
9. J. Brouwers, M.E. Brewster, and P. Augustijns. Supersaturating drug delivery systems: The answer to solubility limited oral bioavailability? *J Pharm Sci.* 98:2549-2572 (2009).
10. H.R. Guzmán, M. Tawa, Z. Zhang, P. Ratanabangkoon, P. Shaw, C.R. Gardner, H. Chen, J.P. Moreau, Ö. Almarsson, and J.F. Remenar. Combined use of crystalline salt forms and precipitation inhibitors to improve oral absorption of celecoxib from solid oral formulations. *J Pharm Sci.* 96:2686-2702 (2007).
11. T. Lee and Y.W. Wang. Initial salt screening procedures for manufacturing ibuprofen. *Drug Dev Ind Pharm.* 35:555-567 (2009).
12. G.G.Z. Zhang, S.Y.L. Paspal, R. Suryanarayanan, and D.J.W. Grant. Racemic species of sodium ibuprofen: Characterization and polymorphic relationships. *J Pharm Sci.* 92:1356-1366 (2003).
13. D. Kashchiev and G.M. Van Rosmalen. Review: Nucleation in solutions revisited. *Cryst Res Technol.* 38:555-574 (2003).
14. N. Rodríguez-Hornedo and D. Murphy. Significance of controlling crystallization mechanisms and kinetics in pharmaceutical systems. *J Pharm Sci.* 88:651-660 (1999).
15. R. Govindarajan, A. Zinchuk, B. Hancock, E. Shalaev, and R. Suryanarayanan. Ionization states in the microenvironment of solid dosage forms: Effect of formulation variables and processing. *Pharm Res.* 23:2454-2468 (2006).
16. A.T.M. Serajuddin, A.B. Thakur, R.N. Ghoshal, M.G. Fakes, S.A. Ranadive, K.R. Morris, and S.A. Varia. Selection of solid dosage form composition through drug–excipient compatibility testing. *J Pharm Sci.* 88:696-704 (1999).
17. G.A. Stephenson, A. Aburub, and T.A. Woods. Physical stability of salts of weak bases in the solid state. *J Pharm Sci.* 100:1607-1617 (2011).
18. G. Leising, R. Resel, F. Stelzer, S. Tasch, A. Lanziner, and G. Hantich. Physical aspects of dexibuprofen and racemic ibuprofen. *J Clin Pharmacol.* 36:3S-6S (1996).
19. N.V. Phadnis and R. Suryanarayanan. Simultaneous quantification of an enantiomer and the racemic compound of ibuprofen by X-ray powder diffractometry. *Pharm Res.* 14:1176-1180 (1997).
20. S. Raghavan, A. Trividic, A. Davis, and J. Hadgraft. Crystallization of hydrocortisone acetate: influence of polymers. *Int J Pharm.* 212:213-221 (2001).

21. R.E. Gordon and S.I. Amin. Crystallization of ibuprofen, US Patent Number 4,476,248, 1984.
22. D. Winn and M.F. Doherty. A new technique for predicting the shape of solution-grown organic crystals. *AIChE J.* 44:2501-2514 (1998).
23. A. Ridell, H. Evertsson, S. Nilsson, and L.O. Sundelöf. Amphiphilic association of ibuprofen and two nonionic cellulose derivatives in aqueous solution. *J Pharm Sci.* 88:1175-1181 (1999).
24. T. Lee and C.W. Zhang. Dissolution enhancement by bio-inspired mesocrystals: the study of racemic (R, S)-(\pm)-sodium ibuprofen dihydrate. *Pharm Res.* 25:1563-1571 (2008).

CHAPTER 4

Combined Use of Crystalline Sodium Salt and Polymeric Precipitation Inhibitors to Improve Pharmacokinetic Profile of Ibuprofen Through Supersaturation

Submitted for publication to AAPS PharmSciTech as: “Combined Use of Crystalline Sodium Salt and Polymeric Precipitation Inhibitors to Improve Pharmacokinetic Profile of Ibuprofen Through Supersaturation”

Jenna L. Terebetski, John J. Cummings, Scott E. Fauty and Bozena Michniak-Kohn

4.1. Introduction

There are many phase and formulation approaches that can be taken to optimize the oral absorption of drugs. One commonly used technique includes the use of a highly soluble salt form of a drug. Since salts are typically thermodynamically stable phases, they can carry minimal risk from a processing and storage perspective (1). In addition, the higher intrinsic aqueous solubility of the ionized form of the drug may enable more rapid and extensive dissolution compared to the free form of the drug. Unfortunately, the pH gradient of the GI tract may limit the solubility enhancement that is offered by salts. This is especially the case for salts of acidic drugs since initial dissolution of the formulation will occur under the acidic conditions of the stomach. Under these conditions, the salt form of an acidic drug can undergo rapid disproportionation, resulting in a phase change to the neutral free acid and subsequent loss of solubilization (2). Therefore, the initial boost in solubility associated with the properties of an acidic salt can be lost prior to initiation of absorption.

Despite this risk of disproportionation, there may be opportunities to prolong the supersaturation that is initially achieved by the rapid dissolution of the salt in the stomach by leveraging the use of polymeric precipitation inhibitors to maintain enhanced solubilization above the intrinsic solubility of the neutral free acid drug. Polymeric precipitation inhibitors have a broad use in the maintenance of supersaturation for amorphous dispersions and emulsion systems (3). The identification of suitable polymers that can inhibit crystallization and extend the dissolution profile of a supersaturated formulation *in vitro* has also led to the identification of formulations that have improved oral bioavailability based on *in vivo* testing (4, 5). Other research demonstrates that the combination of a salt form of celecoxib can have enhanced supersaturation and increased exposure when combined with polymers and surfactants (6). In this previous work, the addition of surfactant at concentrations above its critical micelle concentration was required for the maintenance of supersaturation *in vitro*. Therefore, it is hypothesized that a drug with surfactant-like properties in its salt form may be able to maintain a prolonged state of supersaturation with the presence of polymer, but without the need for additional surfactant.

For this work, we evaluated the feasibility of prolonging the supersaturation of ibuprofen under simulated gastric conditions by combining the highly soluble sodium salt with various polymers that are pharmaceutically acceptable as per the Handbook of Pharmaceutical Excipients (7). In order to circumvent the need for a surfactant component in the formulation, ibuprofen sodium was selected based on its known surfactant-like properties (8). It was hypothesized that formulations that prolonged supersaturation under acidic conditions may increase the C_{\max} and provide an earlier T_{\max}

due to rapid absorption when administered *in vivo*. Therefore, in addition to identifying formulations that enabled supersaturation *in vitro*, the impacts of these formulations on pharmacokinetic parameters were also evaluated *in vivo*. The desired outcome of this work was to identify simple formulations comprised of crystalline drug and polymer blends that could afford rapid onset of action through prolonged supersaturation in the stomach and rapid absorption observed with an increased C_{\max} and earlier T_{\max} , which is of particular interest for a pain reliever such as ibuprofen (9).

4.2. Material and Methods

4.2.1. Materials

(R/S)-(\pm)-ibuprofen (free acid) was purchased from Sigma (Sigma-Aldrich, St. Louis, MO, USA) and the (R/S)-ibuprofen sodium dihydrate was purchased from Fluka (Sigma-Aldrich, St. Louis, MO, USA). Pharmacout 603 (hydroxypropyl methylcellulose, HPMC, Shin-Etsu, JAPAN), Kollidon VA64 (polyvinyl pyrrolidone-vinyl acetate copolymer, PVP-VA, BASF), Carbopol 974P (Carbomer, polyacrylic acid, Lubrizol), Plasdone K12 (polyvinyl pyrrolidone, Ashland), hydroxypropyl methylcellulose acetate succinate (HPMCAS, HF grade, Shin-Etsu), carboxymethylcellulose sodium salt (CMC Na, Sigma), hydroxypropyl cellulose (HPC, SL grade), methylcellulose (MC, 400 cPs, Sigma-Aldrich), Kollidon 25 (polyvinyl pyrrolidone, Sigma), Soluplus (BASF), HPMCP 50 (hydroxypropyl methylcellulose phthalate, Acros), and Klucel EXF (hydroxypropyl cellulose, HPC, Ashland) were used as polymeric excipients.

Sodium chloride, hydrochloric acid, sodium phosphate monobasic, and sodium phosphate dibasic were purchased from Fisher, USA for use in the preparation of the

dissolution buffers. HPLC grade acetonitrile and 85% phosphoric acid were purchased from Sigma-Aldrich (St. Louis, MO, USA) and were used as received. Deionized water was used for all aqueous solutions which were prepared as needed for each experiment.

4.2.2. Methods

4.2.2.1. Supersaturation Screening of Ibuprofen in the Presence of Polymers

Preliminary supersaturation screening of ibuprofen sodium salt in pre-dissolved polymer solutions was conducted using a high-throughput screen to determine potential degree of supersaturation that could be achieved. Dissolution experiments with ibuprofen sodium were performed at 37 °C in simulated gastric fluid (SGF). The formula for SGF was 2 g/L sodium chloride and 1.4 mL/L of 12N hydrochloric acid in deionized water at a final pH of 1.8. For screening studies, polymer was pre-dissolved at a concentration of 1 mg/mL in SGF.

Supersaturation screening was conducted in round bottom high performance liquid chromatography (HPLC) vials on a 1 mL scale, with solid ibuprofen sodium added to each vial at a target concentration of 1 mg/mL. Samples were shaken at 500 rpm on a temperature controlled shaker programmed at 37 °C to enable uniform mixing without the addition of a stir bar that could interfere with particle growth during equilibration. At 20, 40, 60, and 120 minutes, aliquots of the slurries were centrifuge filtered through a MultiScreenHTS-PCF filter plate (Millipore, Billerica, MA, USA) and the filtrate was diluted and assayed using HPLC to determine ibuprofen concentration.

Since excess solid remained in the media, dissolution samples were allowed to equilibrate for 24 hours in order to determine equilibrium solubility of ibuprofen in the presence and absence of polymer. In order to confirm that equilibrium was achieved

within that time, slurries starting from ibuprofen free acid were also evaluated with the same amount of polymer present following 24 hours for comparison. The degree of supersaturation was calculated by dividing the maximum measured concentration of drug in solution during dissolution by its equilibrium solubility determined following 24 hours in the system of interest. The duration of supersaturation was the amount of time that the measured concentration of drug in solution remained above the equilibrium solubility of that system. Measurements of pH of the samples were made using an Accumet pH meter.

All dissolution experiments were conducted in triplicate and data is reported as average concentration of free acid in solution \pm standard deviation.

4.2.2.2. Two-Stage Dissolution of Drug-Polymer Formulations

Based on the supersaturation screening results, polymers that significantly prolonged supersaturation of ibuprofen sodium following addition into SGF were selected for more detailed, larger-scale two-stage biorelevant dissolution experiments. These two-stage dissolution experiments were conducted in triplicate with a USP Apparatus II (paddle) method in a Distek dissolution system 2100C (Distek, Inc., North Brunswick, NJ). In order to differentiate among formulations that may exhibit supersaturation in acidic media, formulations were first subjected to acid stage testing (1 hour in 250 mL of SGF at pH 1.8, prepared as described above). During the transition to the buffer stage of testing, 250 mL of 0.115 M sodium dihydrogen phosphate buffer was added to each vessel for a final volume of 500 mL and final pH of 6.8 ± 0.5 . The use of buffer rather than fasted-state simulated intestinal media was selected since immediate release formulations of ibuprofen have been previously demonstrated to have rapid

dissolution (85% within 30 minutes or less) in pH 6.8 buffer (10). Media was controlled at a temperature of 37.0 ± 0.5 °C for the duration of the experiment and the rotational speed of the paddles was 50 rpm. To each dissolution vessel, 550 mg of 1:1 ibuprofen sodium:polymer blends was added (250 mg of ibuprofen, free acid equivalence). This amount of ibuprofen corresponds to a theoretical 1 mg/mL concentration of ibuprofen in the acid phase which represents a 20-fold level of supersaturation assuming an equilibrium solubility of 0.047 mg/mL in SGF (see Table 4.2). At predetermined intervals (5, 10, 15, 20, 30, 40, 50, 60, 75, 90, 105, 120, and 180 minutes), samples were withdrawn, filtered using a 0.45 μ m PTFE membrane syringe filter (Thermo Fisher Scientific, Waltham, MA), appropriately diluted and analyzed for drug concentration using HPLC.

4.2.2.3. High Performance Liquid Chromatography (HPLC) Analysis

Sample concentrations for the dissolution test and equilibrium solubility studies were determined using an Agilent 1100 Series HPLC instrument. The HPLC method used an Ascentis Express C18 column (2.7 μ m fused-core particle size, 4.6 mm i.d. \times 100 mm length) at 40 °C with a 3-minute linear gradient from 10% to 95% mobile phase A (acetonitrile) and 90% to 5% of mobile phase B (0.1% phosphoric acid) followed by a 1-minute hold at 95% A. The flow rate was 1.8 mL/min and the injection volume was 5 μ L. The samples were analyzed by UV detection at 210 nm. Calibration curves were constructed from peak area measurements using standard solutions of ibuprofen free acid at known concentrations. The retention time of ibuprofen was approximately 3.1 minutes. Linearity was demonstrated from 0.01 to 0.27 mg/mL ($r^2 \geq 0.999$) and the relative

standard deviation of six injections was less than 0.5%. All solubility values will be reported in free acid equivalents.

4.2.2.4. *In vivo* Studies

Pharmacokinetic studies were performed by Merck (West Point, PA). Six, male Wistar Han rats were assigned to each arm of the study. Oral dosage formulations were dispensed into size 9 hard gelatin capsules (Harvard Apparatus, Holliston, MA). The ibuprofen content in each dose was based on the animal weight range of 280-300 grams with a target dose of 25 milligrams per kilogram (mpk). Rats were fasted overnight prior to each dosing session. Plasma samples were collected at 0, 0.25, 0.5, 1, 2, 4, 6, 8 and 24 hours post dosing. EDTA was added to the samples as an anticoagulant and samples were then stored at -20 °C pending analysis of parent drug (ibuprofen) by LC-MS/MS.

4.2.2.5. Plasma Extraction and Chromatographic Analysis

Concentrations of ibuprofen in rat plasma were determined by protein precipitation followed by LC-MS/MS analysis. Calibration curves were generated and verified using standard and quality control (QC) samples prepared from an initial weighing of high purity compound. For the analysis of the plasma samples, standard samples were prepared by adding to 50 µL aliquots of control plasma, 10 µL of standard solutions containing 2.5, 5, 10, 25, 50, 250, 500, 1000, 2500, 5000, 10000, 25000, 50000, 75000, and 125000 ng/mL target compound in 1:1 acetonitrile:water (v:v). This yielded standard samples effectively containing 0.5, 1, 2, 5, 10, 50, 100, 200, 500, 1000, 2000, 5000, 10000, 15000, and 25000 ng/mL of target compounds.

For all unknown samples, 50 µL were used from each sample vial for analysis. To all aliquots of standards and QC samples, 10 µL of 1:1 acetonitrile:water were then

added. This was followed by protein precipitation with 300 μ L of acetonitrile containing 100-200 ng/mL of internal standards (IS) mixture. Sample mixtures were then lightly vortex-mixed. After spinning in a centrifuge for 5 minutes at 4000 rpm, the supernatants were transferred to clean 96-well plates. The sample mixtures were analyzed by LC-MS/MS.

The LC-MS/MS system consisted of a Thermo Scientific LX2 autosampler equipped with two Transcend System pumps and an Applied Biosystems/MSD Sciex API 5000 mass spectrometer. Chromatographic separation of the analytes was achieved on a Waters Acquity HSS T3 column (2.1 x 50 mm, 1.8 μ m particle size) in conjunction with gradient conditions and mobile phases A (0.1% formic acid in water) and B (0.1% formic acid in acetonitrile). Total run time was 3.5 minutes. Mass spectrometric detection of the analytes was accomplished using the Turbo Spray interface operated in the negative ion mode. Analyte response was measured by multiple reaction monitoring (MRM) of transitions unique to each compound.

4.2.2.6. Pharmacokinetic Analysis

Data were acquired and integrated by Sciex Analyst 1.5.1 software. Data were processed using Thermo Electron Corporation Watson v7.3. Peak area ratios of analyte to IS were plotted as a function of the nominal concentrations of the analyte. A line of best fit was generated from the curve points using linear regression type. The equation of this line was used to calculate the concentrations in all samples.

The area under the plasma concentration versus time curve (AUC) was determined using the Watson software (version 7.3). Toxicokinetic calculation method was performed and C_{\max} , T_{\max} , and AUC were reported. Statistical comparisons were

performed by independent Student's *t* test ($\alpha=0.05$). All statistical analysis was performed using SigmaPlot Statistics for Windows version 10.0.

4.3. Results and Discussion

4.3.1. Supersaturation Screening

In order to monitor the degree and duration of supersaturation of ibuprofen in the presence of polymers without the variable of polymer dissolution kinetics, the kinetic solubility profile of ibuprofen sodium was evaluated in the presence of pre-dissolved polymers at a 1:1 weight ratio of drug: polymer. The high polymer loading was selected in order to maximize the potential polymer effect on supersaturation and potentially differentiate among drug:polymer combinations at a fixed ratio. The dissolution profile of the active pharmaceutical ingredient (API) in the absence of polymer was also evaluated under the same conditions in order to differentiate the behavior of ibuprofen sodium disproportionation in SGF from supersaturation influenced by polymer. In the presence of pre-dissolved polymers in SGF (Figure 4.1), prolonged supersaturation was observed for 20 minutes with MC, 60 minutes with HPMC and HPC-SL, and >120 minutes with PVP-VA64 and HPC. In addition, an increase in solubility was observed and maintained for 120 minutes with HPMCAS-HF and Soluplus.

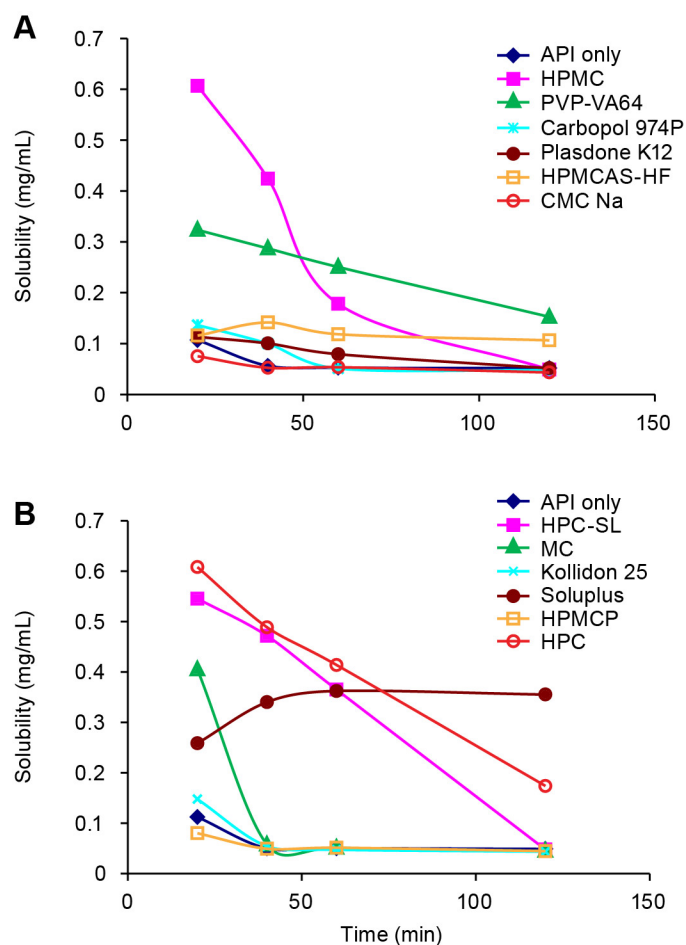


Figure 4.1. Dissolution profiles of 1:1 ibuprofen sodium: pre-dissolved polymer in SGF at 37 °C during supersaturation screen.

Table 4.1 summarizes the degree of ibuprofen supersaturation achieved with pre-dissolved polymers in SGF relative to equilibrium solubility of the same system as well as the duration of supersaturation. The degree of supersaturation was calculated by dividing the maximum measured concentration of drug in solution during dissolution by its equilibrium solubility determined following 24 hours in the system of interest. The duration of supersaturation was the amount of time that the measured concentration of drug in solution remained above the equilibrium solubility of that system.

Table 4.1. Influence of various polymers on maximum degree of supersaturation of ibuprofen following dissolution of ibuprofen sodium in the presence of pre-dissolved polymer in SGF at 37° C.

Polymer	Degree of Supersaturation	Duration of Supersaturation (minutes)
API only	2.4	20
HPMC	18.5	60
PVP-VA64	8.0	>120
Carbopol 974P	5.0	20
Plasdone K12	2.2	20
HPMCAS-HF	1.7	>120
CMC Na	1.5	-
HPC-SL	12.6	60
MC	11.2	20
Kollidon 25	3.0	20
Soluplus	1.4	>120
HPMCP	1.4	-
HPC	12.7	>120

In SGF, the highest degree of supersaturation was observed in the presence of HPMC, HPC, and MC while lower degrees of supersaturation were achieved with PVP-VA64. In general, higher degrees of supersaturation were associated with shorter durations of supersaturation. This was expected based on the greater thermodynamic drive toward precipitation at higher supersaturation values. Since equilibration to the crystalline free acid required nucleation and crystal growth, loss of supersaturation could be related to classical nucleation theory. In general, the difference in chemical potential of a supersaturated solution versus a saturated solution is the driver for crystallization of the thermodynamically stable crystalline phase. In other words, the driving force for nucleation is dependent on the maximum feasible degree of supersaturation that can be achieved in a system (11-13). Alternatively, the PVP-VA64 copolymer system that enabled a more moderate degree of supersaturation was also associated with a prolonged

duration of supersaturation compared to the other systems, suggesting an extended delay in nucleation and/or crystal growth.

Although supersaturation was observed with the PVP-VA64 copolymer, the two evaluated grades of PVP (Plasdone K12 and Kollidon 25) did not enable any supersaturation of ibuprofen. The average molecular weights of PVP-VA64, Kollidon 25, and Plasdone K12 varied from 45000-70000, 28000-34000, and 4000 g/mol, respectively. Although the molecular weight of PVP-VA64 was significantly greater than Kollidon 25, the vinyl pyrrolidone portion of PVP-VA64 accounted for approximately 64% of the mass. Therefore, the average molecular weight attributed to PVP did not differ significantly between PVP-VA64 and Kollidon 25. Likewise, no significant increase in media viscosity was observed when these vinyl pyrrolidone-containing polymers were solubilized in SGF at the 1 mg/mL polymer concentration used in the supersaturation screen. Therefore, the primary difference between PVP-VA64 and PVP was the inclusion of vinyl acetate to the copolymer chain of PVP-VA64, suggesting that the vinyl acetate moiety was contributing to the mechanism of ibuprofen supersaturation in the presence of PVP-VA64.

There were also several polymers that did not have sufficient solubility for complete dissolution at the target polymer concentration of 1 mg/mL and remained as suspensions, including the carbomer polymer (Carbopol 974) and the enteric polymers (HPMCAS-HF and HPMCP). Due to the lack of gastric solubility of these polymers, they were suboptimal candidates to enable large degrees of supersaturation under acidic conditions as exemplified by the lack of supersaturation observed with Carbopol 974 and HPMCP. In the presence of HPMCAS-HF, a modest two-fold increase in degree of

supersaturation was achieved and maintained for the duration of the 120 minute dissolution experiment. The ability of HPMCAS to delay crystal growth was hypothesized as the mechanism of supersaturation for this drug-polymer system. Following loss of supersaturation, observations of irregular particle morphology of ibuprofen crystals and amorphous HPMCAS polymer clustered around the crystals were made by optical microscopy (Figure 4.2). The different ibuprofen free acid crystal morphologies following precipitation in the presence and absence of HPMCAS suggested that adsorption of polymer to the free acid crystal surfaces during precipitation could be modifying the crystal habit and playing a role in delayed crystal growth. Similar observations of crystal habit modification due to varying adsorption of HPMC onto the crystalline faces of hydrocortisone acetate during loss of supersaturation have been reported (14).

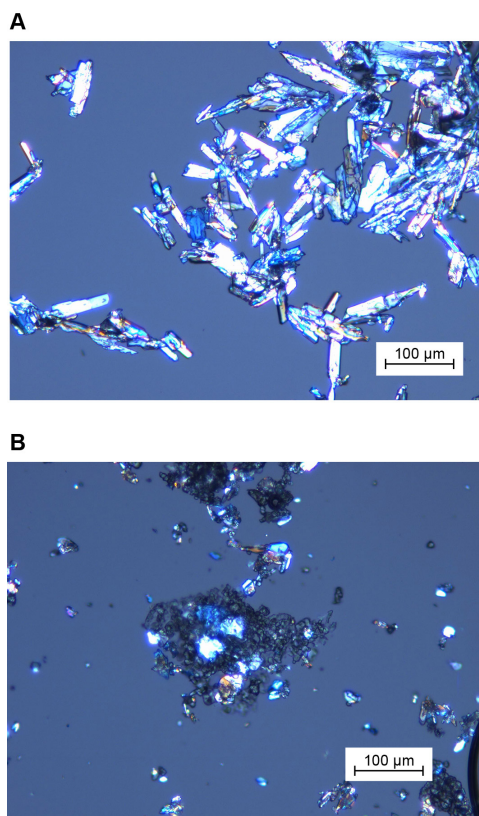


Figure 4.2. Microscopy following dissolution of ibuprofen sodium in SGF (a) without polymer or (b) with HPMCAS-HF at 100x magnification.

The final polymer system that exhibited solubility enhancement in the supersaturation screen relative to the API-only control was Soluplus. However, it was noteworthy that the solubility of drug in solution increased over time rather than decreased to indicate a loss of supersaturation (Figure 4.1b) and no significant degree of supersaturation was observed relative to the equilibrium solubility of the system at 24 hours (Table 4.1). In the case of Soluplus, the increased solubilization of ibuprofen is likely associated with an increase in equilibrium solubility of ibuprofen free acid rather than an actual increase in supersaturation (Table 4.2).

Table 4.2 summarizes the 24 hour solubility data for ibuprofen with and without polymers in SGF. Since the SGF solubility of ibuprofen in the presence of a specific polymer was measured at ~0.04-0.05 mg/mL for both the free acid and the sodium salt, it

was concluded that the ibuprofen sodium salt reached equilibrium as the free acid within the 24 hour time period that was evaluated. Conversion of ibuprofen sodium salt to the free acid in SGF was also confirmed by XRPD (data not shown). Therefore, the solubility of ibuprofen slurried with the various polymers was compared to the control samples without polymer to determine whether any polymers significantly increased the equilibrium solubility of the free acid at the 24 hour time point.

Table 4.2. Influence of various polymers on solubility of ibuprofen following equilibration in SGF containing 1 mg/mL polymer at 37 °C.

Polymer	Ibuprofen Sodium Salt		Ibuprofen Free Acid	
	Solubility at 24 Hours (mg/mL \pm SD)	Final pH of Media	Solubility at 24 Hours (mg/mL \pm SD)	Final pH of Media
API only	0.046 \pm 0.002	2.02	0.047 \pm 0.000	1.82
HPMC	0.033 \pm 0.001	1.86	0.043 \pm 0.005	1.80
PVP-VA64	0.040 \pm 0.002	2.10	0.043 \pm 0.005	1.76
Carbopol 974P	0.027 \pm 0.006	1.89	0.036 \pm 0.004	1.76
Plasdone K12	0.051 \pm 0.004	2.13	0.049 \pm 0.001	1.72
HPMCAS-HF	0.069 \pm 0.039	1.78	0.045 \pm 0.001	1.75
CMC Na	0.049 \pm 0.002	2.14	0.042 \pm 0.012	1.81
HPC-SL	0.043 \pm 0.001	2.20	0.048 \pm 0.001	1.85
MC	0.036 \pm 0.001	2.10	0.047 \pm 0.001	1.82
Kollidon 25	0.050 \pm 0.005	2.13	0.049 \pm 0.002	1.85
Soluplus	0.185 \pm 0.048	2.17	0.206 \pm 0.139	1.81
HPMCP	0.057 \pm 0.006	2.13	0.054 \pm 0.003	1.83
HPC	0.048 \pm 0.004	2.19	0.051 \pm 0.003	1.84

No appreciable increase in solubility was observed in SGF after 24 hours in the presence of any polymer, except Soluplus. Since the solubility of ibuprofen free acid in the presence of Soluplus was in the same region as the ibuprofen sodium salt slurry with Soluplus, it was not believed that ibuprofen sodium was stabilized in this Soluplus system. Therefore the prolonged dissolution profile of ibuprofen in the presence of Soluplus (Figure 4.1b) was associated with ibuprofen free acid reaching a thermodynamically more soluble state rather than maintaining prolonged supersaturation.

This increase in equilibrium solubility is likely due to the polyethylene glycol moiety incorporated into the Soluplus copolymer graft.

4.3.2. Two-Stage Dissolution

Based on the supersaturation screen, polymers that were shown to increase degree and duration of ibuprofen supersaturation following the addition of the ibuprofen sodium salt to SGF were further evaluated by running a biorelevant two-stage dissolution experiment. The polymers evaluated in this experiment included HPMC, PVP-VA64, MC, and HPC. Although HPC-SL also demonstrated an increase in degree and duration of supersaturation, this polymer grade only differed from the other HPC polymer in terms of viscosity. Since increased viscosity can be a contributing factor to enable supersaturation (3), only the higher viscosity grade of HPC was included in the two-stage dissolution studies. In addition, the Soluplus polymer that enhanced intrinsic solubility of ibuprofen was also included in the two-stage dissolution screen. Although an increase in solubilization of ibuprofen was observed in the presence of HPMCAS-HF during the two hour supersaturation screen, the enteric properties of this polymer make it an undesirable candidate to study supersaturation for an immediate release formulation.

During the two-stage dissolution experiment, dissolution of solid blends of ibuprofen sodium with polymer at a one-to-one weight ratio were compared to the dissolution profiles of ibuprofen sodium or ibuprofen free acid alone. Solid blends were selected for this experiment in order to factor in the need for polymer dissolution under biorelevant conditions using formulation compositions that would be similar to those used in *in vivo* studies. The first stage of the dissolution experiment included the addition of solid blends or API only to SGF. The addition of 250 mg ibuprofen (free acid

equivalents) to 250 mL of SGF corresponded to a theoretical 1 mg/mL concentration of ibuprofen in the acid phase, which represented a 20-fold level of supersaturation assuming an equilibrium solubility of 0.047 mg/mL in SGF (Table 4.2). These conditions were intended to differentiate formulations in terms of supersaturation performance. Following 1 hour under acidic conditions, the media was adjusted to pH 6.8 with the addition of 250 mL of phosphate buffer to emulate transition to the intestine where complete dissolution of the drug was anticipated based on previously published solubility data for ibuprofen (10).

Dissolution of ibuprofen in the presence and absence of polymers during the acid stage is illustrated in Figure 4.3. When comparing the dissolution of free acid to sodium salt, a more rapid rate of dissolution was associated with the higher solubility sodium salt form. The initial solubility at the 5 minute time point was 0.16 mg/mL, which is 3.2-fold higher than the equilibrium solubility of ibuprofen. The solubility of the sodium salt slowly decreased toward equilibrium over the 1 hour time-course for SGF dissolution likely due to disproportionation and precipitation of the free acid. Alternatively, the free acid exhibited significantly slower initial dissolution kinetics and did not approach the equilibrium solubility of 0.047 mg/mL until the 60 minute time point.

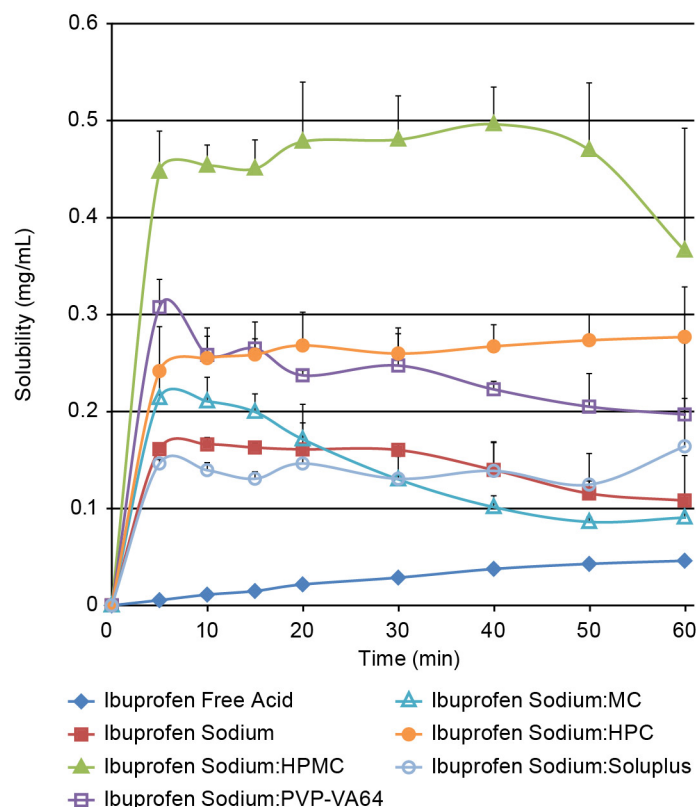


Figure 4.3. Dissolution of ibuprofen free acid and ibuprofen sodium salt with the presence or absence of polymer in SGF at 37 °C.

In the presence of the various polymers, the dissolution of the sodium salt exhibited varying behaviors. The dissolution of ibuprofen sodium in the presence of Soluplus was similar to the dissolution profile of the sodium salt without polymer. Although an increase in equilibrium solubility of ibuprofen was observed in the presence of Soluplus (Table 4.2) and solubility enhancement was initially observed at the 20 minute time-point during the supersaturation screen with pre-dissolved polymer (Figure 4.1b), the slow rate of dissolution associated with the large granules of Soluplus prevented the polymer from providing significant solubility enhancement during this one hour SGF dissolution experiment since full dissolution of Soluplus had not occurred within that period of time. Likewise, the slow dissolution kinetics observed with MC was believed to limit the degree of supersaturation of ibuprofen observed during this acid

stage of the two-stage dissolution experiment. In other words, not enough polymer dissolved to provide maximum supersaturation behavior prior to ibuprofen free acid crystallization. Although a 4-fold increase in degree of supersaturation was observed with ibuprofen sodium in the presence of MC at the 5 minute time-point, loss of supersaturation relative to the sodium salt alone was observed within 20 minutes. This short duration of supersaturation also trended with data obtained from the high-throughput supersaturation screen (Figure 4.1b); however a significantly higher degree of supersaturation was observed with MC during the initial supersaturation screen where polymer was pre-dissolved.

A 4 to 6-fold increase in degree of supersaturation was observed and maintained for the duration of the 1 hour dissolution experiment in SGF when ibuprofen sodium was in the presence of HPC or PVP-VA64. A 9-fold increase in degree of supersaturation was observed when ibuprofen sodium was in the presence of HPMC with loss of supersaturation beginning at 60 minutes. Overall, there was good correlation observed between the acid stage of the dissolution experiment, where blends of ibuprofen sodium with polymer were used, and the supersaturation screening results, where pre-dissolved polymers were evaluated.

Within 30 minutes following pH adjustment to pH 6.8, >85% of ibuprofen dissolution was observed for all formulations, except for the formulation containing MC (Figure 4.4). Therefore, formulations containing ibuprofen alone or with HPMC, HPC, PVP-VA64, or Soluplus met the criteria for an immediate release formulation containing ibuprofen (10). For the ibuprofen sodium:MC formulation, 2 hours of stirring at 50 rpm was required for 85% dissolution of ibuprofen. During the 2 hour dissolution experiment,

visual observations of slow MC wetting and lack of uniform dispersion within the vessel was noted. This suggested that the delayed dissolution of ibuprofen from the MC blends was related to slow MC dissolution. The delayed dissolution of ibuprofen was likely attributed to the low solubility and high viscosity associated with the selected grade of 400 cPs MC. Any ibuprofen from the drug:polymer blend that did not disperse and dissolve prior to initial swelling of the MC polymer was likely trapped in the MC agglomerates. This drug entrapment and the associated slow wetting of MC can explain why ibuprofen exhibited a delayed release profile during this dissolution experiment. Modified drug release due to slow erosion of cellulosic polymers has been previously described (15). In order to more rapidly dissolve the polymer, a lower viscosity grade of MC or an increase in the paddle speed should be considered.

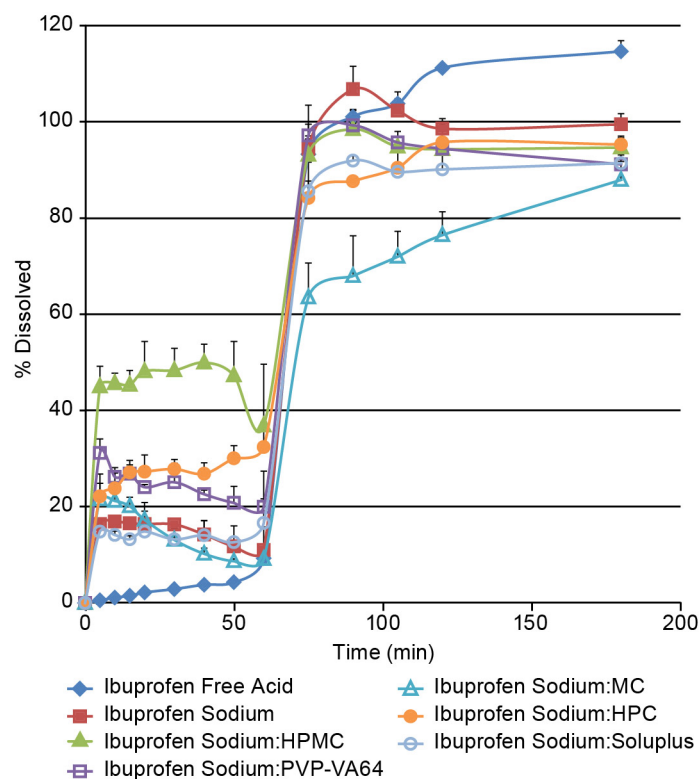


Figure 4.4. Two-stage dissolution profile of ibuprofen with the presence or absence of polymer in SGF for 60 minutes followed by pH adjustment to pH 6.8 at 37 °C.

4.3.3. *In vivo* Studies

In vivo studies were conducted in Wistar Han rats to evaluate the influence of various polymers on the pharmacokinetic parameters of ibuprofen. Each of the polymers evaluated in the two-stage dissolution experiments, including HPMC, PVP-VA64, HPC, MC, and Soluplus, were blended in a 1:1 ratio with ibuprofen sodium and filled into gelatin capsules for oral administration. Size 9 hard gelatin capsules were selected because of their suitability for oral gavage to rats and their rapid disintegration profile, as per the manufacturer's specifications, which would enable drug and polymer to quickly initiate their dissolution in the stomach so that the impact of formulation on C_{\max} and T_{\max} could be observed. The use of capsules also eliminated the potential for suspension inhomogeneity and provided a direct translation to the previously conducted two-stage biorelevant dissolution experiments where solid blends were evaluated. In addition to the drug and polymer formulations, ibuprofen sodium and ibuprofen free acid alone were also dosed for comparison. A dose of 25 mpk (ibuprofen free acid equivalent) was selected based on previous work by Newa et al. which suggested that there are opportunities to detect changes to the pharmacokinetic profile of ibuprofen at this dose since absorption did not seem to be maximized at this dose with a conventional ibuprofen free acid formulation (16).

The average plasma concentrations of various formulations of ibuprofen following oral administration to rats were compared in Figure 4.5 below, with more details found in Figure 4.6. Overall, a delay in the initial onset of absorption was observed with the ibuprofen free acid profile in comparison to all formulations containing ibuprofen sodium. Minimal plasma exposure was observed with the 15 minute time point

for the free acid formulation while all other formulations containing the sodium salt of ibuprofen have significantly higher ibuprofen plasma concentrations at the same time point. In addition, the T_{\max} for ibuprofen free acid was significantly delayed relative to the ibuprofen sodium-containing formulations. Upon initial assessment, a higher C_{\max} was also achieved with some polymer-containing formulations which suggested that these polymers were successfully prolonging supersaturation *in vivo* when compared to the ibuprofen sodium formulation alone. These observations also correlated with the two-stage dissolution experiments, where a significant delay in dissolution of neat ibuprofen free acid is observed relative to the ibuprofen sodium-containing formulations under SGF conditions (Figure 4.3).

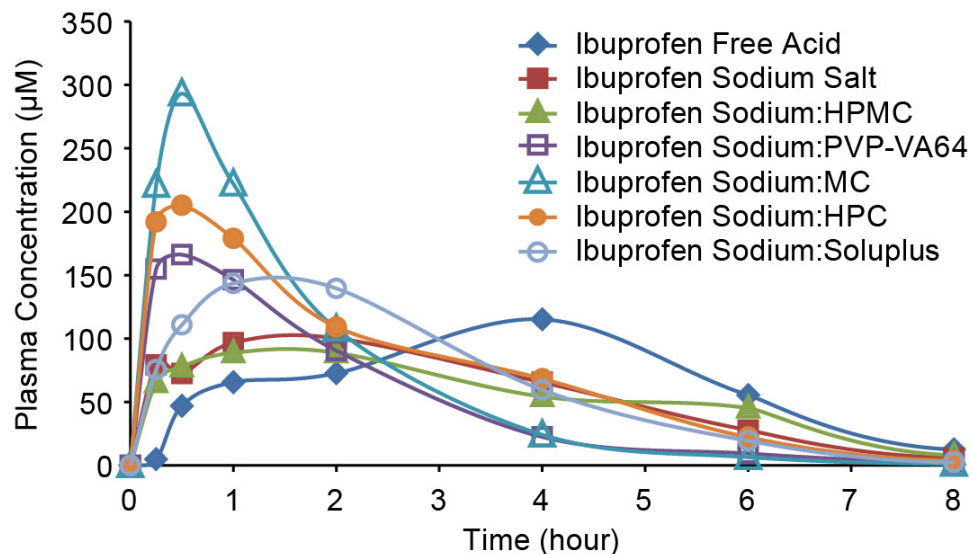


Figure 4.5. Mean plasma concentration of ibuprofen following oral administration in Wistar Han rats (n=6) under fasted conditions at a dose of 25 mpk. Ibuprofen free acid (◆), ibuprofen sodium salt (■), 1:1 ibuprofen sodium:HPMC (▲), 1:1 ibuprofen sodium:PVP-VA64 (□), 1:1 ibuprofen sodium:MC (△), 1:1 ibuprofen sodium:HPC (●), and 1:1 ibuprofen sodium:Soluplus (○).

A head-to-head comparison of ibuprofen sodium to free acid (Figure 4.6a) showed that the higher solubility salt form had an initially faster rate of absorption when compared to the free acid. However, the ibuprofen sodium profile exhibited a trend

toward a decrease in plasma concentration with the 30 minute time point in comparison to the 15 minute time point. Since complete gastric emptying from the stomach of a fasted rat takes 1 hour (17, 18), this decrease in plasma concentration corresponded to an anticipated phase change of the sodium salt to the free acid during transit through the stomach. The need for re-dissolution of the free acid may explain why the T_{\max} of ibuprofen sodium did not differ significantly from the T_{\max} of the free acid formulation (Table 4.3).

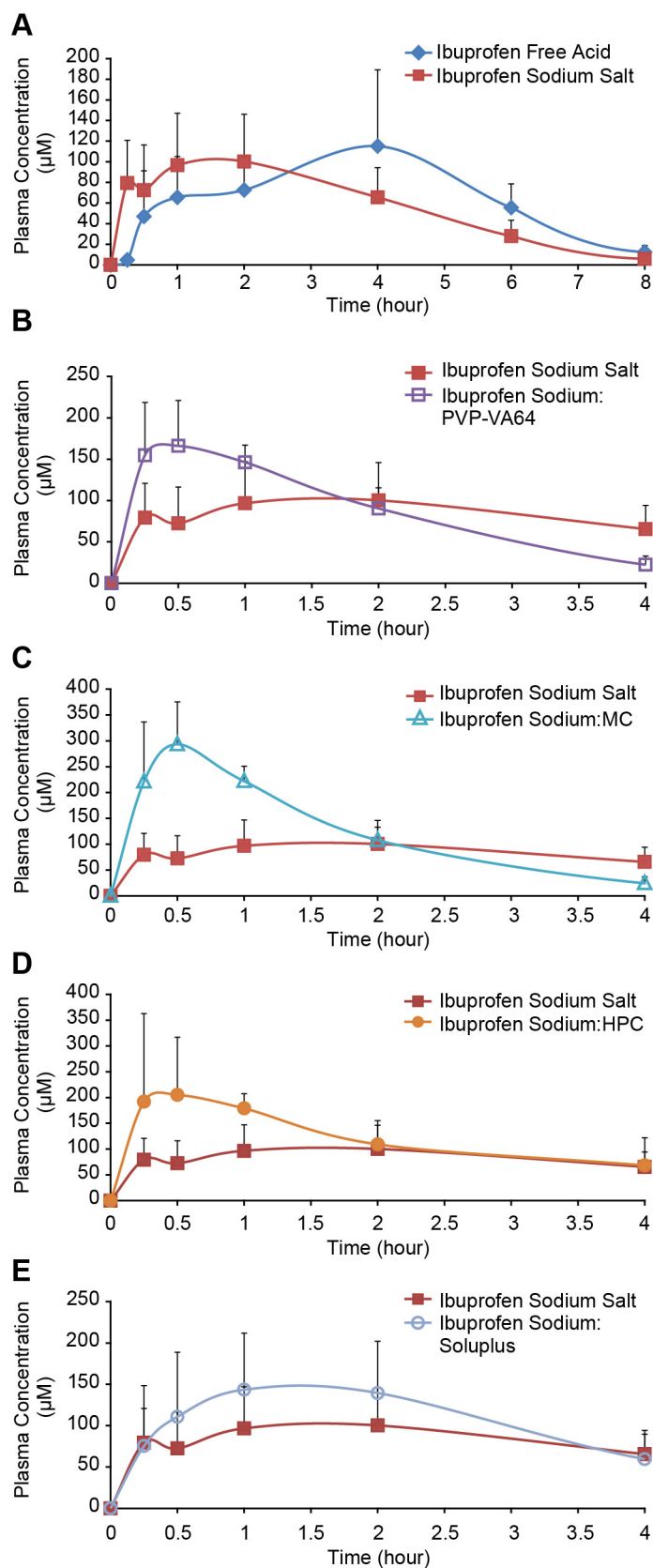


Figure 4.6. Mean (\pm SD) plasma concentration of ibuprofen following oral administration in Wistar Han rats (n=6) under fasted conditions at a dose of 25 mpk. Figures compare the ibuprofen sodium salt (■) profile to (a) ibuprofen free acid (◆), (b) 1:1 ibuprofen sodium:PVP-VA64 (□), (c) 1:1 ibuprofen sodium:MC (△), (d) 1:1 ibuprofen sodium:HPC (●), and (e) 1:1 ibuprofen sodium:Soluplus (○).

When comparing the pharmacokinetic parameters of ibuprofen in various polymer-containing formulations to the control ibuprofen sodium and ibuprofen free acid formulations, significant differences in C_{\max} and T_{\max} were observed (Table 4.3). In general, statistically significant increases in C_{\max} were observed with the PVP-VA64, MC, HPC, and Soluplus formulations along with significant decreases in T_{\max} when compared to the sodium salt control formulation. Alternatively, no significant changes in AUC were observed with any systems, except when comparing the AUC of ibuprofen free acid to the formulation of ibuprofen sodium:PVP-VA64. Due to the absence of intravenous PK data, it is difficult to determine whether maximum bioavailability was already attained with the ibuprofen free acid formulation which could explain the lack of changes in AUC among formulations.

Table 4.3. Ibuprofen pharmacokinetic parameters following oral administration to Wistar Han rats at a dose of 25 mpk.

Formulation	AUC _{0-24h} ($\mu\text{M}\cdot\text{h}$)	C _{max} (μM)	T _{max} (h)
Ibuprofen Free Acid	541 \pm 132	136.2 \pm 61.1	2.6 \pm 1.6
Ibuprofen Sodium	450 \pm 76	130.6 \pm 25.2	1.6 \pm 1.4
1:1 Ibuprofen Sodium:HPMC	434 \pm 91	115.3 \pm 36.4	2.6 \pm 2.1
1:1 Ibuprofen Sodium:PVP-VA64	377 \pm 31*	197.3 \pm 50.5†	0.50 \pm 0.27*
1:1 Ibuprofen Sodium:MC	491 \pm 88	301.0 \pm 79.0*†	0.63 \pm 0.31*
1:1 Ibuprofen Sodium:HPC	556 \pm 117	252.9 \pm 115.2†	0.58 \pm 0.34*
1:1 Ibuprofen Sodium:Soluplus	497 \pm 94	199.8 \pm 43.1†	1.4 \pm 0.7*

(*) significant difference ($P < 0.05$) compared to free acid

(†) significant difference ($P < 0.05$) compared to sodium salt

The inclusion of polymers in the ibuprofen sodium formulations contributed to changes in the PK profiles relative to the sodium salt alone for several systems. Increases in the C_{max} were observed in the presence of PVP-VA64 (Figure 4.6b), MC (Figure 4.6c), and HPC (Figure 4.6d) when compared to ibuprofen sodium alone. In addition, these formulations also had an average T_{max} of 0.5-0.6 hours which is significantly shorter than the ibuprofen free acid formulation (Table 4.3). The early boost in ibuprofen plasma exposure following oral administration was believed to be directly linked to the ability of the polymer to prolong supersaturation under gastric conditions following rapid dissolution of ibuprofen sodium, as demonstrated in the *in vitro* dissolution studies. This *in vivo* profile also correlated with the *in vitro* dissolution profiles previously described in Figure 4.3. A comparison of degree of supersaturation achieved during SGF dissolution of ibuprofen sodium-polymer blends to *in vivo* T_{max} values in Table 4.4 highlights the correlation between supersaturation and faster oral absorption in the presence of PVP-VA64, MC, and HPC.

Table 4.4. Comparison of degree of ibuprofen supersaturation achieved during SGF dissolution of solid drug-polymer blends to pharmacokinetic parameters following oral administration to Wistar Han rats at a dose of 25 mpk.

Formulation	Degree of Supersaturation	T _{max} (h)
Ibuprofen Free Acid	-	2.6 ± 1.6
Ibuprofen Sodium	3.5	1.6 ± 1.4
1:1 Ibuprofen Sodium:HPMC	13.5	2.6 ± 2.1
1:1 Ibuprofen Sodium:PVP-VA64	7.7	0.50 ± 0.27*
1:1 Ibuprofen Sodium:MC	5.9	0.63 ± 0.31*
1:1 Ibuprofen Sodium:HPC	5.4	0.58 ± 0.34*
1:1 Ibuprofen Sodium:Soluplus	0.8	1.4 ± 0.7*

(*) significant difference ($P < 0.05$) compared to free acid

The Soluplus formulation had a significantly higher C_{max} compared to ibuprofen sodium (Table 4.3); however the broad range for the T_{max} of this formulation made this difference more difficult to observe in Figure 4.6e. The increase in C_{max} and earlier T_{max} relative to the ibuprofen free acid formulation was driven by the ability of Soluplus to increase the intrinsic solubility of ibuprofen; however the slow rate of polymer dissolution minimized the ability of Soluplus to have a significant impact on the AUC of this formulation in comparison to the ibuprofen control arms during the time course for absorption. This observation correlated with the two-stage *in vitro* dissolution profile where no significant differentiation between ibuprofen sodium with and without Soluplus was noted (Figure 4.3).

Although a correlation between supersaturation in SGF and early absorption *in vivo* was noted for the PVP-VA64, MC, and HPC formulations, this was not the case for the ibuprofen sodium:HPMC formulation (Table 4.4). No significant difference in the ibuprofen PK profile with the inclusion of HPMC was noted in comparison to ibuprofen sodium alone. This suggested that the presence of the polymer was not affording any supersaturation in the stomach following oral administration to rats. This was contrary to

the *in vitro* dissolution screen in which the presence of HPMC afforded the highest degree of supersaturation for the one hour acid stage of the experiment relative to the other polymers evaluated in this experiment (Figure 4.3). A possible explanation may be that HPMC was enabling supersaturation via a mechanism that was different than the mechanism(s) that were driving supersaturation of ibuprofen in the presence of PVP-VA64, HPC or MC, which may explain the deviation between the *in vitro* and *in vivo* data with this specific formulation. Efforts are ongoing to elucidate the mechanism by which each of these polymers is prolonging supersaturation during *in vitro* dissolution.

4.4. Conclusions

Combining ibuprofen sodium with various pharmaceutically acceptable polymers alone resulted in the identification of several drug-polymer combinations that demonstrated high degrees and extended durations of supersaturation during *in vitro* dissolution experiments under conditions where the highly soluble ibuprofen sodium salt converted to a poorly soluble free acid phase. These formulations included HPMC, PVP-VA64, MC, and HPC. These observations differ significantly from previous work that required the inclusion of surfactant to the salt-polymer formulation to enable supersaturation (6). It is likely that the surfactant-like properties of ibuprofen sodium eliminate the need for addition of surfactant to the formulation to enable supersaturation. This finding results in the feasibility of developing of a more simplistic formulation to achieve desirable supersaturation profiles.

The *in vitro* supersaturation observed with these polymer-ibuprofen formulations translated to an increase in C_{\max} of ibuprofen plasma concentrations relative to ibuprofen

sodium without polymer and a decrease in T_{\max} relative to ibuprofen free acid without polymer for the PVP-VA64, MC, and HPC formulations. Based on these observations, a combination of an appropriate polymer with a salt form of an acidic drug may be a viable formulation approach to prolong supersaturation in the stomach and enable increased C_{\max} and earlier T_{\max} *in vivo* where rapid onset of action is desired for the pharmacokinetic profile of a drug.

4.6. References

1. S.M. Berge, L.D. Bighley, and D.C. Monkhouse. Pharmaceutical salts. J Pharm Sci. 66:1-19 (1977).
2. A. Serajuddin. Salt formation to improve drug solubility. Adv Drug Del Rev. 59:603-616 (2007).
3. D.B. Warren, H. Benameur, C.J.H. Porter, and C.W. Pouton. Using polymeric precipitation inhibitors to improve the absorption of poorly water-soluble drugs: A mechanistic basis for utility. J Drug Targeting:1-28 (2010).
4. S. Xu and W.-G. Dai. Drug Precipitation Inhibitors in Supersaturable Formulations. International journal of pharmaceutics. 453:36-43 (2013).
5. P. Gao and Y. Shi. Characterization of supersaturable formulations for improved absorption of poorly soluble drugs. The AAPS Journal. 14:703-713 (2012).
6. H.R. Guzmán, M. Tawa, Z. Zhang, P. Ratanabanangkoon, P. Shaw, C.R. Gardner, H. Chen, J.P. Moreau, Ö. Almarsson, and J.F. Remenar. Combined use of crystalline salt forms and precipitation inhibitors to improve oral absorption of celecoxib from solid oral formulations. J Pharm Sci. 96:2686-2702 (2007).
7. A.H. Kibbe. Handbook of pharmaceutical excipients, Pharmaceutical Press, London, UK, 2000.
8. A. Ridell, H. Evertsson, S. Nilsson, and L.O. Sundelöf. Amphiphilic association of ibuprofen and two nonionic cellulose derivatives in aqueous solution. J Pharm Sci. 88:1175-1181 (1999).
9. K. Rainsford. Ibuprofen: pharmacology, efficacy and safety. Inflammopharmacology. 17:275-342 (2009).
10. H. Potthast, J.B. Dressman, H.E. Junginger, K.K. Midha, H. Oeser, V.P. Shah, H. Vogelpoel, and D.M. Barends. Biowaiver monographs for immediate release solid oral dosage forms: Ibuprofen. J Pharm Sci. 94:2121-2131 (2005).
11. J. Brouwers, M.E. Brewster, and P. Augustijns. Supersaturating drug delivery systems: The answer to solubility limited oral bioavailability? J Pharm Sci. 98:2549-2572 (2009).

12. D. Kashchiev and G.M. Van Rosmalen. Review: Nucleation in solutions revisited. *Cryst Res Tech.* 38:555-574 (2003).
13. N. Rodríguez-Hornedo and D. Murphy. Significance of controlling crystallization mechanisms and kinetics in pharmaceutical systems. *J Pharm Sci.* 88:651-660 (1999).
14. S. Raghavan, A. Trividic, A. Davis, and J. Hadgraft. Crystallization of hydrocortisone acetate: influence of polymers. *Int J Pharm.* 212:213-221 (2001).
15. K.K. Jain, S.B. Tiwari, and A.R. Rajabi-Siahboomi. Extended-Release Oral Drug Delivery Technologies: Monolithic Matrix Systems. *Drug Delivery Syst*, Vol. 437, Humana Press, 2008, pp. 217-243.
16. M. Newa, K.H. Bhandari, D.X. Lee, J.H. Sung, J.A. Kim, B.K. Yoo, J.S. Woo, H.G. Choi, and C.S. Yong. Enhanced Dissolution of Ibuprofen Using Solid Dispersion with Polyethylene Glycol 20000. *Drug Dev Ind Pharm.* 34:1013-1021 (2008).
17. S. Haruta, K. Kawai, S. Jinnouchi, K.i. Ogawara, K. Higaki, S. Tamura, K. Arimori, and T. Kimura. Evaluation of absorption kinetics of orally administered theophylline in rats based on gastrointestinal transit monitoring by gamma scintigraphy. *J Pharm Sci.* 90:464-473 (2001).
18. C. Scarpignato, M.G. Girone, F. Tirelli, and G. Bertaccini. Inhibition of gastric emptying and secretion by pirenzepine and atropine in rats. *Eur J Pharm Sci.* 101:193-200 (1984).

CHAPTER 5

Combining Ibuprofen Sodium with Cellulosic Polymers: Assessing Impact of Hydrogen Bonding Potential on Degree and Duration of Supersaturation

Submitted for publication to International Journal of Pharmaceutics as: “Combining Ibuprofen Sodium with Cellulosic Polymers: A Deep Dive into Mechanisms of Prolonged Supersaturation”

Jenna L. Terebetski and Bozena Michniak-Kohn

5.1. Introduction

Development of formulations that achieve supersaturation during gastrointestinal transit are a promising approach to enhance the oral absorption of poorly water soluble drugs. Supersaturation occurs when the concentration of drug in solution is above the equilibrium solubility of the thermodynamically stable crystal phase (1, 2). In order to achieve supersaturation, a phase that has increased dissolution or enhanced solubility above the thermodynamically stable form in the gastrointestinal tract is either administered or formed *in vivo*. Examples of rapidly dissolving solid forms that may achieve high intraluminal concentrations include amorphous compounds or crystalline salts that undergo disproportionation in the gastrointestinal tract (3). However, since thermodynamics will drive these phases to the most stable and often least soluble form, the extent of supersaturation associated with phases that are not thermodynamically stable in the local environment may be insufficient to substantially enhance oral exposure unless formulation optimization is conducted to stabilize the supersaturated phase (4).

Significant progress in delaying loss of supersaturation for a metastable amorphous material has been made with the development of stabilized amorphous formulations. In this scenario, the solubility enhancement provided by the amorphous form can be prolonged for extended periods of time through interactions with excipients (5-7). This type of behavior has been referred to as the “parachute effect” (8) and has been shown to translate to improved exposure *in vivo*. For example, a solid dispersion formulation of tacrolimus with HPMC demonstrates prolonged supersaturation *in vitro*. This formulation has also been shown to increase AUC and C_{\max} relative to crystalline tacrolimus when administered orally to dogs (9). The parachute effect, or precipitation inhibition, is a result of excipients interfering in nucleation and/or crystal growth stages of the more stable phase (3). This type of behavior is due to physical or chemical interactions that take place between the drug and excipient which can be influenced by pH, temperature, molecular weight of excipients, viscosity, and the potential for hydrogen bonding (10).

In general, stabilized amorphous systems have a number of potential formulation limitations when compared to equivalent formulations of crystalline material, including increased risk of chemical and physical instability during storage as well as large-scale manufacturing challenges (11). Therefore it is desirable to investigate alternative systems that can achieve supersaturation following oral administration, such as salts. Since salts are stable solid phases that can be included in preclinical and clinical formulations for drug candidates with poor solubility, it is desirable to try to leverage a salt with a favorable pH solubility profile and attempt to sustain supersaturation following oral administration. Although a pharmaceutical salt typically provides solubility enhancement

relative to the free form, salt disproportionation can occur during oral administration if the pKa of an ionizable drug is close to the physiological pH conditions encountered during gastrointestinal (GI) transit (12). Therefore, the solubility enhancement afforded by the salt may be lost, resulting in decreased drug in solution and uncontrolled precipitation of the free form. This behavior could contribute to a reduction in exposure and to an increase in subject-to-subject variability.

Identifying excipients that can prolong the supersaturation initially achieved by a disproportionating salt through precipitation inhibition is a key mitigation plan to maintain solubility enhancement provided by a salt and delay precipitation of the lower solubility free form following disproportionation during GI transit. Guzmán *et al.* have demonstrated that specific combinations of crystalline salt forms of celecoxib with polymers and surfactants can provide both enhanced dissolution and high oral bioavailability (8); however a mechanistic understanding into how these excipients are interacting with celecoxib was not pursued. Depending on the drug-excipient combinations, it is anticipated that a variety of mechanisms could contribute to the prolonged supersaturation.

A significant amount of excipient research has led to the successful development of formulations that delay salt disproportionation during dissolution through the physical modulation of microenvironmental pH at the diffusion boundary layer (13). However, additional efforts to identify systems of salts and polymers that exhibit prolonged supersaturation via chemical interactions following dissolution are, to the authors' knowledge, currently lacking in the literature and are the main focus for this article. Since polymers have variable impact on precipitation inhibition, this work evaluated several

polymers including HPMC, MC and HPC. HPMC has been classified as a broad-spectrum precipitation inhibitor for a variety of drugs (10). Although HPMC has been shown to stabilize supersaturation via a variety of mechanisms, such as increasing aqueous solubility (7, 14), it is the hydrogen bonding potential of HPMC (15, 16) that offers the greatest prospect for inducing a chemical interaction during dissolution of an acidic salt.

The present study investigated the role of HPMC in the supersaturation of ibuprofen, a model BCS II acidic drug (17, 18), during dissolution to simulate oral administration. Ibuprofen is a well-known non-steroidal anti-inflammatory drug (NSAID) which is widely used for its analgesic, antipyretic, and anti-inflammatory effects (19). The commercial form of ibuprofen is the racemic free acid; however, the neutral phase is practically insoluble (18). Since ibuprofen has a pK_a of 4.5-4.6 associated with its carboxylic acid (17), salt formation is feasible. However, disproportionation in the stomach is anticipated for this salt of an acidic drug. For these studies we used the well-characterized dihydrate sodium salt (20, 21) as the supersaturating salt system.

Initial experiments evaluated the dissolution profile of the drug in various media with HPMC in the solid state and pre-dissolved in media. Solubility and viscosity evaluations were conducted to assess the potential for HPMC to play a physical role in supersaturation. As a means to evaluate the role of HPMC in nucleation and crystal growth of ibuprofen, additional dissolution studies were carried out in the presence and absence of free acid seed and characterization of isolated solids was conducted. In order to probe whether specific polymer properties could be attributed to mechanism of supersaturation, additional dissolution studies were run with other cellulosic polymers,

methylcellulose (MC) and hydroxypropyl cellulose (HPC). The impact of these polymers on degree and duration of supersaturation as well as effect on crystal growth were monitored as a means to assess whether the varying degree of polymer hydrophobicity played a role in the mechanism of supersaturation of ibuprofen.

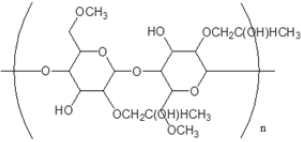
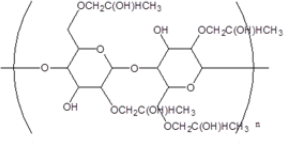
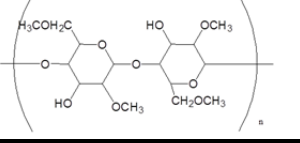
5.2. Materials and Methods

5.2.1. Materials

(*R/S*)-(\pm)-ibuprofen (free acid) was purchased from Sigma (Sigma-Aldrich, St. Louis, MO, USA) and the (*R/S*)-ibuprofen sodium dihydrate was prepared from the free acid and 1.006 molar equivalents of sodium hydroxide. The crystallization for ibuprofen sodium dihydrate was based on the procedures outlined by Lee and Wang (22), but without the need for cosolvent to facilitate precipitation. The final form of ibuprofen sodium dihydrate was confirmed to be the racemic conglomerate (20).

The hydroxypropyl methylcellulose (HPMC, hypromellose) used for this work was Pharmacoat 603, purchased from Shin-Etsu (Tokyo, Japan). Additional polymers included methylcellulose (MC, 400 cPs) purchased from Sigma-Aldrich, USA and Klucel EXF which is a pharmaceutical grade of hydroxypropyl cellulose (HPC) from Ashland, USA. Information about polymer structure and substitution are summarized in Table 5.1.

Table 5.1. Summary of polymer structure and substitution based on manufacturer information.

Polymer	Structure	Methoxyl Degree of Substitution	Methoxyl (%)	Hydroxy-propyl Molar Substitution	Hydroxy-propyl (%)
Pharmacoat 603 (HPMC)		1.8 – 1.9	28 – 30%	0.2	7 – 12%
Klucel EXF (HPC)		-	-	3.4 – 4.4	
Methylcellulose (MC)		1.5 – 1.9	27.5 – 31.5%	-	-

All other materials were of analytical grade and used as received. For dissolution experiments, simulated gastric fluid (SGF) and 50 mM acetate buffer at pH 5.0 were prepared. The recipe for SGF was 2 g/L sodium chloride and 1.4 mL/L of 12N hydrochloric acid in deionized water for a final pH of 1.8.

5.2.2. Methods

5.2.2.1. *In Vitro* Supersaturation Testing and Equilibrium Solubility Assessment

In order to evaluate the supersaturation behavior of ibuprofen following disproportionation of the highly soluble sodium salt to the poorly soluble free acid, dissolution experiments were performed at 25 and 37 °C in SGF and 50 mM acetate buffer at pH 5.0. Preliminary supersaturation experiments were conducted in SGF in order to probe feasibility of supersaturation under biorelevant conditions. However, the majority of experiments were conducted in 50 mM acetate buffer at pH 5.0 in order to fully evaluate potential mechanisms of supersaturation. The pH 5.0 buffer was selected since its pH falls between the pKa of ibuprofen and the pH_{max} of the ibuprofen sodium

salt, which are 4.5-4.6 (17) and 6.9-7.2 (experimentally determined) respectively. The intent was to avoid immediate neutralization of the ibuprofen sodium in the media by selecting a condition that could have slower kinetics of disproportionation and would have a lower degree of supersaturation. For experiments where the polymer was pre-dissolved in media, polymer solutions were prepared at 1 mg/mL in SGF and 2 mg/mL in pH 5 buffer.

Initial dissolution screening was conducted in HPLC vials on a 1 mL scale, with solid ibuprofen sodium added to each vial at a target concentration of 1 mg/mL for SGF studies and 2 mg/mL for dissolution in pH 5 buffer for a final weight ratio of 1:1 ibuprofen sodium:polymer. Samples were mixed at 500 rpm on a temperature controlled shaker programmed at 37 °C. At 20, 40, 60, and 120 minutes, aliquots of slurries were centrifuge filtered through a MultiScreen_{HTS}-PCF filter plate (Millipore, Billerica, MA, USA) and the filtrate was diluted and assayed using high performance liquid chromatography (HPLC) to determine ibuprofen concentration.

Since excess solid remained in the media, dissolution samples were allowed to equilibrate for 24 hours in order to determine equilibrium solubility of ibuprofen in the presence and absence of polymer. The degree of supersaturation was calculated by dividing the maximum concentration of the drug in the solution during dissolution by its solubility at 24 hours. Measurements of pH were made using an Accumet pH meter.

Controlled supersaturation experiments were repeated with ibuprofen sodium in pH 5 buffer with and without 1:1 weight equivalents of pre-dissolved polymer in order to further evaluate conditions that could influence the duration of supersaturation. These samples were prepared on a 10 mL scale to enable additional sampling for an expanded

dissolution profile and isolation of solids for further characterization. For this series of experiments, pre-dissolved HPMC solutions were prepared in pH 5 buffer at a concentration of 2 mg/mL and filtered prior to use in order to avoid the presence of any particulates that could act as seed. In a parallel arm, a small amount of crystalline ibuprofen free acid was added as seed to the ibuprofen sodium:HPMC slurry five minutes into the dissolution experiment. All samples were allowed to shake at 500 rpm under ambient conditions during the study and aliquots were centrifuge filtered and assayed as described above. These controlled dissolution experiments were also repeated with pre-dissolved MC and HPC using identical procedures.

All dissolution experiments were conducted in triplicate and data is reported as average concentration of free acid in solution \pm standard deviation.

5.2.2.2. High Performance Liquid Chromatography (HPLC) Analysis

Sample concentrations for the dissolution test and equilibrium solubility studies were determined using an Agilent 1100 series HPLC instrument. The HPLC method used an Ascentis Express C18 column (2.7 μ m fused-core particle size, 4.6 mm i.d. \times 100 mm length) at 40 °C with a 3-minute linear gradient from 10% to 95% mobile phase A (acetonitrile) and 90% to 5% of mobile phase B (0.1% phosphoric acid) followed by a 1-minute hold at 95% A. The flow rate was 1.8 mL/min and the injection volume was 5 μ L. The samples were analyzed with UV detection at 210 nm. Calibration curves were constructed from peak area measurements using standard solutions of ibuprofen free acid at known concentrations. The retention time of ibuprofen was approximately 3.1 minutes. Linearity was demonstrated from 0.01 to 0.27 mg/mL ($r^2 \geq 0.999$) and the relative

standard deviation of six injections was less than 0.5%. All solubility values will be reported in free acid equivalents.

5.2.2.3. Viscosity

The viscosity of dissolution media with and without polymer was measured on 1 mL samples at 37 °C using a viscometer (Viscolab 3000, Cambridge Viscosity, Medford, MA, USA). A 0.310" piston was selected based on its suitability for low viscosity (0.25-5 cP) measurements.

5.2.2.4. Light Microscopy of Precipitate

The morphology of crystals produced following dissolution were observed using a Zeiss Axiovert 200M polarizing microscope at a magnification of 200x and recorded using an Axiocam HRC digital camera (Carl Zeiss, Inc., Beograd, Austria).

5.2.2.5. X-ray Powder Diffraction (XRPD)

X-ray powder diffractograms were measured on a PANalytical X'Pert PRO X-ray diffractometer (Almelo, The Netherlands). The voltage and current were 45 kV and 40 mA, respectively. Samples were measured in reflection mode in the 2 θ -range from 4-40° using an X'celerator detector. Data were collected using X'Pert Data Collector and viewed using X'Pert HighScore (PANalytical B.V., The Netherlands).

5.2.2.6. Fourier Transform Infrared Spectroscopy (FTIR)

FTIR spectra were measured using a Nicolet Nexus 670 FTIR spectrometer (Nicolet, Madison, WI, USA) with an attenuated total reflectance (ATR) accessory. Samples were placed on the surface of the diamond ATR plate and the ATR assembly was clamped to ensure good contact. Spectra were obtained from 4000-600 cm⁻¹ with a resolution of 2 cm⁻¹ and 32 scans. Raw data was analyzed using OMNIC software. In

order to eliminate the interference of OH-bending and stretching bands associated with residual water, isolated solids were dried for 24 hours before FTIR characterization.

5.3. Results and Discussion

5.3.1. Supersaturation Profiles of Ibuprofen in the Presence of HPMC

In order to assess the supersaturation behavior of ibuprofen with polymer, the kinetic solubility profile of ibuprofen sodium in SGF was evaluated in the presence and absence of pre-dissolved HPMC at a 1:1 weight ratio of drug: polymer. Under the physiologic conditions of the stomach, disproportionation of ibuprofen sodium to the poorly soluble free acid was anticipated to occur rapidly. This was evident in the small amount of ibuprofen that was solubilized following addition of the sodium salt to SGF (Figure 5.1). Alternatively, a 17 fold increase in solubility was observed in the presence of HPMC at the 20 minute time point. Since loss of ibuprofen solubility was observed over time with HPMC, this initial observation of enhanced solubility was indicative of supersaturation. The supersaturation of ibuprofen that was achieved in the presence of HPMC was observed for approximately 40 to 60 minutes. However, significant variability was noted as supersaturation was lost. This variability was attributed to the high degree of supersaturation initially achieved under gastric conditions.

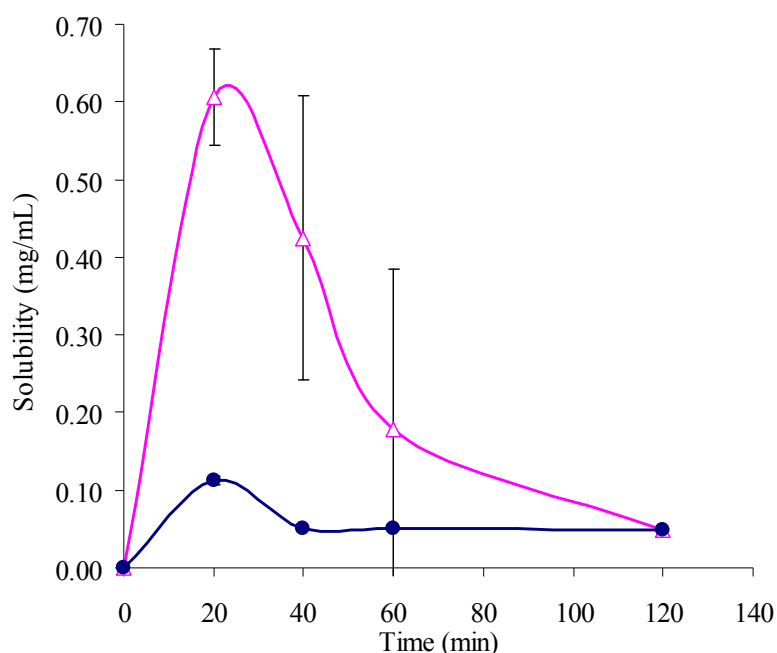


Figure 5.1. Dissolution profile of ibuprofen sodium in SGF at 37 °C without polymer (●) and with pre-dissolved HPMC (Δ). Error bars represent the standard deviation, $n = 3$.

The supersaturation profiles of ibuprofen sodium in pH 5 buffer alone and with 1:1 weight equivalents of HPMC, added either as a solid blend with compound or pre-dissolved in media, were also evaluated in order to explore conditions that prolonged supersaturation. As noted above, the pH 5.0 buffer was selected since its pH falls between the pK_a of ibuprofen and the pH_{max} of the ibuprofen sodium salt, which are 4.5-4.6 (17) and 6.9-7.2 (experimentally determined), respectively. The intent was to avoid immediate neutralization of the ibuprofen sodium in the media by selecting a condition that could have slower kinetics of disproportionation and precipitation of the free acid. In addition, the higher intrinsic solubility of ibuprofen at pH 5 would afford a lower maximum degree of supersaturation which would hopefully contribute to prolonged supersaturation.

As displayed in Figure 5.2, no supersaturation was achieved when ibuprofen sodium was dissolved in pH 5 buffer without HPMC. Based on the kinetic solubility profile, immediate precipitation of the thermodynamically stable crystalline free acid was occurring as the sodium salt was dissolving. This immediate conversion in phase corresponded to no appreciable increase in apparent solubility. Alternatively, supersaturation of ibuprofen in the presence of HPMC was maintained for 40 to 60 minutes when compared to the same system without polymer. The degree of supersaturation was further enhanced with pre-dissolved HPMC in pH 5 buffer when compared to co-blended ibuprofen sodium with polymer. This data suggests that the degree of supersaturation of ibuprofen in the co-blended formulations was rate-limited by the dissolution of polymer. Therefore, the process for supersaturation was likely solution-mediated since polymer needed to be dissolved in order to delay precipitation of ibuprofen.

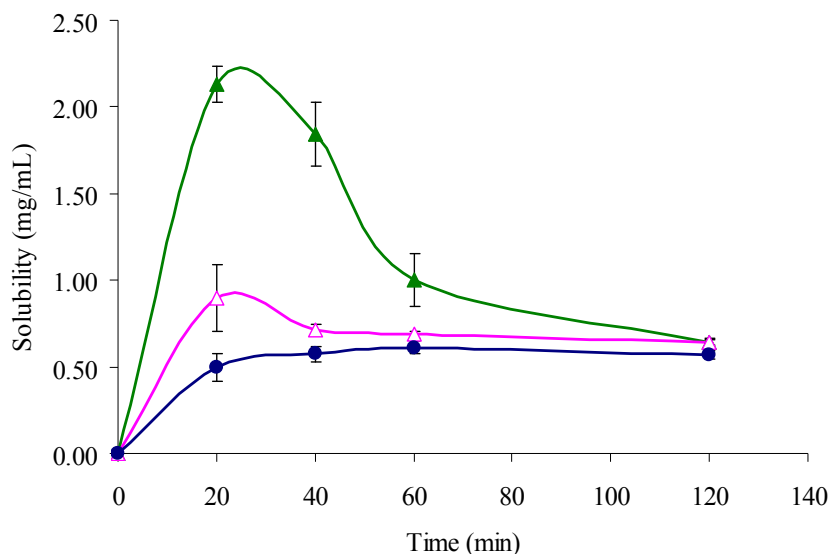


Figure 5.2. Dissolution profile of ibuprofen sodium in pH 5.0 buffer at 37 °C without HPMC (●), with solid HPMC (△), and with pre-dissolved HPMC (▲). Error bars represent the standard deviation, $n = 3$.

The viscosity of the media used during dissolution was measured as a means to explore the proposed solution-mediated mechanism of supersaturation. The presence of 1 mg/mL dissolved HPMC in SGF only shifted the viscosity from 0.64 cP to 0.66 cP at 37 °C, while 2 mg/mL HPMC in pH 5.0 buffer shifted the viscosity from 0.64 cP to 0.68 cP. The lack of a large viscosity enhancement in the presence of HPMC rules out the rheological properties of the polymer as a factor that could be attributed to supersaturation. In addition, supersaturation was higher when polymer was already pre-dissolved compared to the condition with HPMC dissolving along with ibuprofen sodium. The latter could give rise to high local polymer concentrations with increased viscosity. This observation provides further evidence that the role of HPMC, more specifically Pharmacoat 603, to prolong supersaturation was not associated with the viscosity of the polymer even though these studies were run at high polymer loading.

Table 5.2 summarizes the 24 hour solubility data for ibuprofen with and without polymer. No appreciable increase in solubility or shift in pH of the final media was observed in the presence of HPMC, suggesting that the polymer was not playing a role in altering the bulk solution properties of the drug or the vehicle. However, it was noted that there was a significant reduction in the maximum degree of supersaturation in pH 5 buffer compared to SGF. In general, higher degrees of supersaturation are associated with shorter durations of supersaturation since there is a greater thermodynamic drive toward precipitation at higher supersaturation values (23). This suggests that the pH 5 buffer system has a greater potential for enabling prolonged supersaturation of ibuprofen in the presence of polymer as opposed to SGF. Since supersaturation is a transient phenomenon, conducting mechanistic studies under conditions of prolonged durations of

supersaturation is more desirable. Therefore, the decrease in degree of supersaturation and the reduction in variability observed during loss of supersaturation in pH 5 buffer supports further investigation into mechanisms of supersaturation in pH 5 buffer rather than SGF. Therefore the remainder of this paper will focus mainly on supersaturation in pH 5 buffer in order to elucidate mechanisms of drug-polymer interaction.

Table 5.2. Impact of HPMC on solubility of ibuprofen in SGF and pH 5 buffer at 37 °C.

Starting System	Solubility at 20 Minutes (mg/mL \pm SD)	Solubility at 24 Hours (mg/mL \pm SD)	Final pH of Media	Degree of Maximum Supersaturation
1:0 Ibuprofen Sodium:HPMC in SGF	0.05 \pm 0.01	0.030 \pm 0.003	1.80	1.5
1:1 Ibuprofen Sodium:HPMC in SGF	0.60 \pm 0.06	0.035 \pm 0.002	1.82	17.3
1:0 Ibuprofen Sodium:HPMC in pH 5 buffer	0.49 \pm 0.08	0.41 \pm 0.03	5.37	1.2
1:1 Ibuprofen Sodium:HPMC in pH 5 buffer	2.13 \pm 0.11	0.45 \pm 0.04	5.42	4.7

Controlled dissolution experiments were repeated with ibuprofen sodium in pH 5 buffer with and without pre-dissolved HPMC in order to further evaluate conditions that could influence the extent of ibuprofen supersaturation. In order to differentiation between the influence of HPMC on nucleation and crystal growth of the crystalline free acid during loss of supersaturation, pre-dissolved polymer solutions were filtered prior to initiation of dissolution studies as a means to eliminate any particulates that could contribute to nucleation. Another dissolution arm included the addition of a small amount of crystalline ibuprofen free acid which was added as seed in order to examine the influence of polymer on crystal growth.

Figure 5.3 compares the dissolution profiles in pH 5 buffer with HPMC in the presence and absence of seed. In the system lacking seed, supersaturation was maintained for the duration of the two hour dissolution experiment. This was contrary to the HPMC system seeded with crystalline free acid which displayed loss of supersaturation within 2 hours. The significantly prolonged duration of supersaturation in the system without free acid seed indicates that HPMC was playing a role in nucleation inhibition of the free acid in pH 5 buffer. Alternatively, 20 minutes of supersaturation maintenance following crystalline seed addition 5 minutes into the dissolution experiment suggests that HPMC may also play a role in enabling supersaturation by altering crystal growth. Since all of these samples remained suspensions following the two hour dissolution experiment, additional characterization was conducted in order to further probe the differences among these samples. In order to clearly note the differences in precipitate isolated from the three arms of this controlled dissolution experiment, precipitate samples will be referenced as Type A, Type B, and Type C as defined in Table 5.3.

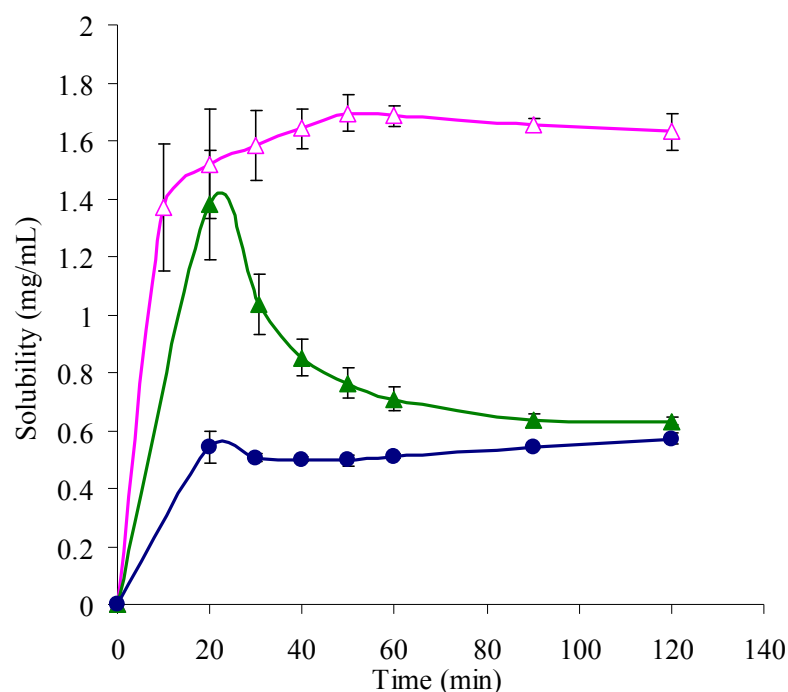


Figure 5.3. Dissolution profile of ibuprofen sodium in pH 5.0 buffer at 25 °C without HPMC (●), with pre-dissolved HPMC void of seed (△), and with pre-dissolved HPMC with seed added (▲). Error bars represent the standard deviation, n = 3.

Table 5.3. Precipitate classification for solids isolated following dissolution of ibuprofen sodium in pH 5.0 buffer.

Precipitate Type	Dissolution Conditions	Time of Precipitate Isolation (supersaturation state)
Type A	Ibuprofen sodium slurried in pH 5 buffer without HPMC	120 minutes (no observation of supersaturation)
Type B	Ibuprofen sodium slurried in pH 5 buffer with pre-dissolved HPMC with seed added	120 minutes (supersaturation was lost)
Type C	Ibuprofen sodium slurried in pH 5 buffer with pre-dissolved HPMC void of seed	120 minutes (supersaturation was maintained)

5.3.2. Phase Characterization of Ibuprofen Following Dissolution

Following the dissolution experiments illustrated in Figure 5.3, an aliquot of each suspension was evaluated by optical microscopy. The ibuprofen isolated from the system

lacking HPMC (Type A, Figure 5.4A) had long needle to rod-like morphology while the sample that exhibited loss of supersaturation following dissolution in the presence of HPMC (Type B, Figure 5.4B) had a distinct plate-like morphology. Although Types A and B reached the same solubility following two hours in pH 5 buffer, the morphologies of these crystals were different. There were also noteworthy differences in the aspect ratios of these crystals, with significantly smaller aspect ratios being associated with crystals isolated from the HPMC system (Type B).

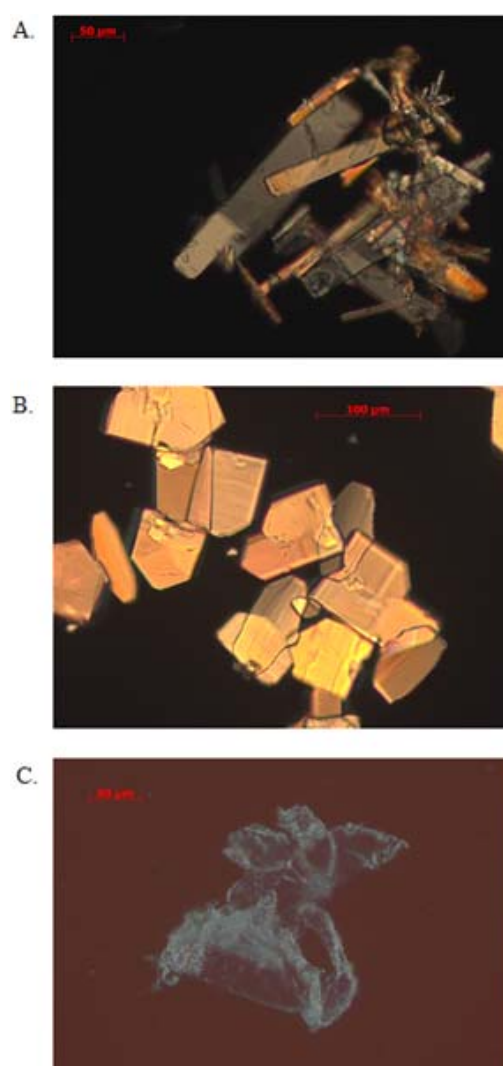


Figure 5.4. Microscopic images at 200x magnification of precipitate following dissolution of ibuprofen sodium in pH 5 buffer for (A) Type A, (B) Type B, and (C) Type C.

Additional characterization was conducted in order to determine whether a polymorph change could account for the disparity in crystal morphology. Type A (Figure 5.5b) had the same XRPD pattern as the control sample of ibuprofen free acid (Figure 5.5a), demonstrating that the ibuprofen sodium salt disproportionated and precipitated as the free acid at these buffer conditions. Type B also exhibited the same XRPD pattern as the ibuprofen free acid control (Figure 5.5c). This data provided evidence that the differences in morphology observed in Figures 4A and 4B were not associated with a different polymorph of the isolated solid following loss of supersaturation. Alternatively, the change in morphology of Type B suggested that HPMC may play a role in altering the growth of ibuprofen free acid crystals as supersaturation was lost during the dissolution experiment.

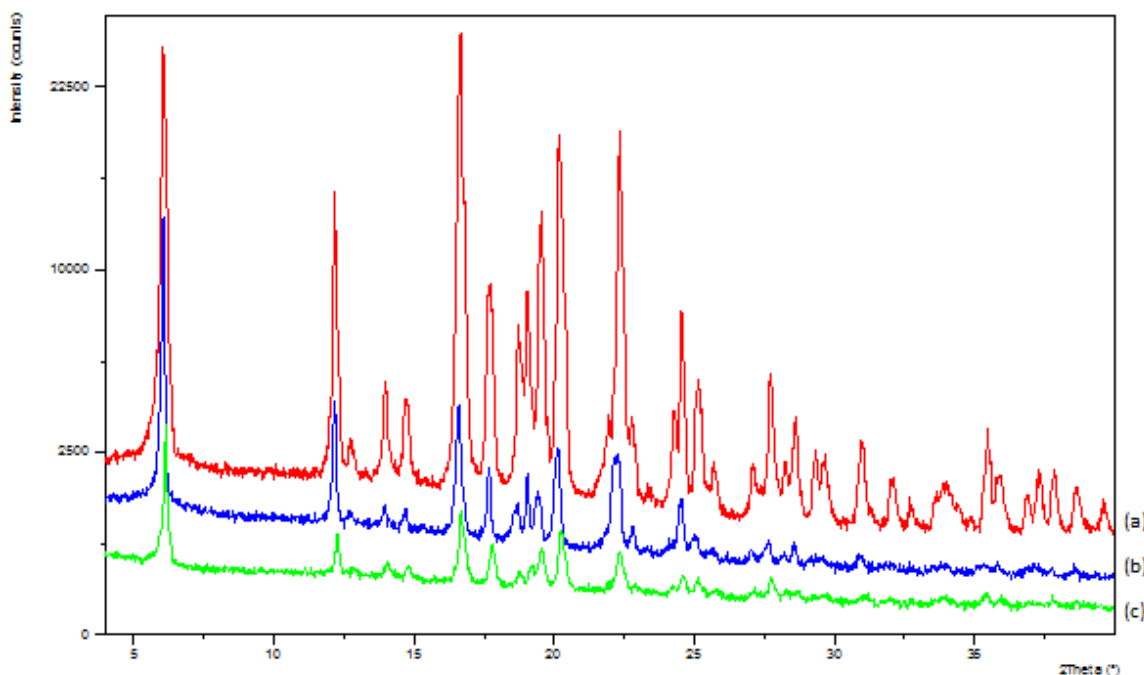


Figure 5.5. XRPD patterns comparing (a) ibuprofen free acid as received to (b) Type A and (c) Type B isolated following dissolution in pH 5 buffer.

The solids isolated from the system with maintained supersaturation (Type C) appeared amorphous with a lack of birefringence under polarized light and no distinct

particle morphology (Figure 5.4C). The lack of birefringence associated with this sample supports the previous suggestion that HPMC may play a role in crystallization inhibition. The XRPD trace of Type C further supported observations by microscopy that ibuprofen was present in the amorphous form based on the presence of the amorphous halo and lack of any distinct crystalline peaks (Figure 5.6). Since loss of supersaturation was observed when seeds were added, as was the case for Type B, it is suggested that Type C is void of any crystalline material since supersaturation of this system can be maintained for at least one month at ambient storage conditions (data not shown). It is therefore hypothesized that HPMC is playing a direct role in inhibiting the nucleation of ibuprofen.

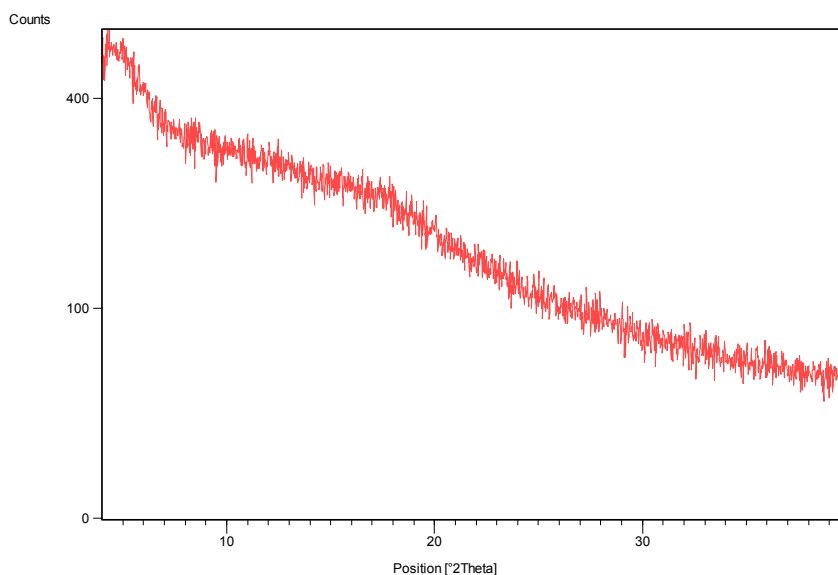


Figure 5.6. XRPD trace of Type C.

5.3.3. Evaluation of Ibuprofen and HPMC by FTIR Spectroscopy

Solids were isolated from ibuprofen slurries in the supersaturated state (Type C) as well as after loss of supersaturation (Type B) in order to further evaluate the role of HPMC in each of these systems. When comparing FTIR of the dry solids isolated from slurries (Types B and C) to ibuprofen free acid and HPMC control spectra (Figure 5.7),

the presence of characteristic HPMC peaks were observed in Type C, which was the solid isolated from the supersaturated system. These HPMC peaks included the O-H stretch at 3500 cm^{-1} and the C-O stretch at $1000\text{--}1200\text{ cm}^{-1}$ (24). In contrast, no HPMC peaks were detected in Type B precipitate. This data suggests that the isolated solid from the supersaturated system (Type C) consisted of ibuprofen co-precipitated with HPMC while no HPMC was present in the solid following loss of supersaturation (Type B).

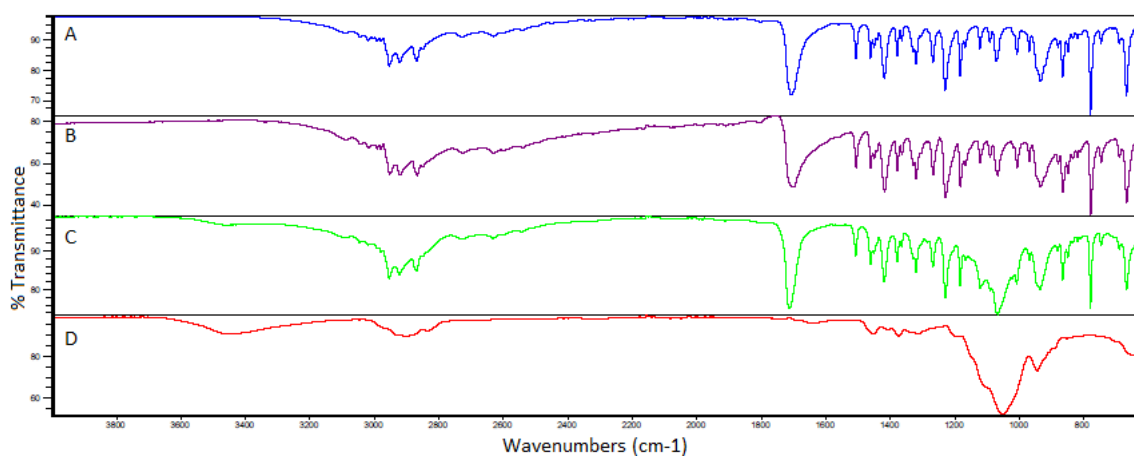


Figure 5.7. FTIR spectra comparing (A) ibuprofen free acid, (B) Type B, (C) Type C, and (D) HPMC.

It is theorized that intermolecular hydrogen bonding between the hydroxyl groups of HPMC and the carbonyl groups of ibuprofen could be responsible for the co-precipitate of these two components in Type C. This intermolecular interaction is likely also inhibiting nucleation of crystalline ibuprofen free acid. In order to probe this hypothesis, the wavenumber region associated with the C=O stretching mode around $1700\text{--}1760\text{ cm}^{-1}$ was examined further for Type C.

Molecular modeling has provided evidence that ibuprofen molecules exist as hydrogen bonded dimers in the free acid crystal lattice (25, 26). This hydrogen bonding was observed in the control spectrum of ibuprofen free acid (Figure 5.7) in the form of a shift in the C=O stretching vibrations from the characteristic free C=O frequency at 1760

cm^{-1} down to the $1725\text{--}1700\text{ cm}^{-1}$ region and a shift in the O-H stretch from 3520 cm^{-1} to a broad band between $3300\text{--}2500\text{ cm}^{-1}$ (24). Since the carbonyl stretch for Type C was maintained in the $1725\text{--}1700\text{ cm}^{-1}$ region, this was evidence that hydrogen bonding was still occurring. Upon closer evaluation in Figure 5.8, a left-shift of the carbonyl peak from 1706 cm^{-1} to 1712 cm^{-1} was observed for Type C when compared to crystalline ibuprofen free acid control. The observed shift in the C=O maxima was not anticipated to be attributed to the presence of ibuprofen in the amorphous form. Published data comparing crystalline ibuprofen free acid to the super-cooled liquid has demonstrated that a reduction in intensity and band broadening is observed for the super-cooled liquid without a shift in the carbonyl peak (27).

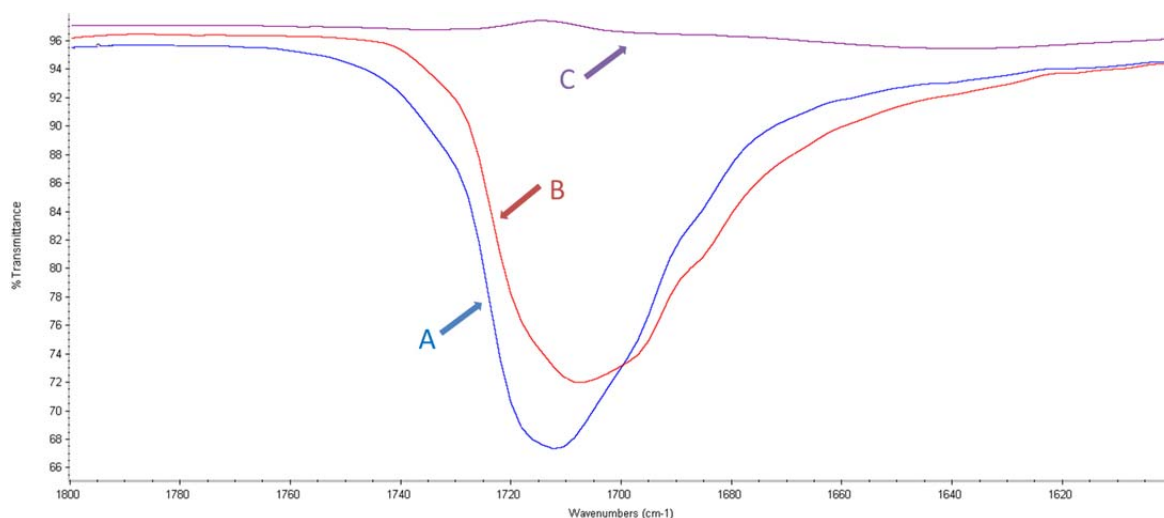


Figure 5.8. FTIR spectra comparing (A) Type C, (B) ibuprofen free acid, and (c) HPMC in the carbonyl region.

The left shift in the maximum of the C=O stretching vibration for Type C indicated that rather than ibuprofen hydrogen bonding with itself, ibuprofen was hydrogen bonding with HPMC when in a supersaturated state. This solid state intermolecular interaction explains why the presence of HPMC was observed in Type C, but not in Type B. This shift in the carbonyl stretch has also been reported in the

literature when an HPMC amorphous solid dispersion was formed with ibuprofen. The authors suggested formation of hydrogen bonding between the drug and polymer following solvent evaporation (15). In summary, for the present study we have provided evidence that the intermolecular hydrogen bonding between ibuprofen free acid and HPMC in the solid state was stabilizing the amorphous ibuprofen and therefore prolonging supersaturation through nucleation inhibition.

The shift of the C=O stretching vibration to a higher frequency indicated that the hydrogen bonding interaction between ibuprofen and HPMC was weaker than the interaction of ibuprofen with itself (28). Once seed was introduced to the supersaturated system, interactions of ibuprofen with itself were favored and the crystal growth process was initiated. As supersaturation was lost, ibuprofen dimer formation replaced the ibuprofen-HPMC interactions. However, since dimers are required for the formation of the crystal lattice, the need for ibuprofen-HPMC interactions to be broken and association of ibuprofen into dimers to occur slowed the crystal growth process. This crystallization process explains the differences in the morphology of crystals for Type A and Type B (Figure 5.4). Specifically, the observations of decreased aspect ratios and larger faces of the ibuprofen crystals grown in the presence of HPMC (Type B) indicate that the polymer was playing a role in the growth of the ibuprofen free acid crystals. Raghavan et al. have made similar observations of crystal habit modification of hydrocortisone acetate in the presence of HPMC and have attributed hydrogen bonding between the drug and polymer to decreased crystallization rates (29).

5.3.4. Role of Other Cellulosic Polymers on Supersaturation of Ibuprofen

The primary mechanism for supersaturation of ibuprofen in the presence of HPMC has been attributed to hydrogen bonding. Therefore, other cellulosic polymers with varying degrees of hydroxyl functionality were evaluated in order to determine whether the polarity of a polymer could be a predictive characteristic to inform on supersaturation potential. In order to assess the degree and extent of supersaturation, the dissolution profiles of ibuprofen sodium in the presence of pre-dissolved MC and HPC in pH 5 buffer void of seed were compared to data without polymer and with pre-dissolved HPMC (Figure 5.9). Supersaturation was maintained in the presence of HPMC, MC and HPC for at least 20 minutes. Although loss of supersaturation was variable for systems containing MC or HPC, there was an observed trend for loss of supersaturation at the 60 minute timepoint for MC and at the 120 minute timepoint for HPC. Alternatively, previous experiments have shown that ibuprofen remained supersaturated in HPMC at 120 minutes and beyond. An evaluation of the solubility of these samples at 24 hours confirmed that there was a deviation among samples containing different polymers. While HPMC systems maintained supersaturation, the HPC system completely lost supersaturation and the MC system exhibited a variable loss of supersaturation. This initial dissolution data suggests that these polymers may interact differently with ibuprofen to enable supersaturation, with HPMC being a better nucleation inhibitor than MC or HPC.

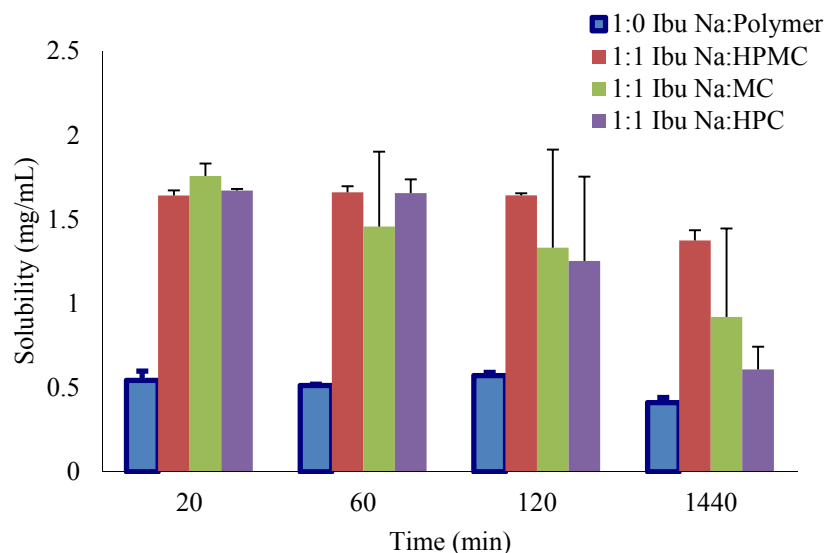


Figure 5.9. Kinetic solubility of ibuprofen sodium in pH 5 buffer at 25 °C with pre-dissolved polymer in the absence of seed. Error bars represent the standard deviation, $n = 3$.

Additional dissolution studies included the addition of crystalline ibuprofen free acid seed in order to examine supersaturation profiles after nucleation. When comparing the dissolution profiles of ibuprofen sodium in pH 5 buffer with various pre-dissolved polymers in the presence of ibuprofen free acid seed (Figure 5.10), it was observed that HPMC and HPC exhibited very similar dissolution profiles. In the presence of either polymer, the high degree of supersaturation was extended for a prolonged period of time, even after seed was added. This suggests that both polymers were able to act as effective supersaturation agents, even after nucleation. The same degree of supersaturation was not achieved with the MC slurry at the 20 minute timepoint; however supersaturation relative to the ibuprofen sodium control was still observed. This data suggests that MC may not facilitate crystal growth inhibition via the same mechanisms as HPMC or HPC.

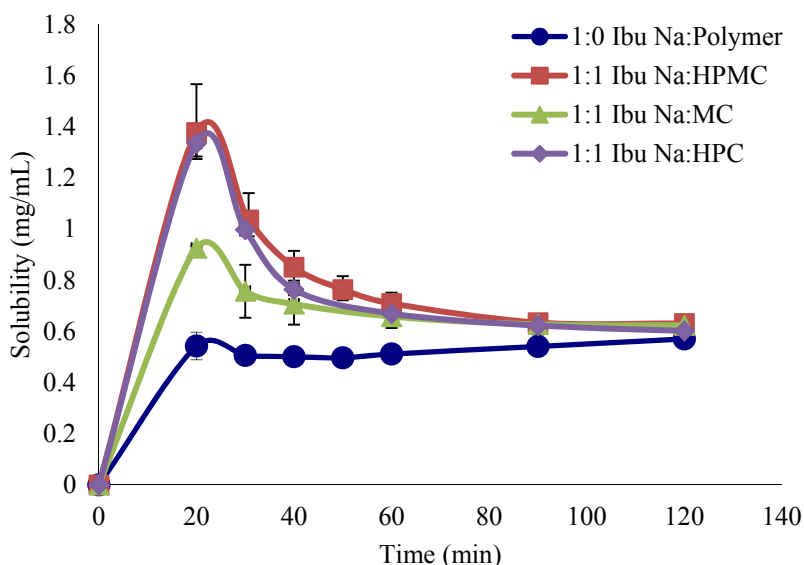


Figure 5.10. Dissolution profile of ibuprofen sodium in pH 5.0 buffer at 25 °C without polymer (●) and with pre-dissolved HPMC (■), HPC (◆), and MC (▲) with seed added. Error bars represent the standard deviation, $n = 3$.

The most striking differences observed with ibuprofen in the presence of these various polymers was in the aspect ratio and morphology of crystals isolated following loss of supersaturation. Figure 5.4 previously illustrated that, following loss of supersaturation in HPMC, ibuprofen free acid crystals had a low aspect ratio and a plate-like morphology when compared to the longer rod-like morphology of ibuprofen free acid in the absence of polymer. Alternatively, higher aspect ratios were observed following loss of supersaturation in the presence of MC and HPC (Figure 5.11). Previous work has shown that during crystal growth of ibuprofen free acid, the presence of solvents that exhibit strong intermolecular hydrogen bonding with ibuprofen yield low aspect ratio crystals (30). Therefore it is hypothesized that a higher degree of hydrogen bonding was occurring with HPMC compared to MC or HPC since the aspect ratios for solids isolated after loss of supersaturation were much smaller when HPMC was present. Additional crystallography data for ibuprofen also draws a correlation between increased

hydrophilicity of media and decreases in aspect ratio of ibuprofen crystals (25, 26). This suggests that polymer hydrophilicity may be predictive of hydrogen bonding potential and prolonged supersaturation of ibuprofen. Since hydrophilicity of the evaluated cellulosic polymers ranges from HPC<MC<HPMC due to the varying degrees of hydrophobic hydroxypropyl substitution on the polymer backbone (31, 32) which was summarized in Table 5.1, hydrogen-bonding potential should also follow the same pattern for these neutral cellulosic polymers.

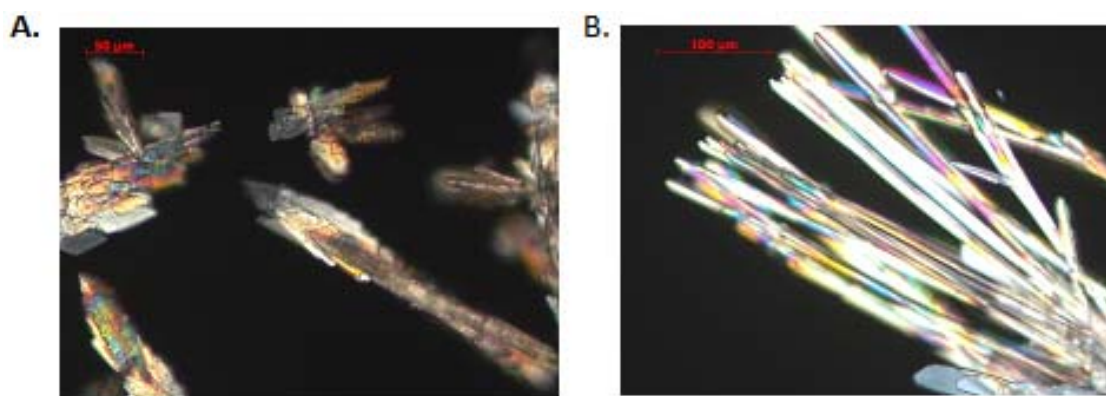


Figure 5.11. Microscopic images at 200x magnification following loss of supersaturation of ibuprofen sodium in pH 5 buffer (A) with pre-dissolved MC and (B) with pre-dissolved HPC in systems void of seed.

It is likely that the reduction in hydrogen bonding potential for MC compared to HPMC can explain why the degree of supersaturation in the presence of MC was significantly reduced when comparing the two dissolution profiles in the presence of seed (Figure 5.10). Rather than hydrogen bonding between ibuprofen and MC interfering with crystal growth, the high viscosity of MC may be the predominant factor attributing to observations of prolonged supersaturation. The rough faces of the ibuprofen crystals following loss of supersaturation in MC (Figure 5.11A) indicated that growth was taking place via a diffusion mechanism and the higher viscosity associated with MC (1.25 cP versus 0.64 cP in pH 5 buffer with and without MC, respectively) could play a role in this

diffusion controlled growth. The correlation between increased media viscosity and decreased drug diffusion during nucleation and crystal growth has been previously highlighted as a potential factor for delayed precipitation during supersaturation (10).

Since the hydrophobicity of HPC is significantly higher than HPMC due to the increased presence of hydroxyalkyl groups (32, 33) as summarized in Table 5.1, it is anticipated that the propensity for hydrogen bonding is less likely. This is supported by the observations of high aspect ratios in Figure 5.11B and loss of supersaturation due to insufficient nucleation inhibition in the absence of seed (Figure 5.9). Therefore, the high aspect ratio and high initial degree of supersaturation observed with HPC suggests that a mechanism other than hydrogen bonding alone is playing a role mechanistically in prolonging supersaturation, and will be the focus of future work.

5.4. Conclusions

Supersaturation of ibuprofen was effectively prolonged with cellulosic polymers. A deep dive into the mechanisms of supersaturation revealed that intermolecular interactions between ibuprofen and HPMC were driving supersaturation rather than physical modulation of bulk solution properties. The soluble sodium salt of ibuprofen enabled high initial degrees of supersaturation to be achieved during dissolution, while HPMC played a role in delaying nucleation and crystal growth of the thermodynamically stable crystalline free acid. Characterization of solids isolated from a supersaturated suspension demonstrated that hydrogen bonding between drug and polymer was stabilizing ibuprofen free acid as an amorphous co-precipitate with HPMC and therefore inhibiting nucleation. Further characterization following loss of supersaturation also

revealed changes in crystal habit and decreases in aspect ratio, further supporting the hypothesis that intermolecular hydrogen bonding between the drug and polymer were altering the growth process of crystalline ibuprofen free acid as supersaturation was lost.

The dissolution behavior of ibuprofen sodium in the presence of pre-dissolved HPMC, MC and HPC were also compared. Differences in crystal morphologies and aspect ratios following loss of supersaturation suggested diverse mechanisms for supersaturation in the presence of each of these polymers. Polymer viscosity was proposed as the primary factor prolonging supersaturation of ibuprofen in the presence of MC, while mechanisms other than hydrogen bonding were likely to be attributed to supersaturation with HPC. Observations of high aspect ratio crystals isolated following loss of supersaturation in the presence of MC and HPC led to the proposal that hydrogen bonding was not the predominant mechanism for supersaturation with these polymer systems. This data also suggested that polymer hydrophilicity may be an important parameter in the prediction of hydrogen bonding potential between drugs and polymers.

This work demonstrated that mechanism of supersaturation was dependent on the specific drug-polymer interactions. These experiments also suggested that certain types of interactions were more effective at maintaining prolonged supersaturation than others. The hydrogen bonding interactions between ibuprofen and HPMC resulted in more effective nucleation inhibition and prolonged supersaturation than MC, which primarily prolonged supersaturation through physical modification of media viscosity. In conclusion, these results suggest that an intermolecular interaction, as opposed to a physical interaction, may be more effective at prolonging supersaturation of ibuprofen, at least during *in vitro* dissolution. It is unclear how these varying mechanisms of

supersaturation will translate to changes in exposure, and this will therefore be the focus of future work.

5.5. References

1. B. Hancock and M. Parks. What is the True Solubility Advantage for Amorphous Pharmaceuticals? *Pharm Res.* 17:397-404 (2000).
2. S.M. Berge, L.D. Bighley, and D.C. Monkhouse. Pharmaceutical salts. *J Pharm Sci.* 66:1-19 (1977).
3. J. Brouwers, M.E. Brewster, and P. Augustijns. Supersaturating drug delivery systems: The answer to solubility limited oral bioavailability? *J Pharm Sci.* 98:2549-2572 (2009).
4. G. Kwei, L. Novak, L. Hettrick, E. Reiss, D. Ostovic, A. Loper, C. Lui, R. Higgins, I.W. Chen, and J. Lin. Regiospecific Intestinal Absorption of the HIV Protease Inhibitor L-735,524 in Beagle Dogs. *Pharm Res.* 12:884-888 (1995).
5. D.E. Alonzo, G.G.Z. Zhang, D. Zhou, Y. Gao, and L.S. Taylor. Understanding the behavior of amorphous pharmaceutical systems during dissolution. *Pharm Res.* 27:608-618 (2010).
6. H. Konno, T. Handa, D.E. Alonzo, and L.S. Taylor. Effect of polymer type on the dissolution profile of amorphous solid dispersions containing felodipine. *Eur J Pharm Biopharm.* 70:493-499 (2008).
7. F. Usui, K. Maeda, A. Kusai, and K. Nishimura. Inhibitory effects of water-soluble polymers on precipitation of RS-8359. *Int J Pharm.* 154:59-66 (1997).
8. H.R. Guzmán, M. Tawa, Z. Zhang, P. Ratanabanangkoon, P. Shaw, C.R. Gardner, H. Chen, J.P. Moreau, Ö. Almarsson, and J.F. Remenar. Combined use of crystalline salt forms and precipitation inhibitors to improve oral absorption of celecoxib from solid oral formulations. *J Pharm Sci.* 96:2686-2702 (2007).
9. K. Yamashita, T. Nakate, K. Okimoto, A. Ohike, Y. Tokunaga, R. Ibuki, K. Higaki, and T. Kimura. Establishment of new preparation method for solid dispersion formulation of tacrolimus. *Int J Pharm.* 267:79-91 (2003).
10. D.B. Warren, H. Benameur, C.J.H. Porter, and C.W. Pouton. Using polymeric precipitation inhibitors to improve the absorption of poorly water-soluble drugs: A mechanistic basis for utility. *J Drug Targeting*:1-28 (2010).
11. T.f. Vasconcelos, B. Sarmiento, and P. Costa. Solid dispersions as strategy to improve oral bioavailability of poor water soluble drugs. *Drug Discovery Today.* 12:1068-1075 (2007).
12. A. Serajuddin. Salt formation to improve drug solubility. *Adv Drug Delivery Rev.* 59:603-616 (2007).
13. M. Hawley and W. Morozowich. Modifying the diffusion layer of soluble salts of poorly soluble basic drugs to improve dissolution performance. *Mol Pharmaceutics.* 7:1441-1449 (2010).
14. T. Loftsson, H. Friariksdoottir, and T.K. Guamundsdottir. The effect of water-soluble polymers on aqueous solubility of drugs. *Int J Pharm.* 127:293-296 (1996).

15. M. Iervolino, B. Cappello, S.L. Raghavan, and J. Hadgraft. Penetration enhancement of ibuprofen from supersaturated solutions through human skin. *Int J Pharm.* 212:131-141 (2001).
16. H. Wen, K.R. Morris, and K. Park. Hydrogen bonding interactions between adsorbed polymer molecules and crystal surface of acetaminophen. *J Colloid Interface Sci.* 290:325-335 (2005).
17. H. Potthast, J.B. Dressman, H.E. Junginger, K.K. Midha, H. Oeser, V.P. Shah, H. Vogelpoel, and D.M. Barends. Biowaiver monographs for immediate release solid oral dosage forms: Ibuprofen. *J Pharm Sci.* 94:2121-2131 (2005).
18. N.A. Kasim, M. Whitehouse, C. Ramachandran, M. Bermejo, H. LennernÃ¶s, A.S. Hussain, H.E. Junginger, S.A. Stavchansky, K.K. Midha, and V.P. Shah. Molecular properties of WHO essential drugs and provisional biopharmaceutical classification. *Mol Pharmaceutics.* 1:85-96 (2004).
19. K. Rainsford. Ibuprofen: pharmacology, efficacy and safety. *Inflammopharmacology.* 17:275-342 (2009).
20. G.G.Z. Zhang, S.Y.L. Paspal, R. Suryanarayanan, and D.J.W. Grant. Racemic species of sodium ibuprofen: Characterization and polymorphic relationships. *J Pharm Sci.* 92:1356-1366 (2003).
21. T. Lee, Y. Chen, and C. Zhang. Solubility, Polymorphism, Crystallinity, Crystal Habit, and Drying Scheme of (R, S)-(6)-Sodium Ibuprofen Dihydrate. *Pharm Technol.* 31:72 (2007).
22. T. Lee and Y.W. Wang. Initial salt screening procedures for manufacturing ibuprofen. *Drug Dev Ind Pharm.* 35:555-567 (2009).
23. D. Kashchiev and G.M. Van Rosmalen. Review: Nucleation in solutions revisited. *Cryst Res Technol.* 38:555-574 (2003).
24. N.P.G. Roeges. A guide to the complete interpretation of infrared spectra of organic structures, Wiley hichester etc., 1994.
25. D. Winn and M.F. Doherty. A new technique for predicting the shape of solution-grown organic crystals. *AIChE Journal.* 44:2501-2514 (1998).
26. D. Winn and M.F. Doherty. Modeling crystal shapes of organic materials grown from solution. *AIChE Journal.* 46:1348-1367 (2000).
27. A.R. Bras, J.P. Noronha, A.M.M. Antunes, M.M. Cardoso, A. Schonhals, F. Affouard, M. Dionisio, and N.T. Correia. Molecular motions in amorphous ibuprofen as studied by broadband dielectric spectroscopy. *J Phys Chem B.* 112:11087-11099 (2008).
28. E. Karavas, E. Georgarakis, and D. Bikiaris. Application of PVP/HPMC miscible blends with enhanced mucoadhesive properties for adjusting drug release in predictable pulsatile chronotherapeutics. *Eur J Pharm Biopharm.* 64:115-126 (2006).
29. S. Raghavan, A. Trividic, A. Davis, and J. Hadgraft. Crystallization of hydrocortisone acetate: influence of polymers. *Int J Pharm.* 212:213-221 (2001).
30. C. Acquah, A.T. Karunanithi, M. Cagnetta, L.E.K. Achenie, and S.L. Suib. Linear models for prediction of ibuprofen crystal morphology based on hydrogen bonding propensities. *Fluid Phase Equilib.* 277:73-80 (2009).
31. F. Tian, D.J. Saville, K.C. Gordon, C.J. Strachan, J.A. Zeitler, N. Sandler, and T. Rades. The influence of various excipients on the conversion kinetics of

- carbamazepine polymorphs in aqueous suspension. *J Pharm Pharmacol.* 59:193-201 (2007).
32. E.D. Klug. Some properties of water-soluble hydroxyalkyl celluloses and their derivatives. *J Polym Sci, Part C: Polym Symp.* 36:491-508 (1971).
 33. Y. Qiu, Y. Chen, G.G.Z. Zhang, L. Liu, and W. Porter. *Developing solid oral dosage forms: pharmaceutical theory & practice*, Academic Press, 2009.

CHAPTER 6

Probing the Speciation of Ibuprofen in the Presence of Polymers during *In Vitro* Supersaturation

Planned submission for publication to Drug Development and Industrial Pharmacy as:

“Probing the Speciation of Ibuprofen in the Presence of Polymers during *In Vitro* Supersaturation”

Jenna L. Terebetski and Bozena Michniak-Kohn

6.1. Introduction

Development of poorly water-soluble drugs is challenging due to the limitations of drug solubilization and subsequent poor absorption following oral administration. One approach to enhance bioavailability of low solubility drugs is through administration of a supersaturating formulation (1, 2). Supersaturation occurs when an excess of drug is solubilized above the equilibrium solubility of the thermodynamically stable species. This can be achieved initially through formation of a metastable phase following administration and stabilized through the use of excipients. Various species have been proposed to contribute to measured concentrations of dissolved drug during supersaturation. In the case of amorphous spray dried dispersions, dissolved drug was described as including free drug, drug in micelles, and drug in drug/polymer colloids (3). Alternatively, administration of a soluble salt in a pH modified formulation can prolong the presence of ionized species with enhanced solubility even under conditions where the unionized species is favored (4). Stabilization of the metastable phase during GI transit

has been attributed to various interactions between the drug and excipients and a number of reviews detail these potential mechanisms of supersaturation (1, 5, 6). However, additional investigation into contributions of speciation during supersaturation is required to further enhance the understanding of the mechanisms of supersaturation. This can provide important insight into developing high performing formulations for challenging compounds.

Previous work has demonstrated that the dissolution of the highly water-soluble sodium salt of ibuprofen in simulated gastric conditions exhibited prolonged supersaturation under conditions where the poorly soluble free acid phase was thermodynamically stable. In order for supersaturation to be prolonged, inclusion of a polymer such as PVP-VA64, MC, or HPMC was required (Chapter 4). In this study, kinetic dynamic light scattering (DLS) experiments were conducted with ibuprofen sodium and polymer formulations. The presence of aggregate or micelle formation was monitored as a means to correlate solution speciation to supersaturation. Solids isolated following ultracentrifugation were also evaluated via microscopy in order to characterize the species that were contributing to supersaturation. Finally, the influence of polymers on the pKa of ibuprofen was also evaluated.

6.2. Materials and Methods

6.2.1. Materials and Sample Preparation

(R/S)-(±)-ibuprofen (free acid) was purchased from Sigma (Sigma-Aldrich, St. Louis, MO, USA) and the (R/S)-ibuprofen sodium dihydrate was purchased from Fluka (Sigma-Aldrich, St. Louis, MO, USA). Pharmacoat 603 (hydroxypropyl methylcellulose,

HPMC, Shin-Etsu, JAPAN), Kollidon VA64 (polyvinyl pyrrolidone-vinyl acetate copolymer, PVP-VA, BASF, GERMANY), and methylcellulose (MC, 400 cPs, Sigma-Aldrich, USA) were used as polymeric excipients. Formulation blends of ibuprofen sodium with each polymer were prepared individually at a 1:1 weight:weight ratio with gentle mixing.

Sodium chloride and hydrochloric acid were purchased from Fisher (Pittsburg PA, USA) for use in the preparation of the dissolution buffers. HPLC grade acetonitrile and 85% phosphoric acid were purchased from Sigma-Aldrich (St. Louis, MO, USA) and were used as received. Deionized water was used for all aqueous solutions which were prepared as needed for each experiment. Dissolution experiments with ibuprofen sodium were performed at 37 °C in simulated gastric fluid (SGF). The formula for SGF was 2 g/L sodium chloride and 1.4 mL/L of 12N hydrochloric acid in deionized water at a final pH of 1.8.

6.2.2. Methods

6.2.2.1. Speciation of Ibuprofen Sodium in Aqueous Media

Solution behavior of ibuprofen sodium was interrogated by using the DynaPro Plate Reader (Wyatt Technology, Santa Barbara, CA, USA) to measure the hydrodynamic radii of particles in solution. Critical aggregate concentration (CAC) and critical micelle concentration (CMC) determination of ibuprofen was conducted in water with ibuprofen sodium concentrations ranging from 0.01 to 150 mg/mL using dynamic light scattering.

Drug concentrations were also evaluated by HPLC following filtration through 0.45 μ m PTFE membrane syringe filters (Thermo Fisher Scientific, Waltham, MA) or

ultracentrifugation using an Optima TLX ultracentrifuge equipped with a TLA 120.2 rotor (Beckman Coulter, Inc., Brea, CA) in order to determine the impact of sample handling on recovery of the solubilized species.

6.2.2.2. Dissolution of Drug-Polymer Formulations

In order to explore speciation behavior of ibuprofen during supersaturation when combining the sodium salt with various polymers, large-scale biorelevant dissolution experiments were conducted in triplicate with a USP Apparatus II (paddle) method in a Distek dissolution system 2100C (Distek, Inc., North Brunswick, NJ). Kinetic solubility profiles of each formulation were monitored in acidic media (2 hours in 250 mL of SGF at pH 1.8, prepared as described above). Media was controlled at a temperature of 37.0 ± 0.5 °C for the duration of the experiment and the rotational speed of the paddles was 50 rpm. To each dissolution vessel, 550 mg of 1:1 ibuprofen sodium:polymer blends was added (250 mg of ibuprofen, free acid equivalence). This amount of ibuprofen corresponded to a theoretical 1 mg/mL concentration of ibuprofen in the acidic media which represented a maximum achievable supersaturation level of 20-fold assuming an equilibrium solubility of 0.047 mg/mL in SGF (see Table 6.1). At predetermined intervals (10, 30, 60, and 120 minutes), samples were withdrawn, filtered using a 0.45 μ m PTFE membrane syringe filter (Thermo Fisher Scientific, Waltham, MA) and appropriately diluted for analysis of drug concentration using high performance liquid chromatography (HPLC). In order to investigate the possibility of sub-450 nm particles or colloids passing through the 0.45 μ m syringe filter, filtered samples were also ultracentrifuged using an Optima TLX ultracentrifuge equipped with a TLA 120.2 rotor (Beckman Coulter, Inc., Brea, CA). Ultracentrifugation was performed at 80,000 rpm for

20 minutes. Supernatant was then diluted and analyzed by HPLC to measure only solubilized species at each time point.

All dissolution experiments were conducted in triplicate and data were reported as average concentration of free acid in solution \pm standard deviation.

6.2.2.3. High Performance Liquid Chromatography (HPLC) Analysis

Ibuprofen concentrations during the kinetic solubility studies were determined using an Agilent 1100 Series HPLC instrument. The HPLC method used an Ascentis Express C18 column (2.7 μ m fused-core particle size, 4.6 mm i.d. \times 100 mm length) at 40 °C with a 3-minute linear gradient from 10% to 95% mobile phase A (acetonitrile) and 90% to 5% of mobile phase B (0.1% phosphoric acid) followed by a 1-minute hold at 95% A. The flow rate was 1.8 mL/min and the injection volume was 5 μ L. The samples were analyzed with UV detection at 210 nm. Calibration curves were constructed from peak area measurements using standard solutions of ibuprofen free acid at known concentrations. The retention time of ibuprofen was approximately 3.1 minutes. Linearity was demonstrated from 0.01 to 0.27 mg/mL ($r^2 \geq 0.999$) and the relative standard deviation of six injections was less than 0.5%. All solubility values will be reported in free acid equivalents.

The supersaturation ratio was calculated by dividing the measured concentration of drug in solution during dissolution by its equilibrium solubility determined following 24 hours in the system of interest. Table 6.1 summarizes the 24 hour solubility data previously generated in Chapter 4.

Table 6.1. Solubility of ibuprofen sodium following 24 hours in SGF with and without 1 mg/mL polymer at 37 °C (data initially reported in Chapter 4).

Polymer	Solubility at 24 Hours (mg/mL \pm SD)	Final pH of Media
Ibuprofen Sodium Only	0.046 \pm 0.002	2.02
HPMC	0.033 \pm 0.001	1.86
PVP-VA64	0.040 \pm 0.002	2.10
MC	0.036 \pm 0.001	2.10

6.2.2.4. Dynamic Light Scattering (DLS) Studies

The hydrodynamic radii of particles in solution were determined by using the DynaPro Plate Reader (Wyatt Technology, Santa Barbara, CA, USA), which is a dynamic light scattering instrument. Varying concentrations of ibuprofen sodium in water were evaluated by DLS in order to determine the critical aggregate concentration (CAC) and critical micelle concentration (CMC) of the sodium salt in aqueous media. Kinetic solubility samples isolated during dissolution studies of ibuprofen sodium with polymers were also evaluated in order to probe speciation during supersaturation. In order to analyze samples by DLS, aliquots were filtered through 0.45 μ m filters in order to eliminate any dust or solid particles and transferred to a 386 well assay plate for DLS analysis. The supernatant following ultracentrifugation was also analyzed by DLS. Each sample was analyzed 10 times with a single acquisition lasting 3 seconds at a controlled temperature of 25 °C. Data was analyzed using DYNAMICS 7.0 (Wyatt Technology, Santa Barbara, CA, USA) software. The autocorrelation function of scattered light intensity was used to determine the acceptability of data, and the hydrodynamic radius of particles was reported only when a valid correlation function was obtained (7).

6.2.2.5. Optical Microscopy Studies

The presence of crystal formation during dissolution of ibuprofen sodium with and without polymers was monitored using a Zeiss Axiovert 200M polarizing microscope

at a magnification of 100x and recorded using an Axiocam HRC digital camera (Carl Zeiss, Inc., Beograd, Austria). Aliquots from dissolution baths were transferred directly to slides for visual observations of crystallization during dissolution testing. In addition, sediment isolated following 0.45 μm filtration and subsequent ultracentrifugation was also characterized under polarized light in order to evaluate the presence of crystallinity in the samples.

6.2.2.6. X-ray Powder Diffraction (XRPD) Analysis

X-ray powder diffractograms of solids isolated following the 2 hour dissolution experiments were measured on a PANalytical X'Pert PRO X-ray diffractometer (Almelo, The Netherlands). The voltage and current were 45 kV and 40 mA respectively. Samples were measured in reflection mode in the 2θ -range from 4-40° using an X'celerator detector. Data were collected using X'Pert Data Collector and viewed using X'Pert HighScore (PANalytical B.V., The Netherlands).

6.2.2.7. pKa Determination

The pKa values of ibuprofen in the presence and absence of PVP-VA64, MC, or HPMC were determined through spectrophotometric titration. The titrations were performed with the Sirius T3 instrument GLpKa (Sirius Analytical Instruments, East Sussex, UK) using a double junction electrode. The electrode was standardized from pH 1.8 to 12.2 and the KOH titrant was standardized against potassium hydrogen phthalate. Each sample was dissolved in ionic strength adjusted (ISA) water (0.15 M potassium chloride in water) to create a stock solution of 20.0 mg/ml. An aliquot of each stock solution was added to a titration vial and diluted up to 1.5 ml with ISA water. The starting pH of each solution was adjusted with 0.5 M potassium hydroxide. Each solution

was titrated with 0.5 M hydrochloric acid from about pH 9 to 1.8 at 25 °C in ISA water. For spectrophotometric analysis, spectra were recorded from 200-700 nm. The pKa values were calculated using T3 Simulator v.1.1 software. It was noted that solubilization of ibuprofen was maintained for the duration of the titrations, so addition of cosolvent was not required.

6.3. Results and Discussion

6.3.1. Evaluating Speciation of Ibuprofen Sodium in Aqueous Media

The behavior of ibuprofen sodium in water was evaluated by dynamic light scattering in order to confirm the surfactant-like nature of ibuprofen in solution and validate the utility of DLS to assess speciation of ibuprofen during dissolution experiments. Throughout the evaluated concentration range of 0.01 to 150 mg/mL, ibuprofen sodium remained solubilized with a clear solution being maintained for the duration of the experiment. A significant increase in particle size to ~60 nm radius was observed at a concentration above 17 mg/mL with a corresponding increase in the intensity of the scattered light (Figure 6.1). Wang and Matayoshi have previously defined the critical aggregate concentration (CAC) as the concentration of a compound where molecular aggregation first begins to form. They also noted a nonlinear increase in intensity during light scattering measurements at this point (8). These results are consistent with the CAC of ibuprofen sodium in water occurring around 17 mg/mL, which indicates that ibuprofen has the ability to form large soluble aggregates with a mean particle radius of 60 nm at this concentration. However, it was also noted that above a concentration of 41 mg/mL, a significant reduction in particle size was observed

along with a continued increase in intensity, with mean particle radii ranging from 1.4 to 3.2 nm. This transition in particle size is likely due to formation of micelles rather than larger solubilized aggregates. The concentration at which this occurs corresponds to the previously reported CMC for ibuprofen sodium in water at 25 °C, which was determined to be 180 mM or 41.1 mg/mL by fluorescence probe techniques (9). In addition, it has been previously reported that micelles of ibuprofen have an average particle size of 1.1 – 2 nm diameter using DLS analysis (10). The correlation between CMC observations between DLS and fluorescence approaches supports the utility of DLS as a technique to characterize ibuprofen speciation in solution.

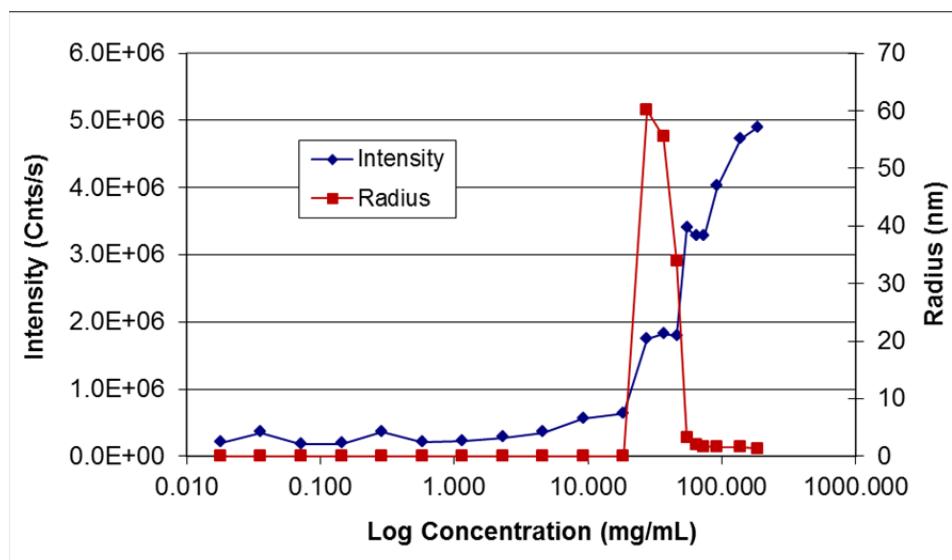


Figure 6.1. Normalized intensity (♦) or hydrodynamic radius (■) as a function of ibuprofen sodium concentration in water at 25 °C.

Drug concentrations of ibuprofen sodium alone in water above the CAC and CMC were also measured via different isolation methods in order to determine the effect of potential speciation during dissolution experiments in the presence of added polymer. Drug concentrations were measured following either filtration through 0.45 µm syringe filters or ultracentrifugation at 80,000 rpm for 20 minutes. Table 6.2 illustrates the full

recovery of ibuprofen following filtration or ultracentrifugation when dissolved at concentrations above the CAC and CMC. This is consistent with the observation of clear solutions and solubilized aggregates or micelles that were being detected by DLS in Figure 6.1. This also indicates that solubilized species, regardless of size, are measurable following either filtration or ultracentrifugation. When taking a closer look at the hydrodynamic radii of the solubilized particles during DLS evaluation of these samples, both the larger aggregates and smaller micelles remained intact following filtration, with aggregates observed at a concentration of 28.9 mg/mL and micelles observed at a concentration of 59.2 mg/mL. Alternatively, ultracentrifugation disrupted the stabilization of the larger aggregates at 28.0 mg/mL, with no large particles being detected by DLS following ultracentrifugation. Since the total measured drug concentration did not change following ultracentrifugation, the solubilized aggregates were not physically separated from the remainder of solubilized ibuprofen and were likely broken up. It is anticipated that only solid particles or amorphous colloids could be separated during ultracentrifugation (11). Therefore, ultracentrifugation was used as the method to quantify fully dissolved species, including solubilized free drug and solubilized drug-polymer monomers, micelles, and aggregates during these reported dissolution/supersaturation experiments. Alternatively, syringe filtration was used to quantify drug in non-solubilized drug/polymer colloids or solid nanoparticles in addition to fully dissolved species.

Table 6.2. Measured drug concentration and DLS evaluation of ibuprofen sodium in water at 25 °C following 0.45 μ m filtration or ultracentrifugation (n=3).

Theoretical Ibuprofen Concentration (mg/mL)	Measured Concentration (mg/mL \pm SD)		Radius (nm \pm SD)	
	Filtration	Ultracentrifugation	Filtration	Ultracentrifugation
28.9 ^a	29.6 \pm 0.4	28.7 \pm 0.6	27.4 \pm 2.6	0.4 \pm 0.1
59.2 ^b	59.4 \pm 0.4	58.8 \pm 1.4	1.0 \pm 0.1	0.9 \pm 0.0

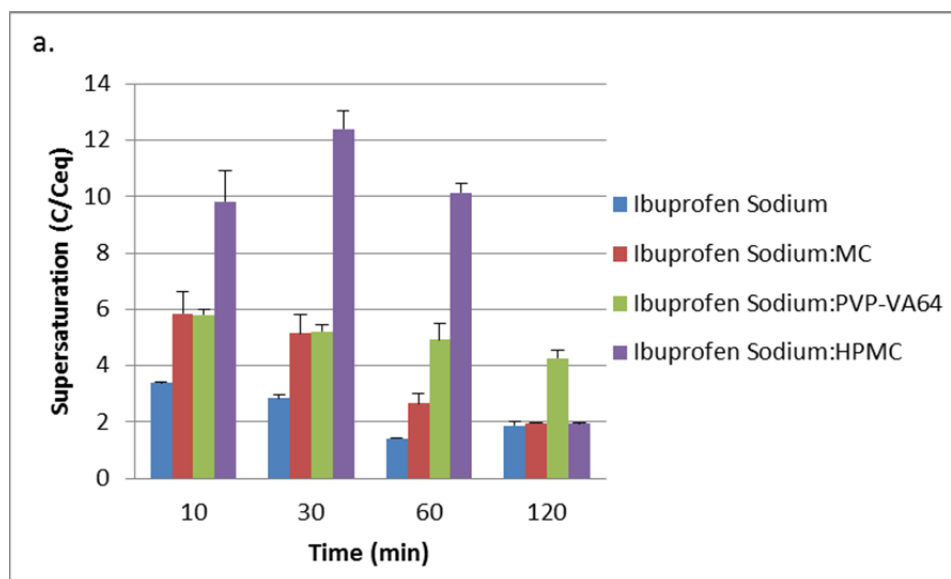
^a Concentration was between the CAC and CMC of ibuprofen sodium in water

^b Concentration was above the CMC of ibuprofen sodium in water

6.3.2. Characterization of Drug-Polymer Formulations during Dissolution

Dissolution studies were conducted in SGF at 37 °C with ibuprofen sodium alone or with MC, PVP-VA64, or HPMC. Samples were removed at the appropriate time points and filtered prior to analysis. The solubility of the filtrate was measured and reported as supersaturation ratio relative to 24 hour solubility data as a function of time for each formulation and summarized in Figure 6.2a. Minor solubility enhancement was observed initially following dissolution of ibuprofen sodium in SGF, with a three-fold increase in solubilized ibuprofen at 10 minutes relative to equilibrium solubility. Due to disproportionation of the sodium salt under acidic conditions and equilibration of the free acid, significant solubility enhancement was not maintained beyond 30 minutes. Modest solubility enhancement (6-fold) was observed with ibuprofen:MC formulations, but was lost over the 120 minute dissolution experiment, with loss of supersaturation relative to the ibuprofen sodium only formulation within 120 minutes. In contrast, a 4-6 fold increase in supersaturation was observed and maintained for ibuprofen sodium in the presence of PVP-VA64 for the duration of the experiment. Alternatively, a much higher degree of supersaturation was obtained for ibuprofen sodium:HPMC, with a 10 to 12-fold increase in solubilized ibuprofen sodium for the first 60 minutes in SGF. However, this was followed by loss of supersaturation at 120 minutes.

Similar patterns in duration of supersaturation for each of the drug:polymer formulations were also observed following isolation of fully dissolved species via ultracentrifugation (Figure 6.2b); however, the degree of supersaturation was not as large when compared to supersaturation determined following filtration. The maximum degree of supersaturation measured following ultracentrifugation was only 4-fold over 24 hour solubility values. This degree of supersaturation was observed for ibuprofen sodium with MC or HPMC at 10 minutes, but only maintained for 60 minutes with HPMC. The supersaturation achieved with MC was comparable to the HPMC formulations for the first 10 minutes following ultracentrifugation. The differences in degree and duration of supersaturation with each polymer formulation following isolation of solubilized drug via filtration and ultracentrifugation suggested that each polymer was enabling supersaturation of ibuprofen differently.



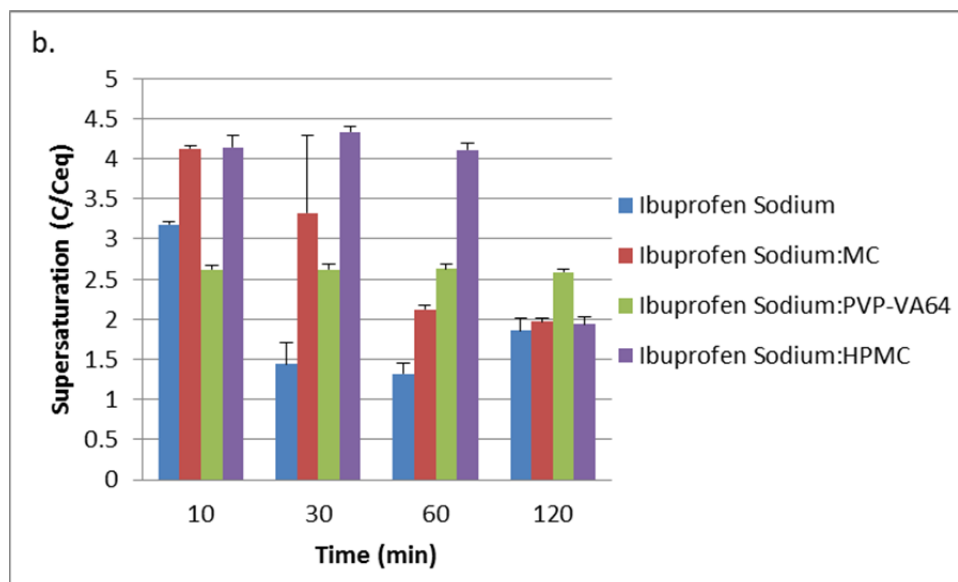
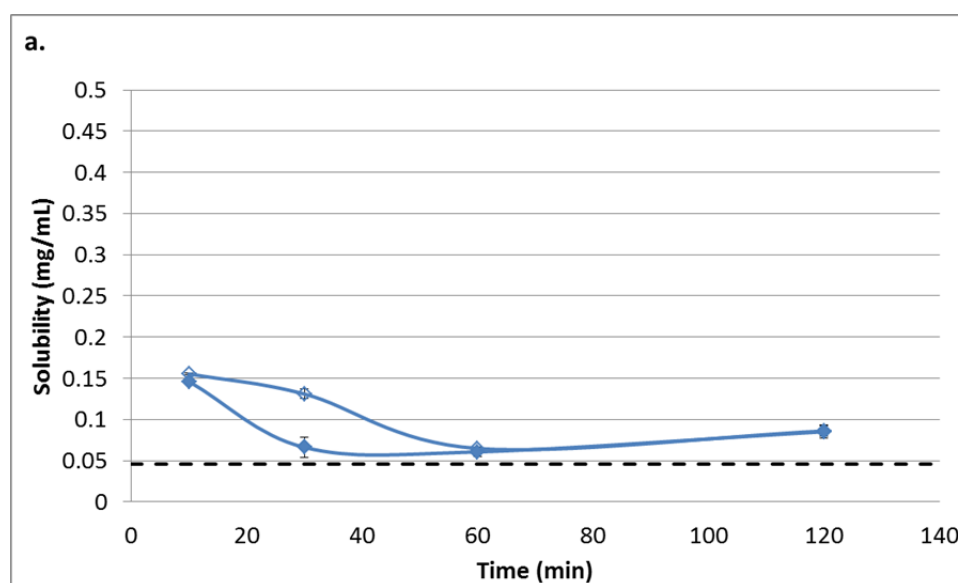


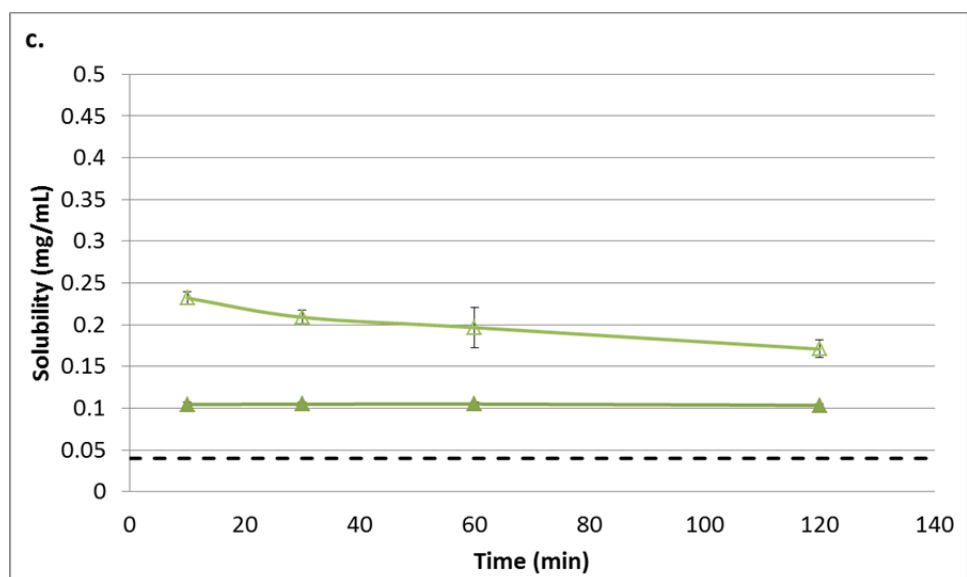
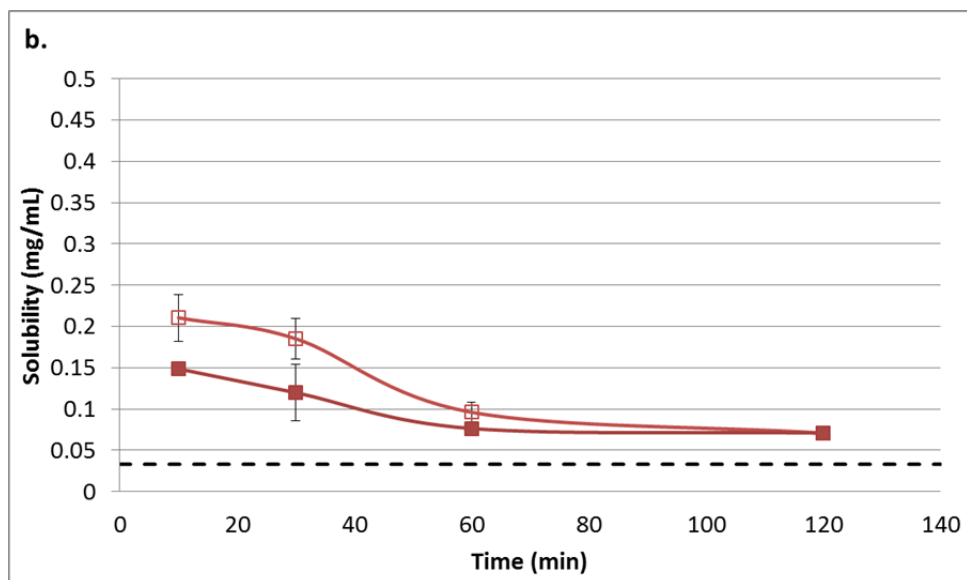
Figure 6.2. Supersaturation profiles of ibuprofen following addition of ibuprofen sodium formulations to SGF. Ibuprofen concentration was determination by (a) filtration or (b) ultracentrifugation.

The dissolution profiles of ibuprofen during supersaturation in SGF were examined for each formulation by comparing the solubility measured following filtration or ultracentrifugation in Figure 6.3. During dissolution of ibuprofen sodium in SGF (Figure 6.3a), the initial 3-fold increase in supersaturation at 10 minutes was observed following both filtration and ultracentrifugation. This lack of deviation in measured solubility following both approaches indicated that the observed supersaturation was associated with only fully dissolved ibuprofen rather than any colloidal particles or crystalline nanoparticles of free acid. The loss of supersaturation between 30 and 60 minutes correlated with an equilibration of ibuprofen free acid in SGF.

The measured solubility differed when filtration or ultracentrifugation were used for ibuprofen in the presence of MC (Figure 6.3b), PVP-VA64 (Figure 6.3c), or HPMC (Figure 6.3d) when ibuprofen was still at a supersaturated state. Overall, higher measured solubility was associated with the filtered samples while the ultracentrifuged samples had lower measured solubility. Nevertheless, the solubility of ibuprofen following

ultracentrifugation remained above the 24 hour solubility of each system for the duration that supersaturation was maintained. This supported the observation that supersaturation of ibuprofen was achieved in the presence of each of these polymers, with a portion of the supersaturated species being fully dissolved. The 1.5 to 2.5 fold increase in the solubility of the filtered samples versus the ultracentrifuged samples indicated that non-solubilized species with a particle size <450 nm were able to pass through the filter and contribute to the supersaturation reported in Figure 6.2a; however these non-solubilized species were removed from the sample during ultracentrifugation.





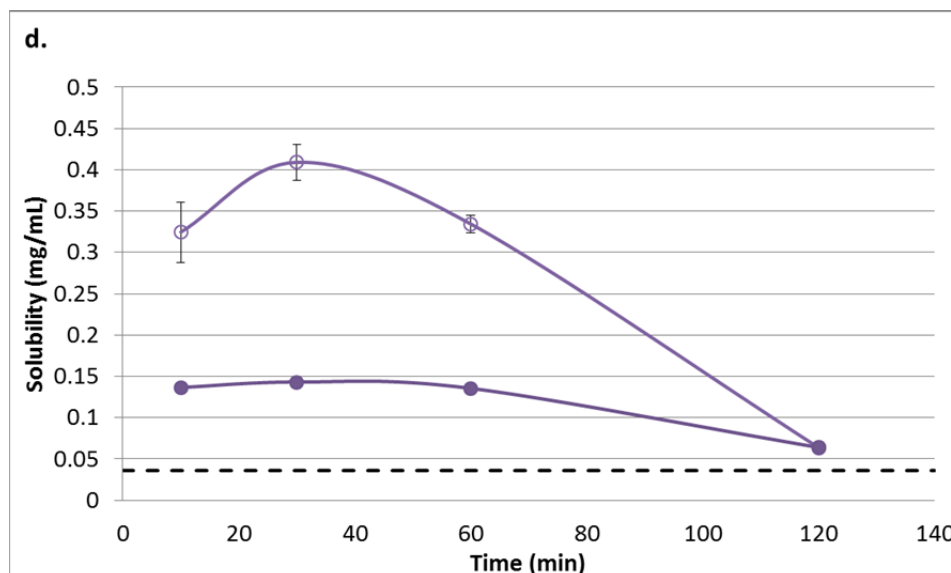


Figure 6.3. Ibuprofen solubility profiles in SGF at 37 °C for (a) ibuprofen sodium alone or ibuprofen sodium with (b) MC, (c) PVP-VA64, or (d) HPMC. Ibuprofen concentrations were determined following filtration (open symbols) and ultracentrifugation (closed symbols). The *dashed line* represents the 24 hour solubility of ibuprofen with polymer in SGF.

In order to confirm that non-solubilized nanoparticles or colloids were contributing to the measured supersaturation of ibuprofen in the presence of polymers, particle size evaluation of filtrate isolated during dissolution in SGF was conducted by dynamic light scattering (Table 6.3). Friesen *et al.* has previously noted that species capable of passing through a 0.45 μm filter include free drug, drug in micelles, and drug/polymer colloids (3). No particles were observed for ibuprofen sodium alone in SGF following 10 to 120 minutes. This corresponded to the proposal that initial supersaturation of ibuprofen observed following addition of the sodium salt to SGF at 10 minutes was associated with fully dissolved species rather than non-solubilized particles that passed through the 0.45 μm filter since solubility measured following filtration and ultracentrifugation was the same (Figure 6.3a). Since initial characterization of ibuprofen sodium by dynamic light scattering was able to detect aggregates and micelles (Figure

6.1), the supersaturation of ibuprofen sodium was associated with an increase in solubilized ibuprofen monomers that were below the limits of detection by DLS.

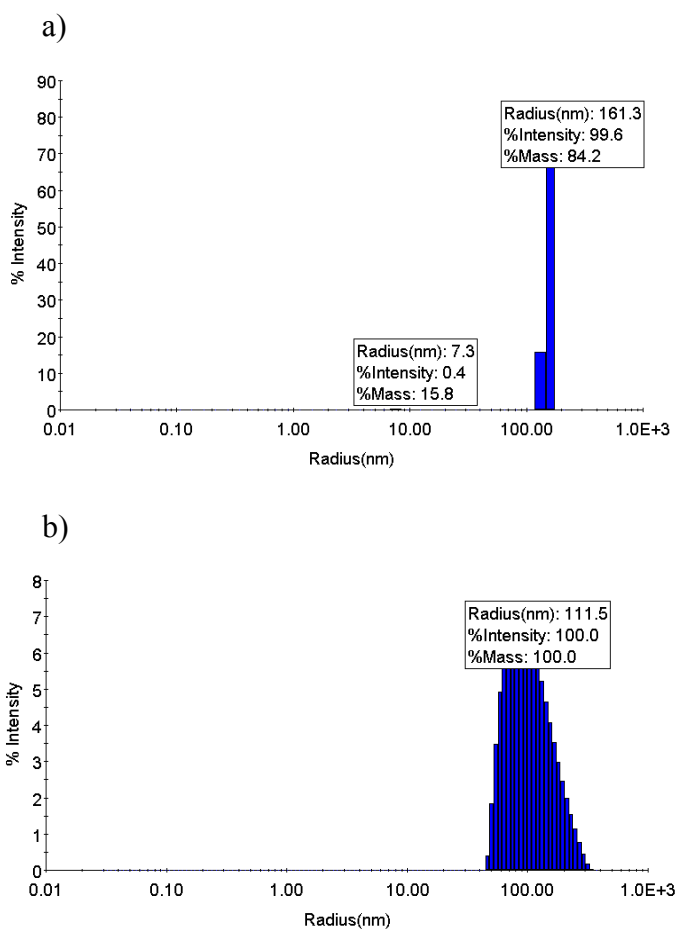
Table 6.3. Particle size data during dissolution of ibuprofen sodium in SGF in the presence and absence of polymer following filtration.

System	Radius (nm \pm SD)		
	10 minutes into SGF dissolution	120 minutes into SGF dissolution	Polymer Only in SGF
Ibuprofen Sodium	-	-	-
1:1 Ibuprofen Sodium:MC	155.1 \pm 4.0	17.3 \pm 0.4	28.9
1:1 Ibuprofen Sodium:PVP-VA64	106.5 \pm 10.7	106.2 \pm 3.6	8.9
1:1 Ibuprofen Sodium:HPMC	86.0 \pm 1.8	6.4 \pm 1.4	7.1

In contrast, nanoparticles with a mean radius of 86 to 155 nm were detected in the filtrate at 10 minutes for ibuprofen sodium formulations in the presence of MC, PVP-VA64, or HPMC (Table 6.3). Upon closer evaluation of the particle size distributions obtained during DLS analysis, a mixture of small particles with an average radius of 7.3 nm and larger particles with an average radius of 161 nm were observed for ibuprofen supersaturated in the presence of MC (Figure 6.4a). Based on the percent intensity and percent mass, the majority of species detected by DLS were the larger nanoparticles. Since the average particle size of MC only in SGF was determined to be 29 nm, the smaller species were likely associated with polymer monomers or small polymer aggregates while the larger aggregates were associated with ibuprofen. Since the concentration of ibuprofen in SGF was well below the reported CMC for ibuprofen (Figure 6.1), it is unlikely that ibuprofen micelles were contributing to this particle size distribution. For the particle size distributions of ibuprofen in PVP-VA64 (Figure 6.4b)

and HPMC (Figure 6.4c), large nanoparticles 86 to 111 nm in radius were observed.

Since no species with particles below 50 nm were detected by DLS, the polymer aggregates for PVP-VA64 and HPMC themselves, which were reported to have average particle radii of 7-9 nm (Table 6.3), were likely associated with ibuprofen as these larger particles. Previous work has demonstrated that ibuprofen adsorbs to HPMC in the form of mixed polymer-drug micelles when below the CMC of ibuprofen (9). Therefore, mixed aggregates of ibuprofen with polymer are proposed to be contributing to the supersaturation observed with the filtered samples during initial dissolution of the sodium salt with PVP-VA64 or HPMC in SGF.



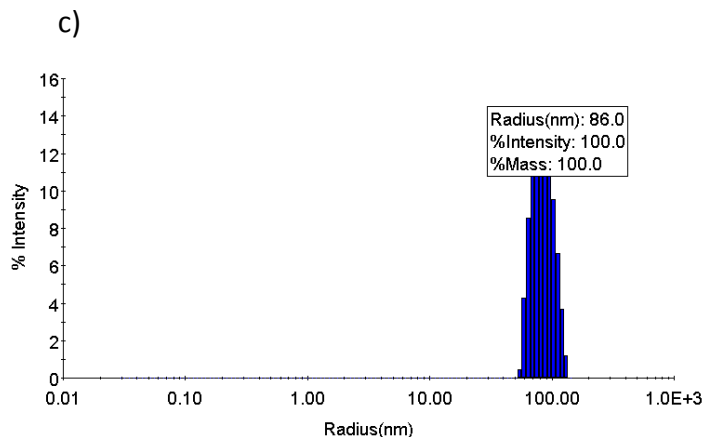
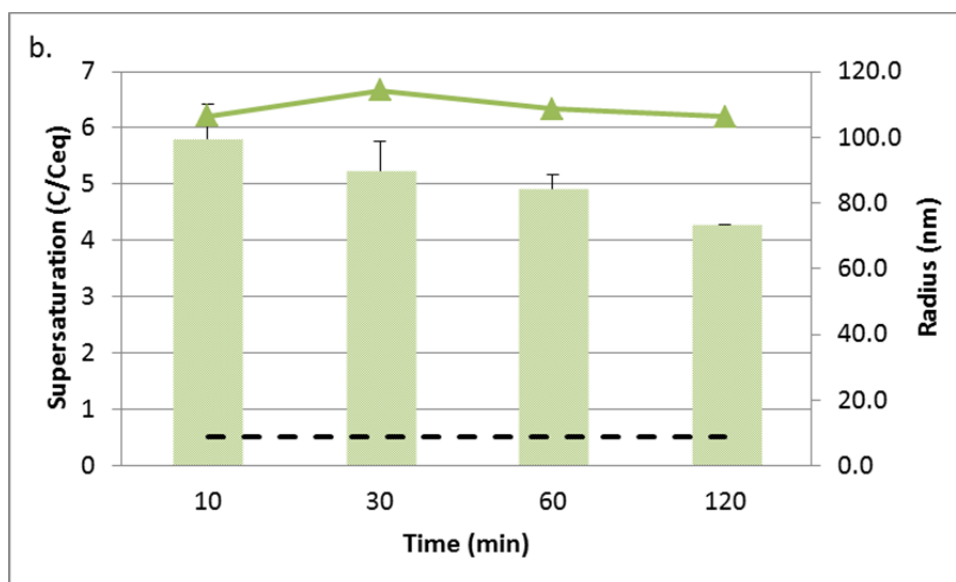
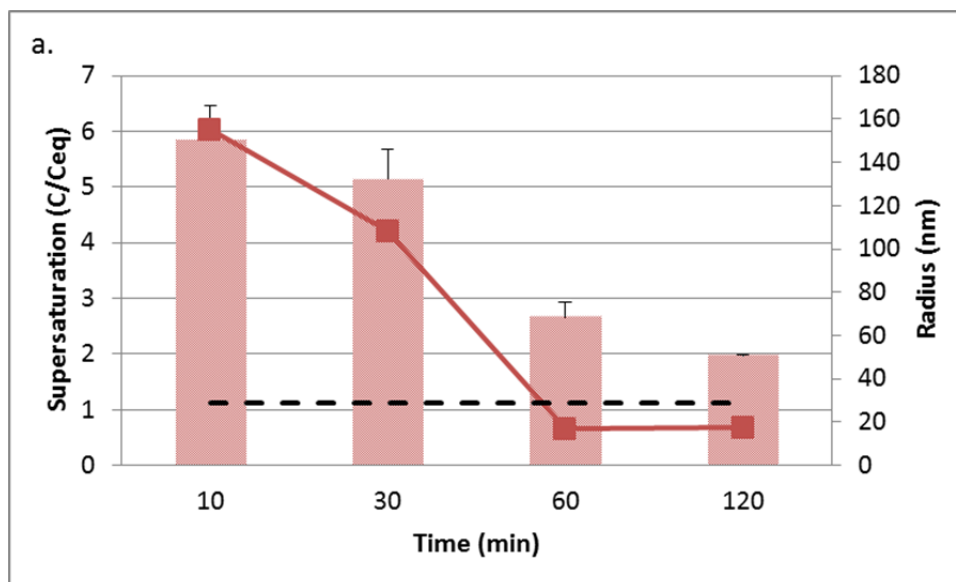


Figure 6.4. Particle size distribution by dynamic light scattering of ibuprofen with (a) MC, (b) PVP-VA64, and (c) HPMC in SGF at 10 minutes following filtration.

When comparing the DLS data of freshly filtered aliquots from 10 minutes to 120 minutes (Table 6.3), reduction in particle size was observed for the MC and HPMC formulations. These were also the same formulations that exhibited loss of supersaturation following 120 minutes in SGF (Figures 6.5a and 5c, respectively). The particles that were detected in these formulations at the end of the experiment were similar in size to the solubilized polymer particles detected in the polymer only solutions of SGF. In contrast, minimal change in aggregate size of particles observed from 10 to 120 minutes was noted for the ibuprofen sodium:PVP-VA64 formulation which maintained supersaturation for the duration of the experiment (Figure 6.5b). In summary, the presence of large particles, approximately 90 to 150 nm in mean radius, were observed when ibuprofen was in the supersaturated state in the presence of MC, PVP-VA64, or HPMC. Differences in particle size of these nanoparticle species can be attributed to the varying influence of each polymer on supersaturation rather than the formation of a common species during supersaturation since PVP-VA64 and HPMC was proposed to be included in these drug-polymer aggregates.



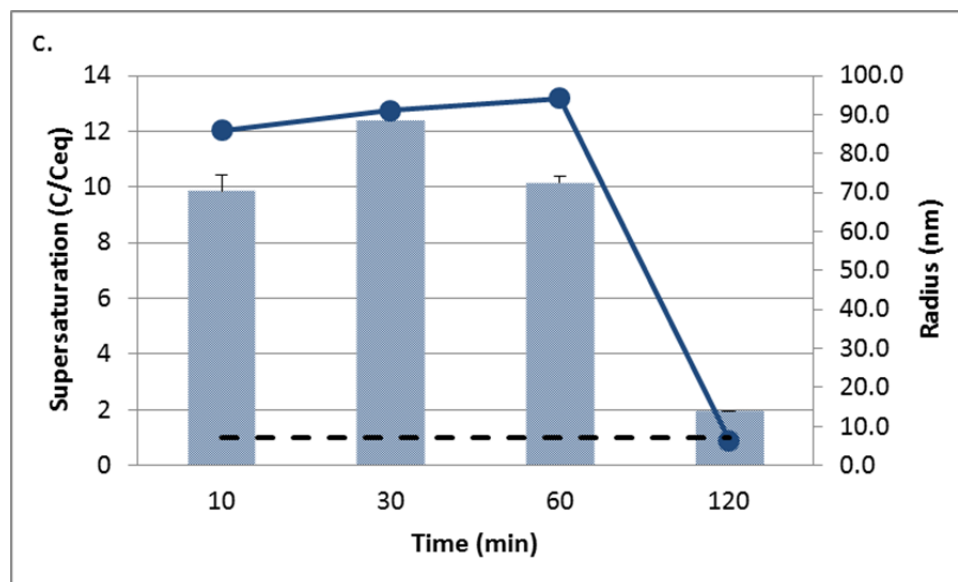


Figure 6.5. Comparison of ibuprofen supersaturation to particle size of filtrate as a function of time during dissolution in SGF of ibuprofen sodium with (a) MC, (b) PVP-VA64, or (c) HPMC. The bars represent the supersaturation of ibuprofen determined in triplicate and the error bars indicate standard deviation. The solid line represents average particle size data determined by DLS. The *dashed line* represents the particle size of polymer alone in SGF determined by DLS.

Dynamic light scattering was also conducted for ibuprofen samples in SGF following ultracentrifugation rather than filtration alone at 10 and 120 minutes (Table 6.4). Similar to the filtered samples of ibuprofen without polymer, no measurable particles were observed during DLS analysis of ultracentrifuged aliquots of ibuprofen sodium supersaturated in SGF at 10 minutes. Alternatively, ultracentrifuged samples containing ibuprofen and polymer were determined to have species with a mean radius similar in size to particles detected with polymer only controls in SGF. Based on the particle speciation evaluation of ibuprofen sodium summarized in Table 6.2, detection of large solubilized aggregates was not feasible following ultracentrifugation since it was proposed that ultracentrifugation disrupted aggregate stability while the micelles remained intact. Ultracentrifugation has also been previously described as a method to

separate colloidal particles from solubilized species (11). Therefore it was not surprising that the large nanoparticles were no longer detected following ultracentrifugation.

Table 6.4. DLS data during dissolution of ibuprofen sodium in SGF in the presence and absence of polymer following ultracentrifugation.

System	Radius (nm \pm SD)		
	10 minutes into SGF dissolution	120 minutes into SGF dissolution	Polymer Only in SGF
Ibuprofen Sodium	-	-	-
1:1 Ibuprofen Sodium:MC	10.0 \pm 3.3	23.0 \pm 1.3	22.5
1:1 Ibuprofen Sodium:PVP-VA64	3.2 \pm 2.8	8.6 \pm 2.2	6.3
1:1 Ibuprofen Sodium:HPMC	4.7 \pm 0.6	5.3 \pm 0.1	5.4

In order to determine whether the nanoparticles in the hundred nanometer range detected following filtration were associated with solubilized aggregates, colloids, or precipitated solid, pellets were isolated following ultracentrifugation of filtered samples at 10 minutes when supersaturation was observed for ibuprofen in the presence of MC, PVP-VA64, and HPMC. Observations by optical microscopy (Figure 6.6) illustrated that solid particles were present in the filtrate and separated from the solubilized species during ultracentrifugation. In the presence of MC, isolated pellets contained birefringent, crystalline particles. In contrast, amorphous aggregates were observed with the PVP-VA64 and HPMC systems based on observations of irregularly shaped particles that lacked birefringence. Significant reductions in ibuprofen concentration were noted following ultracentrifugation of supersaturated samples (Figures 6.3b-d), which demonstrated that the pellets isolated following ultracentrifugation consisted of non-solubilized drug. Although the DLS data of species in solution during supersaturation

indicated that polymer remained present in the solution following ultracentrifugation (Table 6.4), solubilized polymer was not quantified. Therefore, it is possible that the pellets isolated during supersaturation consisted of a colloidal mixture of drug and polymer. Since the presence of polymer was required to prolong supersaturation, it is proposed that amorphous ibuprofen colloids were successfully stabilized as aqueous suspensions due to the interactions of drug with PVP-VA64 or HPMC. This work also indicates that *in situ* formation of stabilized amorphous drug/polymer colloids may be successfully achieved with simple formulation compositions, including a highly soluble crystalline salt and polymer. Previous work has shown that the formation of stable amorphous drug/polymer nanostructures during oral administration of a spray-dried dispersion contributes to enhanced bioavailability (3). Therefore, it is anticipated that the formation of amorphous ibuprofen colloids during administration of ibuprofen sodium with PVP-VA64 or HPMC may also translate to increases in *in vivo* exposure.

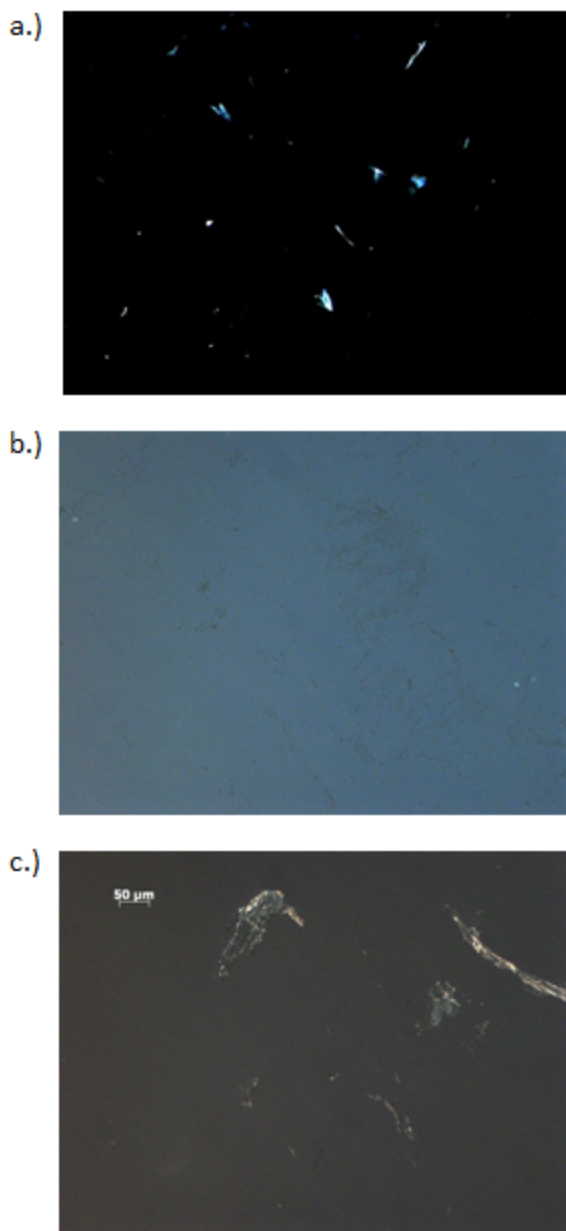


Figure 6.6. Polarized optical microscopy of pellets isolated via ultracentrifugation of filtrate following 10 minutes of ibuprofen sodium dissolution with (a) MC, (b) PVP-VA64, or (c) HPMC, at 100x magnification.

Initiation of ibuprofen crystallization during dissolution of drug-polymer formulations in SGF was determined by optical microscopy of the dissolution media over time (Figure 6.7). Initiation of ibuprofen crystallization was observed within 10 minutes for ibuprofen sodium alone or with MC even though supersaturation was still achieved during this time. The higher degree of supersaturation observed in the presence of MC,

even following ultracentrifugation, may be due to the ability of MC to slow the crystal growth of ibuprofen relative to the ibuprofen sodium control sample. This proposed decrease in crystal growth corresponded to observations of decreased particle size with the inclusion of MC during dissolution. Previous work suggested that the viscosity enhancement afforded by MC was the major parameter slowing the crystal growth of ibuprofen (Chapter 5).

The ability of ibuprofen to maintain supersaturation following nucleation was also observed with the PVP-VA64 and HPMC formulations. In the presence of HPMC or PVP-VA64, crystalline particles were first observed at 30 and 60 minutes, respectively. However, loss of supersaturation was not observed until after 60 minutes for the HPMC formulation and loss of supersaturation did not occur within 120 minutes for the PVP-VA64 formulation. Observations of prolonged supersaturation due to reduced crystal growth rate have been previously reported (12). Even though crystalline particles were observed in the media with the PVP-VA64 formulations at 60 minutes, isolated solid from ultracentrifuged samples remained amorphous. Alonzo et al. described two mechanisms of amorphous solid crystallization which included crystallization of the solid material or crystallization from the supersaturated solution (13). Since supersaturation was maintained for the duration of the dissolution experiment in the presence of PVP-VA64, minimal crystallization from solution was occurring. Therefore the crystallization was coming from the amorphous solid; however, the presence of polymer was substantially slowing the rate of crystal growth. Since the rate of crystal growth is proportional to the difference between the actual solution concentration and the equilibrium concentration (14); the higher degree of supersaturation associated with the

HPMC formulations relative to the PVP-VA64 formulation resulted in higher rates of crystal growth with the HPMC formulations.

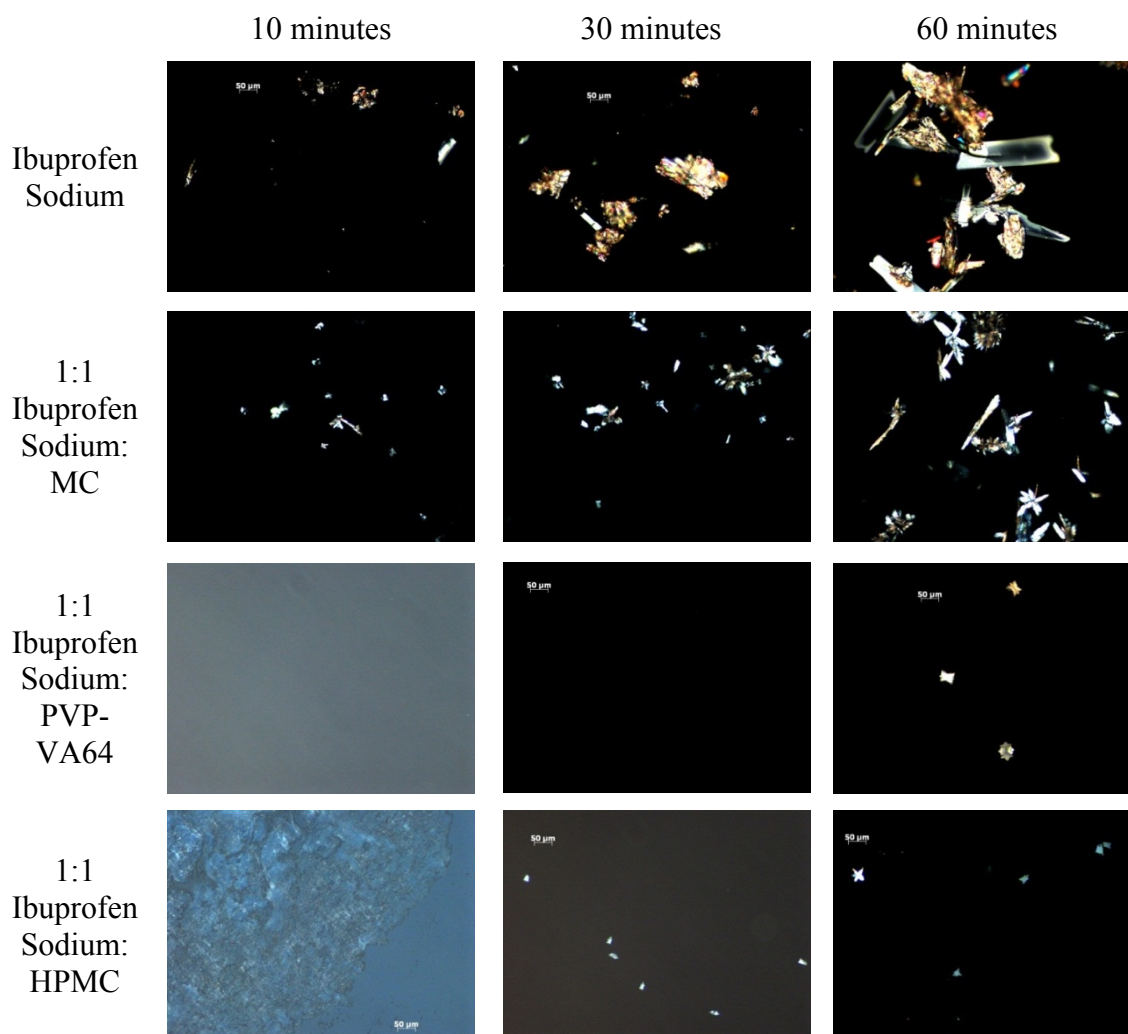


Figure 6.7. Optical microscopy following isolation of slurries from dissolution baths at 100x magnification.

XRPD analysis was conducted on isolated solids following two hours in SGF at 37 °C in order to confirm that the precipitate characterized following loss of supersaturation was the crystalline free acid of ibuprofen. Within 2 hours, ibuprofen sodium converted to the free acid in the presence and absence of each polymer formulation (Figure 6.8). Since the two known forms of ibuprofen, the S(+) enantiomer and the racemic form, have substantially different XRPD patterns (15, 16), XRPD

analysis was sufficient to confirm that the racemic form of the free acid was isolated from each system following dissolution in the presence and absence of polymer. Although supersaturation was still observed with the PVP-VA64 formulation, a sufficient portion of the solid isolated from the dissolution bath consisted of the crystalline free acid. This indicates that PVP-VA64 plays a role in maintaining supersaturation by slowing the crystal growth of the free acid through stabilization of the drug-polymer colloid which was still observed via DLS at the 120 minute time point (Figure 6.5b). Similar observations of stabilized triclosan colloidal suspensions with particles ranging in size from 90-250 nm have been reported in the presence of HPMC (17) and attributed to crystal growth inhibition and controlled nucleation due to hydrogen bonding between the drug and polymer (18).

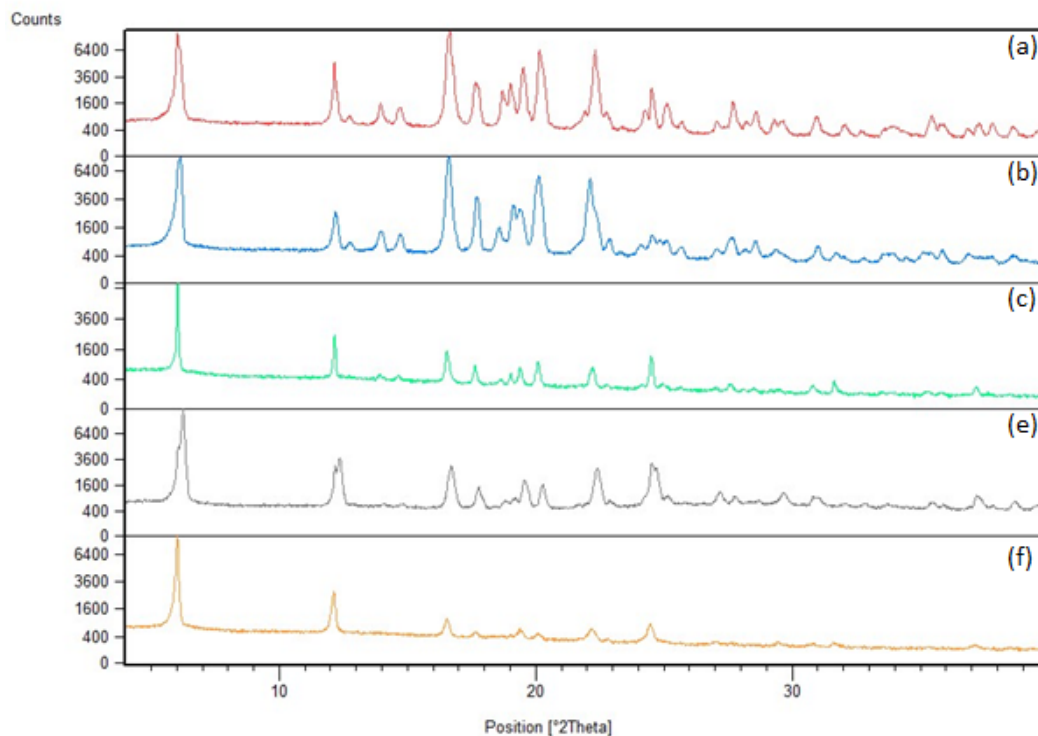


Figure 6.8. XRPD patterns comparing (a) ibuprofen free acid as a reference to ibuprofen sodium slurried in SGF at 37°C for 2 hours (b) alone, or with (c) PVP-VA64, (d) HPMC, or (e) MC.

6.3.3. pKa Determination

The influence of each polymer on the pKa of ibuprofen was experimentally determined by spectrophotometric titration in order to determine whether the observations of prolonged supersaturation during dissolution in SGF with MC, PVP-VA64 or HPMC could be due to thermodynamically changing the free energy of disproportionation. Previous work has demonstrated that mixed micelle formation of chlorpromazine and trifluoperazine with ionic surfactants resulted in a pKa shift for both compounds (19). However, Table 6.5 illustrates that the presence of polymer did not influence the pKa of ibuprofen. Therefore rapid disproportionation of ibuprofen sodium was anticipated in SGF regardless of the polymer. Nevertheless, modulation of microenvironmental pH has been shown to prolong supersaturation through the inclusion of pH modifying excipients with drug and polymer (20); however, the lack of ionizable groups on the polymers evaluated in this study suggest that the polymers used were also unable to modify the microenvironmental pH of the dissolution media in order to prolong supersaturation through delayed disproportionation of the highly soluble sodium salt. Therefore observations of ibuprofen supersaturation in the presence of these polymers are due to interactions occurring between the free acid of ibuprofen and each polymer.

Table 6.5. pKa values for ibuprofen in ISA water obtained by spectrophotometric titration in the absence and presence of polymer.

System	pKa
Ibuprofen	4.26 ± 0.005
Ibuprofen + MC	4.24 ± 0.001
Ibuprofen + PVP-VA64	4.27 ± 0.008
Ibuprofen + HPMC	4.24 ± 0.005

6.4. Conclusions

Supersaturation was observed during dissolution of ibuprofen sodium in SGF when MC, PVP-VA64, or HPMC was included in the formulation. By comparing ibuprofen solubility measurements following filtration or ultracentrifugation, it was determined that a portion of ibuprofen supersaturation was associated with non-solubilized colloids or crystalline nanoparticles while another component was attributed to a kinetic enhancement in fully dissolved species. This was confirmed by dynamic light scattering analysis and characterization of isolated solids via optical microscopy. During supersaturation in MC, the presence of crystalline nanoparticles was contributing to measured supersaturation following filtration, while amorphous colloids were present in supersaturated samples with PVP-VA64 or HPMC. Observations of crystalline particles in the dissolution media while supersaturation was still maintained suggested that each of these polymers was playing a role in prolonging supersaturation through delayed crystal growth of ibuprofen free acid. In addition, the absence of an ibuprofen pKa shift in the presence of any of these polymers indicated that a prolonged presence of ionized species in solution was likely not contributing to observations of prolonged supersaturation.

6.5. References

1. J. Brouwers, M.E. Brewster, and P. Augustijns. Supersaturating drug delivery systems: The answer to solubility limited oral bioavailability? *J Pharm Sci.* 98:2549-2572 (2009).
2. P. Gao and Y. Shi. Characterization of supersaturatable formulations for improved absorption of poorly soluble drugs. *AAPS J.* 14:703-713 (2012).
3. D.T. Friesen, R. Shanker, M. Crew, D.T. Smithey, W. Curatolo, and J. Nightingale. Hydroxypropyl methylcellulose acetate succinate-based spray-dried dispersions: an overview. *Mol Pharmaceutics.* 5:1003-1019 (2008).
4. M. Hawley and W. Morozowich. Modifying the diffusion layer of soluble salts of poorly soluble basic drugs to improve dissolution performance. *Mol Pharmaceutics.* 7:1441-1449 (2010).

5. D.B. Warren, H. Benameur, C.J.H. Porter, and C.W. Pouton. Using polymeric precipitation inhibitors to improve the absorption of poorly water-soluble drugs: A mechanistic basis for utility. *J Drug Targeting*:1-28 (2010).
6. S. Xu and W.-G. Dai. Drug Precipitation Inhibitors in Supersaturable Formulations. *Int J Pharm.* 453:36-43 (2013).
7. X. Li, S.D. Wettig, and R.E. Verrall. Isothermal titration calorimetry and dynamic light scattering studies of interactions between gemini surfactants of different structure and Pluronic block copolymers. *J Colloid Interface Sci* 282:466-477 (2005).
8. J. Wang and E. Matayoshi. Solubility at the Molecular Level: Development of a Critical Aggregation Concentration (CAC) Assay for Estimating Compound Monomer Solubility. *Pharm Res.* 29:1745-1754 (2012).
9. A. Ridell, H. Evertsson, S. Nilsson, and L.O. Sundelöf. Amphiphilic association of ibuprofen and two nonionic cellulose derivatives in aqueous solution. *J Pharm Sci.* 88:1175-1181 (1999).
10. T. Lee and C.W. Zhang. Dissolution enhancement by bio-inspired mesocrystals: the study of racemic (R, S)-(±)-sodium ibuprofen dihydrate. *Pharm Res.* 25:1563-1571 (2008).
11. S.B. Murdande, M.J. Pikal, R.M. Shanker, and R.H. Bogner. Solubility advantage of amorphous pharmaceuticals, part 3: Is maximum solubility advantage experimentally attainable and sustainable? *J Pharm Sci.* 100:4349-4356 (2011).
12. L. Lindfors, S. Forssen, J. Westergren, and U. Olsson. Nucleation and crystal growth in supersaturated solutions of a model drug. *J Colloid Interface Sci.* 325:404-413 (2008).
13. D.E. Alonzo, G.G.Z. Zhang, D. Zhou, Y. Gao, and L.S. Taylor. Understanding the behavior of amorphous pharmaceutical systems during dissolution. *Pharm Res.* 27:608-618 (2010).
14. J. Garside, A. Mersmann, and N. J. Measurement of Crystal Growth and Nucleation Rates, Rugby: Institute of Chemical Engineering, 2002.
15. G. Leising, R. Resel, F. Stelzer, S. Tasch, A. Lanziner, and G. Hantich. Physical aspects of dexibuprofen and racemic ibuprofen. *J Clin Pharmacol.* 36:3S-6S (1996).
16. N.V. Phadnis and R. Suryanarayanan. Simultaneous quantification of an enantiomer and the racemic compound of ibuprofen by X-ray powder diffractometry. *Pharm Res.* 14:1176-1180 (1997).
17. S. Raghavan, K. Schuessel, A. Davis, and J. Hadgraft. Formation and stabilisation of triclosan colloidal suspensions using supersaturated systems. *Int J Pharm.* 261:153-158 (2003).
18. S. Raghavan, A. Trividic, A. Davis, and J. Hadgraft. Crystallization of hydrocortisone acetate: influence of polymers. *Int J Pharm.* 212:213-221 (2001).
19. W. Caetano and M. Tabak. Interaction of chlorpromazine and trifluoperazine with ionic micelles: electronic absorption spectroscopy studies. *Spectrochim Acta, Part A.* 55:2513-2528 (1999).
20. T.T.D. Tran, P.H.L. Tran, and B.J. Lee. Dissolution-modulating mechanism of alkalizers and polymers in a nanoemulsifying solid dispersion containing ionizable and poorly water-soluble drug. *Eur J Pharm Biopharm.* 72:83-90 (2009).

APPENDIX A

Physical Characterization of Ibuprofen Free Acid and Sodium Salt

A.1. Physical Characterization of Ibuprofen

Ibuprofen has the chemical name of (R/S)-2-(4-(2-methylpropyl)phenyl)propanoic acid. The chemical structure of the free acid is illustrated in Figure A.1 and the chemical structure of the sodium salt appears in Figure A.2. The molecular weight of the free acid is 206.29 g/mol while the sodium salt has a molecular weight of 228.26 g/mol.

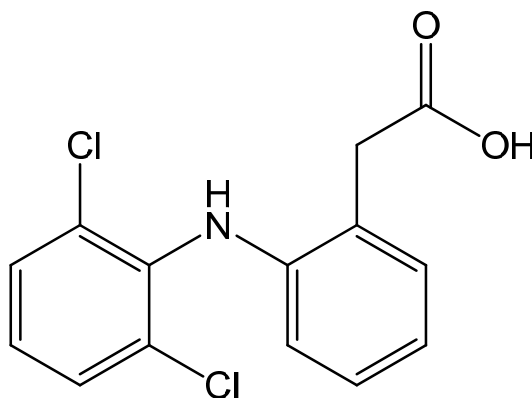


Figure A.1. Structure of ibuprofen free acid.

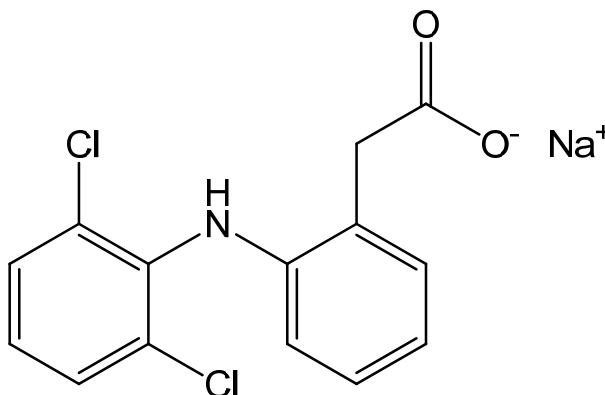


Figure A.2. Structure of ibuprofen sodium.

A.1.1. Materials

(R/S)-(\pm)-ibuprofen (free acid) was purchased from Sigma (Sigma-Aldrich, St. Louis, MO, USA) and the (R/S)-ibuprofen sodium dihydrate was prepared from the free

acid and 1.006 molar equivalents of sodium hydroxide. The crystallization for ibuprofen sodium dihydrate was based on the procedures outlined by Lee and Wang (1), but without the need for cosolvent to facilitate precipitation.

A.1.2. Methods

A.1.2.1. X-ray Powder Diffraction (XRPD)

X-ray powder diffractograms were measured on a PANalytical X'Pert PRO X-ray diffractometer (Almelo, The Netherlands). The voltage and current were 45 kV and 40 mA, respectively. Samples were measured in reflection mode in the 2θ -range from 4-40° using an X'celerator detector. Data were collected using X'Pert Data Collector and viewed using X'Pert HighScore (PANalytical B.V., The Netherlands).

A.1.2.2. Light Microscopy

The morphology of crystals were observed using a Zeiss Axiovert 200M polarizing microscope at a magnification of 200x and recorded using an Axiocam HRC digital camera (Carl Zeiss, Inc., Beograd, Austria).

A.1.2.3. Differential Scanning Calorimetry (DSC)

DSC was performed using an MDSC 2910 calorimeter (TA Instruments Co., USA). Samples were heated in Tzero aluminum pans with lids that were not crimped (TA Instruments Co., USA) at a heating rate of 10 °C/minute in a nitrogen environment.

A.1.2.4. Thermal Gravimetric Analysis (TGA)

TGA was performed using a TGA Q5000 (TA Instruments Co., USA). Samples were placed on a tared platinum pan and heated at a ramp rate of 10 °C/minute from 25 to 300 °C.

A.1.2.5. Microtrac Assessment of Particle Size

Particle size of solid compound was measured using a SRA150 Microtrac. 100% Isopar G was used as the media and the flow rate was set at 60%. Compound was suspended in Isopar G with 0.25% lecithin prior to addition to cell for particle size measurement. The set zero was 30 seconds, followed by a run time of 10 seconds. 3 runs were acquired and averaged prior to data reporting following 30 seconds of sonication.

A.1.3. Results of Ibuprofen Free Acid Characterization

Based on XRPD analysis, the ibuprofen material was crystalline as received (Figure A.3). Since the two known forms of ibuprofen, the S(+) enantiomer and the racemic form, have substantially different XRPD patterns (2, 3), XRPD analysis confirmed that the racemic form of the free acid was characterized during this analysis. The measured melting point of 78.2 °C (Figure A.5) also conforms with the previously reported melting point for the racemic form of ibuprofen free acid (1, 4).

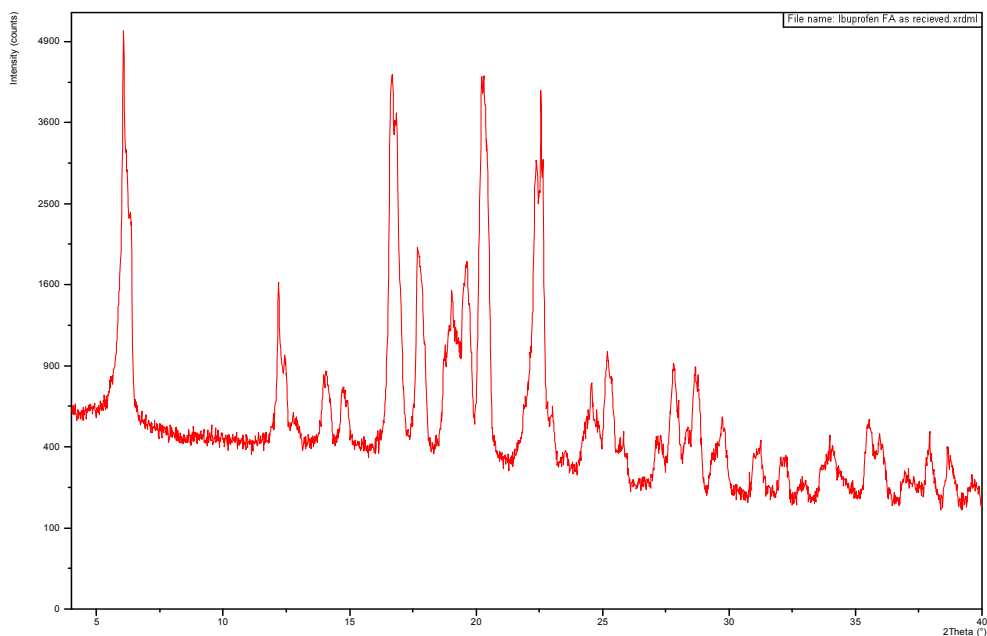


Figure A.3. XRPD of ibuprofen free acid.



Figure A.4. Microscopy of ibuprofen free acid at 200x magnification.

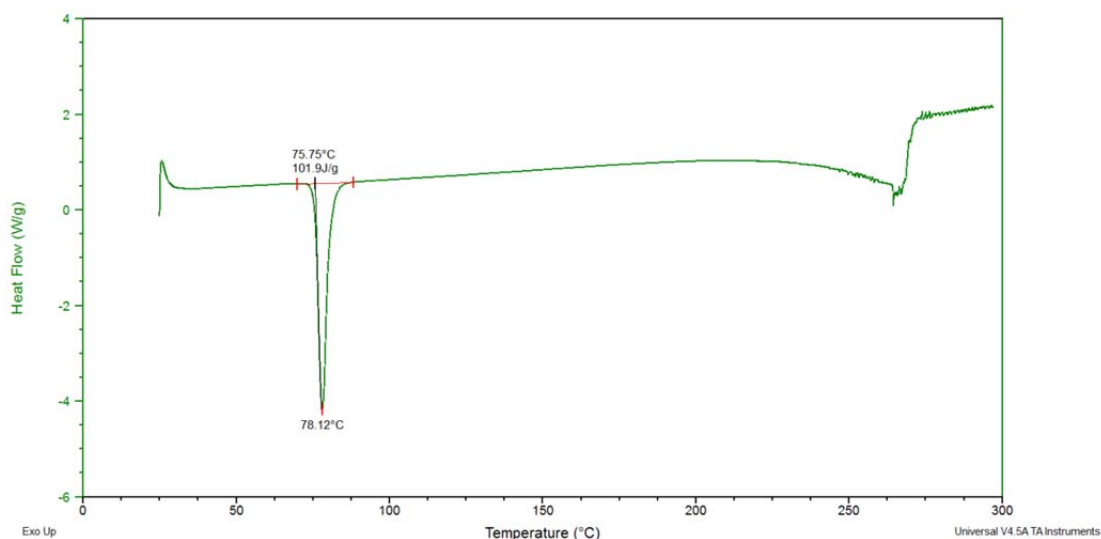


Figure A.5. DSC trace of ibuprofen free acid.

A.1.4. Results of Ibuprofen Sodium Characterization

Based on XRPD analysis (Figure A.6) and observations by optical microscopy (Figure A.7), the ibuprofen sodium was isolated as a crystalline solid. The thermal analysis of the solid (Figure A.8) illustrated a broad endotherm around 99.36 °C which corresponds to the loss of two moles of water (13.44% weight loss from 25-100 °C). The loss of water is followed by the melt at 201.15 °C. Based on XRPD and DSC data, the material was prepared as the racemic conglomerate of ibuprofen sodium dihydrate (5).

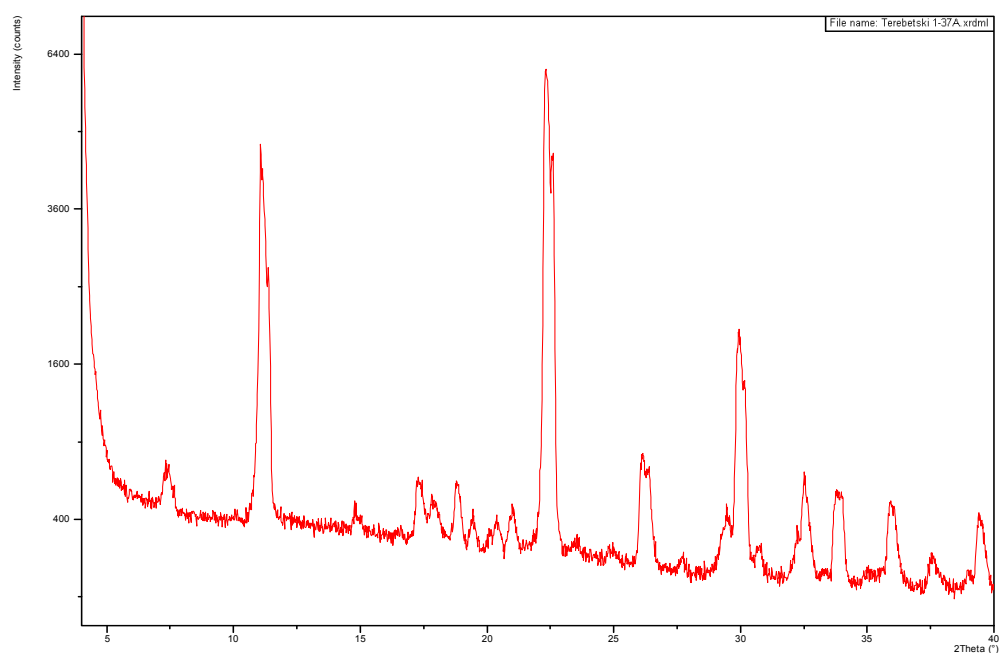


Figure A.6. XRPD of ibuprofen sodium dihydrate.

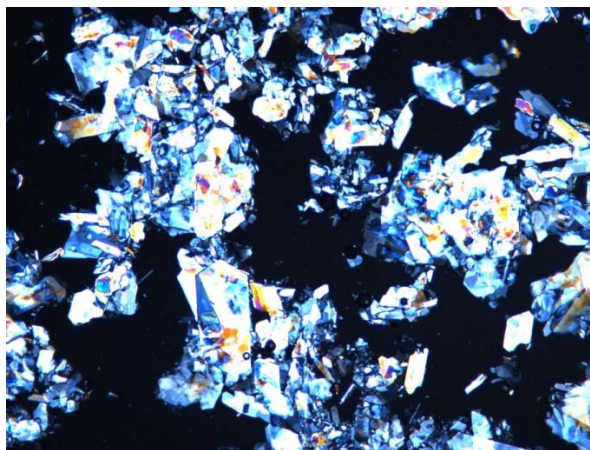


Figure A.7. Microscopy of ibuprofen sodium dihydrate at 200x magnification.

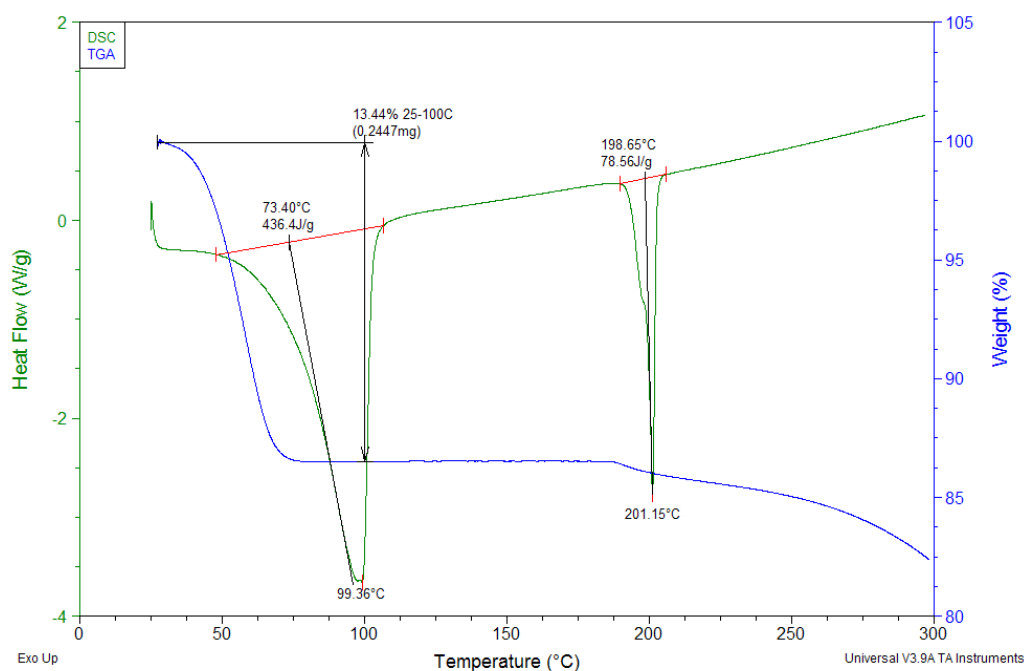
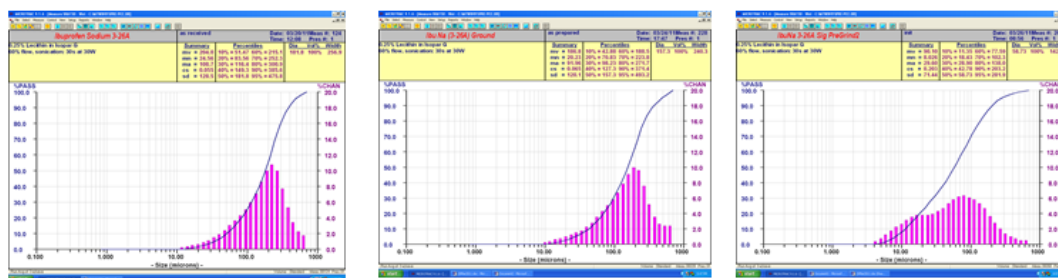


Figure A.8. Overlay of DSC and TGA of ibuprofen sodium dihydrate.

Ibuprofen sodium dihydrate crystals had a plate-like morphology (Figure A.7). Table A.1 and Figure A.9 illustrate the broad particle size distribution for this material. Following crystallization and isolation, the initial particle size of ibuprofen sodium salt had a mean volume of 204 microns, with 95% of particles having a particle size <276 micron. Significant particle size reduction of ibuprofen was feasible through grinding, with a resulting mean particle size of 90 microns. In order to enable rapid dissolution of ibuprofen sodium, ibuprofen sodium dihydrate was ground prior to use in any additional studies.

Table A.1. Particle size distribution data for ibuprofen sodium dihydrate.

Sample	Mean Volume (microns)	Standard Deviation	95 Percentile (microns)
Ibuprofen Sodium, as prepared	204.0	128.5	475.8
Ibuprofen Sodium, ground	186.8	120.1	493.2
Ibuprofen Sodium, ground significantly	90.10	71.44	281.9

**Figure A.9.** Summary of particle size data for ibuprofen sodium dihydrate.

A.2. pKa Titration for Ibuprofen Sodium

A.2.1. Methods

A.2.1.1. pKa Determination

The pKa value of ibuprofen was determined through spectrophotometric titration. The titration was performed with the Sirius T3 instrument GLpKa (Sirius Analytical Instruments, East Sussex, UK) using a double junction electrode. The electrode was standardized from pH 1.8 to 12.2 and the KOH titrant was standardized against potassium hydrogen phthalate. Ibuprofen sodium was dissolved in ionic strength adjusted (ISA) water (0.15 M potassium chloride in water) to create a stock solution of 20.0 mg/ml. An aliquot of stock solution was added to a titration vial and diluted up to 1.5 ml with ISA water. The starting pH was adjusted with 0.5 M potassium hydroxide. The solution was titrated with 0.5 M hydrochloric acid from about pH 9 to 1.8 at 25 °C in ISA water. For spectrophotometric analysis, spectra were recorded from 200-700 nm. The pKa values were calculated using T3 Simulator v.1.1 software. It was noted that solubilization of

ibuprofen was maintained for the duration of the titrations, so addition of cosolvent was not required.

A.2.2. Results for pKa Determination of Ibuprofen Sodium

Based on spectrophotometric titration, the pKa of ibuprofen is 4.25 in ISA water (Figure A.10). This is slightly lower than the previously published pKa value of 4.5 (6).

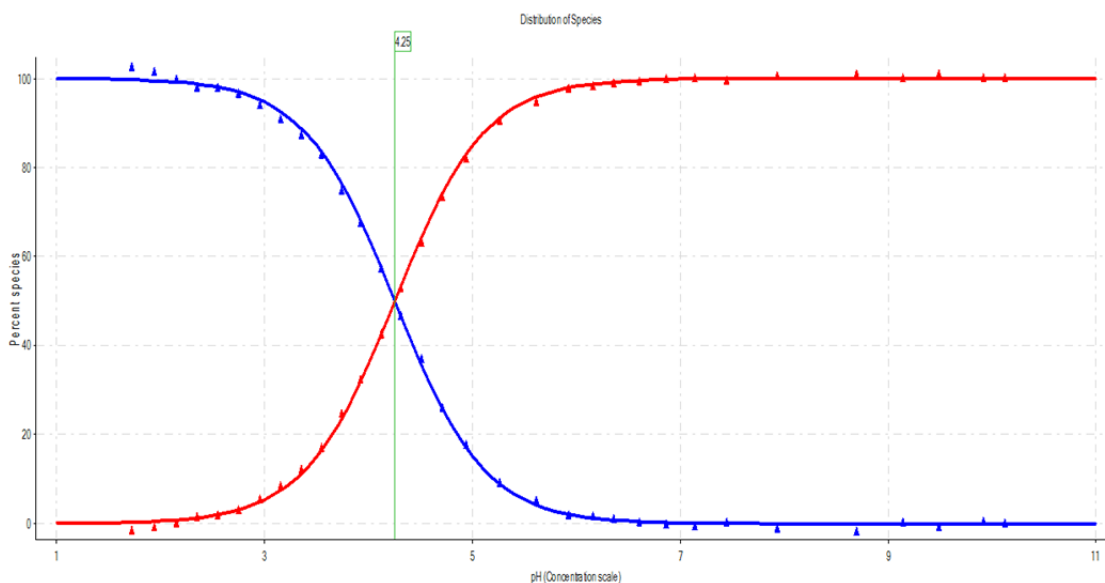


Figure A.10. pKa determination of ibuprofen sodium in ISA water (unionized species in blue and ionized species in red).

A.3. pH-Dependent Solubility Profile of Ibuprofen Sodium

A.3.1. Methods

A.3.1.1. Equilibrium Solubility as a Function of pH

Solid ibuprofen sodium and free acid was slurried in aqueous buffers from pH 1.5 to 12 for multiple days in order to determine equilibrium solubility of ibuprofen at 37 °C. Samples were filtered periodically and diluted with mobile phase for HPLC analysis.

Measurements of pH were also made using an Accumet pH meter. Additional solid was added in cases where complete dissolution of compound was observed.

A.3.1.2. High Performance Liquid Chromatography (HPLC) Analysis

Sample concentrations for equilibrium solubility studies were determined using an Agilent 1100 series HPLC instrument. The HPLC method used an Ascentis Express C18 column (2.7 μm fused-core particle size, 4.6 mm i.d. \times 100 mm length) at 40 $^{\circ}\text{C}$ with a 3-minute linear gradient from 10% to 95% mobile phase A (acetonitrile) and 90% to 5% of mobile phase B (0.1% phosphoric acid) followed by a 1-minute hold at 95% A. The flow rate was 1.8 mL/min and the injection volume was 5 μL . The samples were analyzed with UV detection at 210 nm. Calibration curves were constructed from peak area measurements using standard solutions of ibuprofen free acid at known concentrations. The retention time of ibuprofen was approximately 3.1 minutes.

A.3.2. Results of pH-Dependent Solubility Assessment

The pH solubility profile for ibuprofen sodium illustrates the low solubility associated with the free acid and the very high solubility of the sodium salt when in aqueous media (Figure A.11). Based on the pH solubility curve, the pKa is around 4.25-4.5 while the pH_{max} for the sodium salt occurs at pH 6.9-7.2.

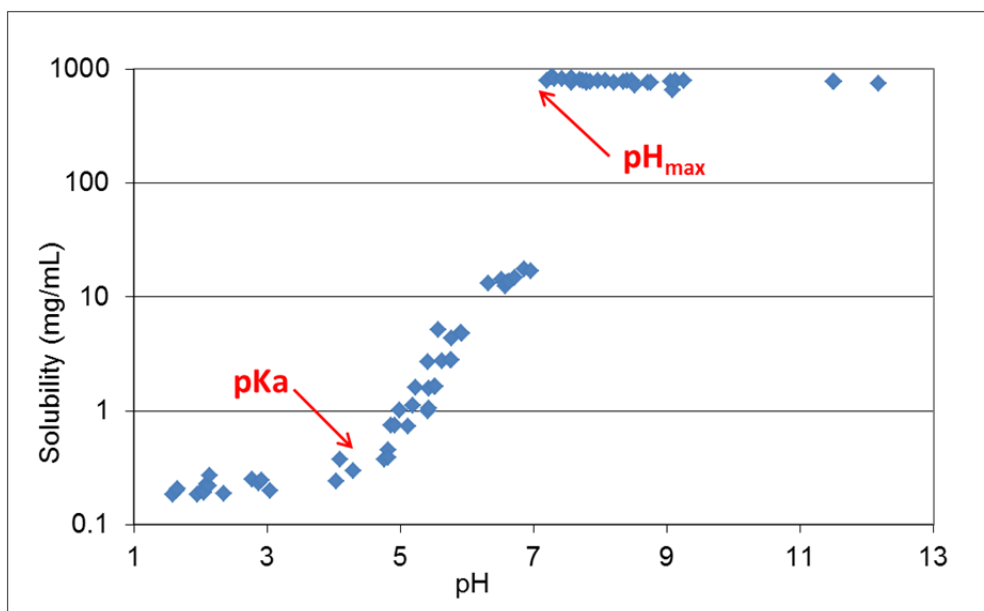


Figure A.11. pH solubility profile of ibuprofen sodium dihydrate at 37 °C.

A.4. References

1. T. Lee and Y.W. Wang. Initial salt screening procedures for manufacturing ibuprofen. *Drug Dev Ind Pharm.* 35:555-567 (2009).
2. G. Leising, R. Resel, F. Stelzer, S. Tasch, A. Lanziner, and G. Hantich. Physical aspects of dexibuprofen and racemic ibuprofen. *J Clin Pharmacol.* 36:3S-6S (1996).
3. N.V. Phadnis and R. Suryanarayanan. Simultaneous quantification of an enantiomer and the racemic compound of ibuprofen by X-ray powder diffractometry. *Pharm Res.* 14:1176-1180 (1997).
4. A.J. Romero and C.T. Rhodes. Stereochemical aspects of the molecular pharmaceutics of ibuprofen. *J Pharm Pharmacol.* 45:258-262 (1993).
5. G.G.Z. Zhang, S.Y.L. Paspal, R. Suryanarayanan, and D.J.W. Grant. Racemic species of sodium ibuprofen: Characterization and polymorphic relationships. *J Pharm Sci.* 92:1356-1366 (2003).
6. H. Potthast, J.B. Dressman, H.E. Junginger, K.K. Midha, H. Oeser, V.P. Shah, H. Vogelpoel, and D.M. Barends. Biowaiver monographs for immediate release solid oral dosage forms: Ibuprofen. *J Pharm Sci.* 94:2121-2131 (2005).

APPENDIX B

HPLC Method Validation of Ibuprofen

B.1. HPLC Method Validation

B.1.1. Materials

(R/S)-(±)-ibuprofen (free acid) was purchased from Sigma (Sigma-Aldrich, St. Louis, MO, USA) and the (R/S)-ibuprofen sodium dihydrate was purchased from Fluka (Sigma-Aldrich, St. Louis, MO, USA). HPLC grade acetonitrile and 85% phosphoric acid were purchased from Sigma-Aldrich (St. Louis, MO, USA). Deionized water from the house line was used for all aqueous solutions and these were prepared as needed for each experiment.

B.1.2. Method

An Agilent 1100 series HPLC instrument with Degasser G1379A, Quarternary Pump G1311A, Temperature-Controlled Autosampler G1329A/B, Column Compartment G1316A, Diode Array Detector G1315B, and Empower Pro software was used for ibuprofen method validation. The optimized chromatographic method conditions included: column - Ascentis Express C18, 2.7 μm fused-core particle size, 4.6 mm i.d. \times 100 mm length; column temperature – 40 °C; injection volume – 5 μL ; UV detection wavelength – 210 nm; mobile phase: A = acetonitrile, B = 0.1% phosphoric acid in HPLC water (3-minute linear gradient from 10% to 95% mobile phase A and 90% to 5% of mobile phase B followed by a 1-minute hold at 95% A); flow rate – 1.8 mL/min; run time – 4 minutes; sample diluents – 1:1 acetonitrile:water.

B.1.3. Standard Preparation

Standards were prepared by weighing 10.2 mg of ibuprofen free acid into a clean 50 mL volumetric flask. The flask was then diluted to volume with 1:1 acetonitrile:water (this sample is the 204.0 µg/mL standard). Using volumetric pipettes, 0.875 mL of the 204.0 µg/mL standard was transferred to an HPLC vial and diluted to a final volume of 1 mL with 1:1 acetonitrile:water. The sample was capped and vortexed to prepare the 178.5 µg/mL standard. This process was repeated, resulting in calibration standards of 204.0, 178.5, 153.0, 127.5, 102.0, 51.0, 25.5, 10.2, 5.10, 1.02, 0.51, and 0.20 µg/mL standards.

B.1.4. Method Validation

Results of standards ranging from 0.20 µg/mL to 204.0 µg/mL are shown in Table B.1 below. Each standard was injected in triplicate. At concentrations <1.02 µg/mL, significant variability is observed with high associated percent RSD of these injections. While the limit of detection (LOD) is <0.20 µg/mL, the limit of quantitation (LOQ) is between 0.51 and 1.02 µg/mL.

Table B.1. Ibuprofen standard concentrations with average chromatogram peak area, standard deviation, and relative standard deviation of three separate runs.

Concentration (µg/mL)	AVG (mV*s)	SD	% RSD
0	0	0	-
0.20	1516	230.57	15.21
0.51	3553	212.18	5.97
1.02	6752	33.87	0.50
5.10	32763	256.50	0.78
10.2	65430	187.44	0.29
25.5	161289	112.82	0.07
51.0	315199	463.50	0.15
102.0	624480	521.69	0.08
127.5	776141	2898.55	0.37
153.0	919234	1934.80	0.21
178.5	1051759	4103.23	0.39
204.0	1176622	3482.60	0.30

Linearity of the current method was observed with standards ranging from 1.0 µg/mL to 178.5 µg/mL, with an R^2 value of 0.9994 (Figure B.1). When the standards range from 1.0 µg/mL - 204.0 µg/mL, loss of linearity is initiated with an R^2 value decreasing to 0.9987.

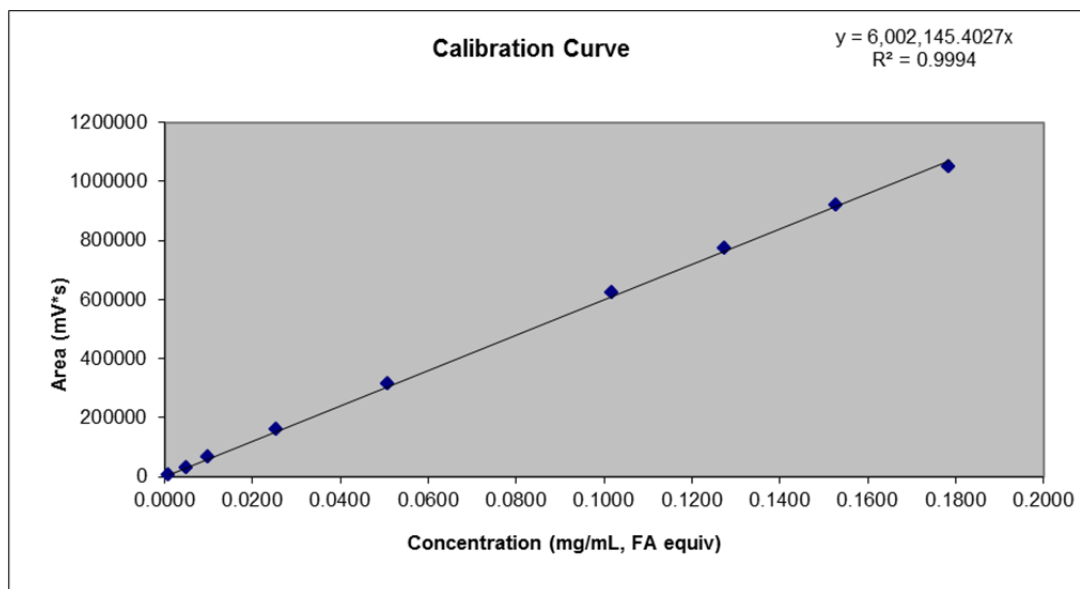


Figure B.1. Average ibuprofen standard curve, with standard concentrations ranging from 1.0 – 178.5 µg/mL.

Precision measures the degree of reproducibility among individual test results when the method is applied repeatedly to the same or similar samples. The current method passed the test for repeatability as determined by the percent RSD of six replicates at a concentration of 102.0 µg/mL. The average area of the 102.0 µg/mL standard was 625056.50 mV*s, with a standard deviation of 847.65 and a % RSD of 0.14, which meets the precision criteria for RSD <0.5%.

In order to understand the intermediate precision of the method, intra- and inter-day variabilities were tested over two days with calibration curves generated separately on the same day as well as on two separate days, respectively, with standard solutions ranging in concentration from 1.0 to 178.5 µg/mL. Intra-day precision was tested by

comparing the calibration curves for Run 1 and Run 4 which were prepared and analyzed on the same day. The % RSD of the slope of the best fit line was 0.15% for the intra-day precision analysis. Inter-day precision was tested over two days by comparing calibration curves generated with Run 4 and Run 5. The % RSD of the slope of the best fit line was 0.43% which is lower than the requirement of 2% for intermediate precision.

B.1.5. Specificity

B.1.5.1. Filter Validation

The use of filters will be important when preparing dissolution and solubility samples of ibuprofen where removal of excess solids will be required to accurately measure ibuprofen solubility. Methods of filtration will include centrifuge filtration through 0.45 μm Millipore Ultrafree-MC centrifuge filters via 10 minutes of centrifugation as well as syringe filtration with Titan 3, 17mm, 0.45 μm PTFE syringe filters. In order to confirm minimal retention of solubilized ibuprofen during filtration, aliquots of three varying concentrations of ibuprofen sodium solutions in water were passed through filters in triplicate. In order to better understand risk of filter retention, 3 mL of three varying concentrations of ibuprofen water solutions were also passed through the Titan 3 0.45 μm PTFE syringe filter in triplicate, with the first 2 mL discarded and the final 1 mL retained for further analysis. Samples were analyzed and compared to their unfiltered equivalents. Results shown in Tables B.2-B.4 indicate that use of either filtration method (centrifuge or syringe filter) is acceptable. In addition, there is no need to saturate the filter prior to retaining sample in order to minimize ibuprofen retention on the filter.

Table B.2. Filter validation set for centrifuge filtration.

Concentration (mg/mL)	Average Area (mV*s) Filtered Sample	SD	% RSD	Average Area (mV*s) Unfiltered Sample	% Claim
0.994	542718.33	1694.89	0.31	542166.00	100.10
0.0994	275889.00	1970.33	0.71	277074.67	99.57
0.00994	28059.00	191.16	0.68	28420.67	98.73

Table B.3. Filter validation set for syringe filtration.

Concentration (mg/mL)	Average Area (mV*s) Filtered Sample	SD	% RSD	Average Area (mV*s) Unfiltered Sample	% Claim
0.994	542249.33	1679.94	0.31	542166.00	100.02
0.0994	275927.33	612.88	0.22	277074.67	99.59
0.00994	28155.33	231.65	0.82	28420.67	99.07

Table B.4. Filter validation set for syringe filtration (with 2 mL discarded prior to analysis).

Concentration (mg/mL)	Average Area (mV*s) Filtered Sample	SD	% RSD	Average Area (mV*s) Unfiltered Sample	% Claim
0.994	542644.67	1709.06	0.31	542166.00	100.09
0.0994	277279.67	174.64	0.06	277074.67	100.07
0.00994	28395.67	145.19	0.51	28420.67	99.91

B.1.5.2. Solution Stability

Solution stability of ibuprofen in 1/1 acetonitrile/water was evaluated by using the autosampler. The temperature was uncontrolled so that samples were kept under ambient laboratory conditions. The samples were also continuously exposed to laboratory light. Approximately every hour, the 50.0 µg/mL standard was analyzed for up to 22 hours. The data shown in Table B.5 below indicates that ibuprofen is stable in 1/1 acetonitrile/water for at least 22 hours and therefore degradation by hydrolysis, photolysis or adhesion to glassware is not a concern with runs lasting up to 22 hours.

Table B.5. Solution stability of 50.0 µg/mL standard following 22 hours of storage at ambient conditions.

Average Area (mV*s)	65577.72
SD	311.36
% RSD	0.47
Minimum Area (mV*s)	65141.00
Maximum Area (mV*s)	66502.00

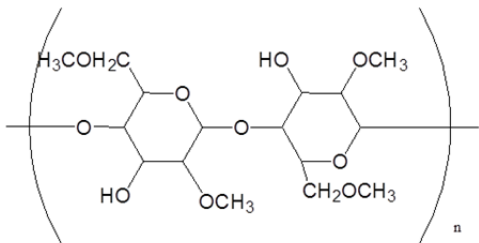
APPENDIX C

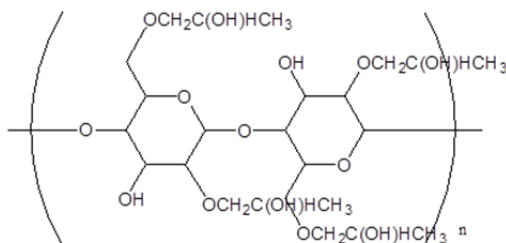
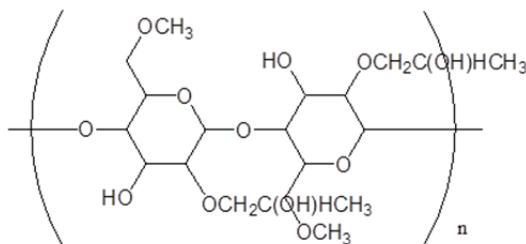
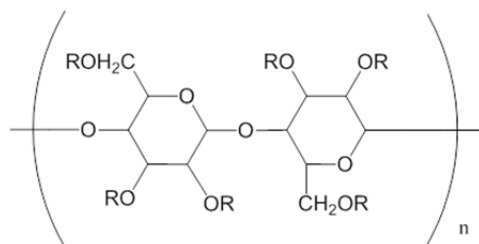
Polymer Summary

C.1. Description of Polymers Evaluated

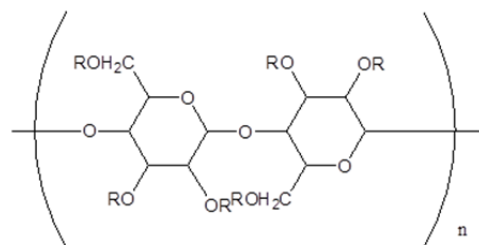
A wide array of pharmaceutically acceptable polymers were evaluated during this research. Pharmaceutical acceptability was based on inclusion in the Handbook of Pharmaceutical Excipients (1). The following polymers were used as polymeric excipients: Pharmacoat 603 (hydroxypropyl methylcellulose, HPMC, Shin-Etsu, JAPAN), Kollidon VA64 (polyvinyl pyrrolidone-vinyl acetate copolymer, PVP-VA, BASF), Poly(acrylic acid) (PAA, Aldrich), Carbopol 974P (Lubrizol), Plasdene K12 (polyvinyl pyrrolidone, Ashland), hydroxypropyl methylcellulose acetate succinate (HPMCAS, HF grade, Shin-Etsu), carboxymethylcellulose sodium salt (CMC Na, Sigma), hydroxypropyl cellulose (HPC, SL grade), methylcellulose (MC, 400 cPs, Sigma-Aldrich), Kollidon 25 (polyvinyl pyrrolidone, Sigma), Carbopol 934P (Lubrizol), Soluplus (BASF), HPMCP 50 (hydroxypropyl methylcellulose phthalate, Acros), and Klucel EXF (hydroxypropyl cellulose, HPC, Ashland). Table C.1 summarizes polymer nomenclature, structure, functionality, solubility, and grades used for this work.

Table C.1. Summary of polymer structure and property information.

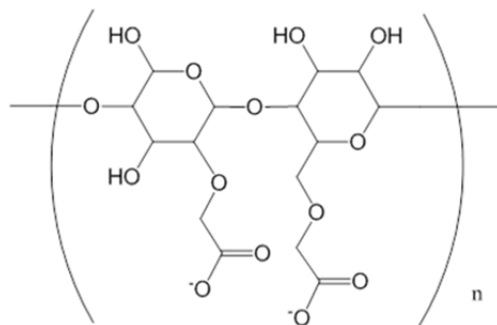
Methylcellulose (MC, Methocel, Metolose)	
	<p>Functionality: Alcohol</p> <p>Solubility: water soluble</p> <p>Grades Used: MC 400 cP</p>

Hydroxypropyl cellulose (HPC, Klucel)**Functionality:** Alcohol**Solubility:** water soluble**Grades Used:** Klucel EXF; HPC-SL (lower viscosity)**Hydroxypropyl methylcellulose (HPMC, Hypromellose)****Functionality:** Alcohol**Solubility:** water soluble**Grades Used:** Pharmacoat 603**Hydroxypropyl methylcellulose phthalate (HPMCP)****Functionality:** Carboxylic acid, carbonyl, alcohol**Solubility:** soluble at high pH**Grades Used:** HPMCP 50

R = H
CH₃
CH₂CH(CH₃)OH
COC₆H₄COOH

Hydroxypropyl methylcellulose acetate succinate (HPMCAS)**Functionality:** Carboxylic acid, carbonyl, alcohol**Solubility:** soluble at high pH**Grades Used:** HF (Copolymer ratio acetyl/succinoyl = 2/1)

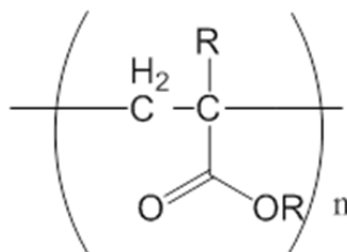
R = H
CH₃
CH₂CH(CH₃)OH
COCH₃
COCH₂CH₂COOH

Carboxymethylcellulose, sodium salt (CMC Na)

Functionality: Carboxylic acid, alcohol

Solubility: water soluble

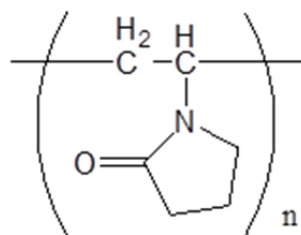
Grades Used: CMC Na

Poly(acrylic acid) (PAA, Carbomer, Carbopol)

Functionality: Carboxylic acid

Solubility: water soluble, but pH dependent viscosity

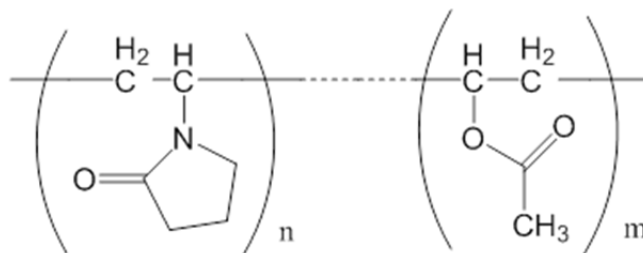
Grades Used: PAA, Carbopol 934 PNF, Carbopol 974PNF

Polyvinyl pyrrolidone (PVP, Povidone, Kollidon, Plasdone)

Functionality: Amide

Solubility: water soluble

Grades Used: Plasdone K12, Kollidon 25

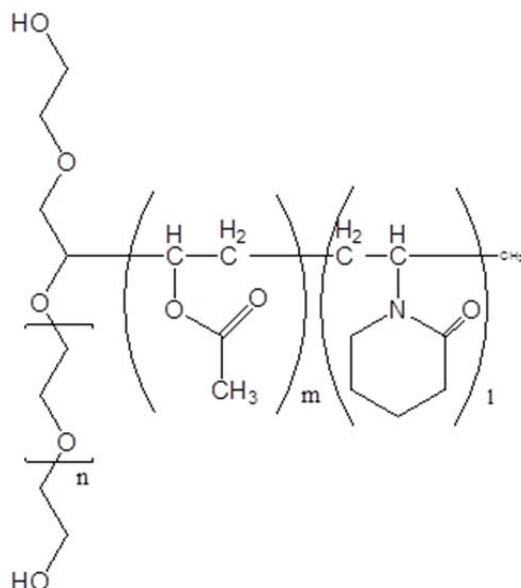
Polyvinyl pyrrolidone-vinyl acetate copolymer (PVP-VA, Copovidone)

Functionality: Amide, ester

Solubility: water soluble

Grades Used: Kollidon VA64

Polyvinyl caprolactam-polyvinyl acetate-polyethylene glycol graft copolymer (Soluplus)



Functionality: Ester, amide, alcohol

Solubility: water soluble

Grades Used: Soluplus

C.2. Particle Size Distribution of Polymers Evaluated

C.2.1. Methods

C.2.1.1. Microtrac Assessment of Particle Size

Particle size of each polymer was measured using a SRA150 Microtrac. Isopar G was used as the media and the flow rate was set at 60%. Polymers were suspended in Isopar G with 0.25% lecithin prior to addition to cell for particle size measurement. The set zero was 30 seconds, followed by a run time of 10 seconds. 3 runs were acquired and averaged prior to data reporting, and data was acquired for samples that were not sonicated and were then sonicated for 30 seconds. For polymers that exhibited large particle size distributions (PSD), polymers were also ground with mortar and pestle then re-analyzed.

C.2.2. Results of Polymer Particle Size Assessment

The mean particle size of each polymer is reported in Table C.2. The majority of polymers had an average particle size of ~100 microns; however, Soluplus and HPMCP had substantially larger particles, with a mean particle size of ~300 microns. Grinding of the polymers had a moderate impact on reducing particle size.

Table C.2. Average particle size of each polymer evaluated.

Polymer	Mean Particle Size (microns)	
	0 sec sonication	30 sec sonication
Pharmacoat 603	69.36	68.60
CMC Na Salt	105.1	113.6
Kollidon VA64	98.07	85.71
Soluplus	302.6	304.2
Soluplus - Ground	250.7	250.6
Poly(acrylic acid)	80.16	44.03
Carbopol 974P	93.32	39.66
Plasdone K12	56.77	54.06
HPMCAS-HF	7.767	7.715
HPMCP 50	305.5	312.8
HPMCP 50 - Ground	235.6	241.2
HPC-SL	111.1	115.0
MC 400 centipoise	77.97	83.70
Kollidon 25	75.18	76.12
Carbopol 934 PNF	129.1	100.0
HPC	87.58	92.72

C.3. Viscosity Assessment of Polymers in Dissolution Media

C.3.1. Methods

C.3.1.1. Media Preparation

Media prepared for viscosity measurements included simulated gastric fluid (SGF) and 50 mM acetate buffer at pH 5.0. The recipe for SGF was 2 g/L sodium chloride and 1.4 mL/L of 12N hydrochloric acid in deionized water for a final pH of 1.8. Polymer were pre-dissolved in media, with target concentrations of 1 mg/mL and 2 mg/mL in SGF and pH 5 buffer, respectively. These concentrations were selected based on polymer loading in supersaturation experiments with ibuprofen.

C.3.1.2. Viscosity Measurements

The viscosity of dissolution media with and without polymer was measured on 1 mL samples at 37 °C using a viscometer (Viscolab 3000, Cambridge Viscosity, Medford, MA, USA). A 0.310" piston was selected based on its suitability for low viscosity (0.25-5 cP) measurements.

C.3.2. Results of Viscosity Measurements for Pre-Dissolved Polymer in Dissolution Media

The effects of pre-dissolved polymers on media viscosity in SGF and pH 5 buffer are summarized in Tables C.3 and C.4, respectively. In SGF, Carbopol 974P, MC, and Carbopol 934 PNF significantly increased media viscosity relative to the media only control. Likewise, these polymers also exhibited increased media viscosity in pH 5 buffer. Poly(acrylic acid), HPMCAS-HF, and CMC Na also increased media viscosity in pH 5 buffer.

Table C.3. Influence of polymer on media viscosity at 1 mg/mL in SGF at 37 °C.

Polymer	Viscosity (cP)		Temperature (°C)	
	Mean	Std Dev	Mean	Std Dev
Media Only	0.64	0.01	37.25	0.20
Pharmacoat 603	0.66	0.01	37.02	0.05
PVP-VA64	0.67	0.01	37.02	0.05
Poly(acrylic acid)	not determined; suspension settled			
Carbopol 974P	0.89	0.11	37.07	0.06
Plasdone K12	0.63	0.01	37.04	0.01
HPMCAS-HF	0.64	0.01	37.05	0.07
CMC Na Salt	0.70	0.01	37.08	0.12
HPC-SL	0.67	0.02	37.16	0.17
MC 400 cP	0.89	0.02	37.00	0.06
Kollidon 25	0.66	0.01	37.02	0.02
Carbopol 934 PNF	0.84	0.08	36.99	0.03
Soluplus	0.67	0.00	37.01	0.03
HPMCP 50	0.64	0.00	36.99	0.04
HPC	0.71	0.02	37.04	0.02

Table C.4. Influence of polymer on media viscosity at 1 mg/mL in pH 5 buffer at 37 °C.

Polymer	Viscosity (cP)		Temperature (°C)	
	Mean	Std Dev	Mean	Std Dev
Media Only	0.71	0.03	37.04	0.07
Pharmacoat 603	0.82	0.05	37.05	0.04
PVP-VA64	0.71	0.01	37.01	0.03
Poly(acrylic acid)	4.69	0.67	37.12	0.21
Carbopol 974P	1.84	0.13	37.00	0.03
Plasdone K12	0.65	0.00	36.98	0.05
HPMCAS-HF	0.71	0.05	37.00	0.04
CMC Na Salt	0.93	0.02	36.99	0.03
HPC-SL	0.69	0.02	36.99	0.02
MC 400 cP	1.25	0.17	37.00	0.05
Kollidon 25	0.66	0.01	37.04	0.06
Carbopol 934 PNF	1.50	0.33	37.02	0.07
Soluplus	0.68	0.02	37.03	0.06
HPMCP 50	0.71	0.01	37.16	0.16
HPC	0.78	0.01	37.01	0.06

C.4. Solubility of Evaluated Polymers in Dissolution Media

C.4.1. Methods

C.4.1.1. Visual Assessment of Polymer Solubility

The threshold solubility of each of the polymers used in dissolution and supersaturation experiments was evaluated in Simulated Gastric Fluid (SGF), pH 1.8 at 37 °C. Since all dissolution experiments with ibuprofen in SGF were conducted with polymer concentrations of 1 mg/mL, the threshold concentration for solubility assessment was also 1 mg/mL. Solid polymer was mixed into SGF via shaking at 500 rpm.

Observations about polymer solubility were made following 2 hours of equilibration.

Measurements of pH were also made using an Accumet pH meter.

C.4.2. Results of Polymer Threshold Solubility Assessment in Dissolution Media

The majority of polymers evaluated in the threshold solubility study were solutions at the target concentration of ~1 mg/mL, as summarized in Table C.5. However, several polymers exhibited lower solubility within the span of this 2 hour experiment.

The polymers that were not in solution at the target concentration included Poly(acrylic acid), Carbopol 974P, Carbopol 934 PNF, HPMCAS-HF, and HPMCP. Due to the acidic functionality incorporated into each of these polymers, this observation of poor solubility in gastric pH was anticipated since the polymer remains unionized in the media. Aside from solubility observations, it was also noted that solubilization of each of these polymers did not significantly shift the pH of the media.

Table C.5. Threshold solubility of polymers in SGF following 2 hours of equilibration at 37 °C.

Polymer	Solubility (mg/mL)	pH
Pharmacoat 603	> 0.9	1.9
CMC Na Salt	> 0.9	2.0
Kollidon VA64	> 1.1	1.9
Soluplus - Ground	~ 3.9	1.9
Poly(acrylic acid)	< 1.1	1.8
Carbopol 974P	< 0.8	1.9
Plasdone K12	> 0.8	1.9
HPMCAS-HF	< 0.8	1.8
HPMCP 50 - Ground	< 1.0	1.9
HPC-SL	> 0.9	1.8
MC 400 centipoise	> 0.9	1.9
Kollidon 25	> 1.0	1.9
Carbopol 934 PNF	< 0.8	1.8
HPC	> 0.9	1.9

C.5. References

1. A.H. Kibbe. Handbook of pharmaceutical excipients, Pharmaceutical Press, London, UK, 2000.

APPENDIX D

Influence of Polymers on pKa of Ibuprofen

D.1. Influence of Polymers on pKa of Ibuprofen

The pKa values of ibuprofen in the presence and absence of Pharmacoat 603 (hydroxypropyl methylcellulose, HPMC, Shin-Etsu, JAPAN), Kollidon VA64 (polyvinyl pyrrolidone-vinyl acetate copolymer, PVP-VA, BASF), methylcellulose (MC, 400 cPs, Sigma-Aldrich), Klucel EXF (hydroxypropyl cellulose, HPC, Ashland), hydroxypropyl cellulose (HPC, SL grade), Soluplus (BASF), Plasdone K12 (polyvinyl pyrrolidone, Ashland), and Kollidon 25 (polyvinyl pyrrolidone, Sigma) were determined through spectrophotometric titration.

D.1.1. Methods for pKa Determination

The titrations were performed with the Sirius T3 instrument GLpKa (Sirius Analytical Instruments, East Sussex, UK) using a double junction electrode. The electrode was standardized from pH 1.8 to 12.2 and the KOH titrant was standardized against potassium hydrogen phthalate. Each sample was dissolved in ionic strength adjusted (ISA) water (0.15 M potassium chloride in water) to create a stock solution of 20.0 mg/ml. An aliquot of each stock solution was added to a titration vial and diluted up to 1.5 ml with ISA water. The starting pH of each solution was adjusted with 0.5 M potassium hydroxide. Each solution was titrated with 0.5 M hydrochloric acid from about pH 9 to 1.8 at 25 °C in ISA water. For spectrophotometric analysis, spectra were recorded from 200-700 nm. The pKa values were calculated using T3 Simulator v.1.1 software. It was noted that solubilization of ibuprofen was maintained for the duration of the titrations, so addition of cosolvent was not required.

D.1.2. Results for Ibuprofen pKa Determination in Presence of Polymers

None of the polymers evaluated dramatically shifted the pKa of ibuprofen as summarized in Table D.1.

Table D.1. pKa of ibuprofen in the presence of polymers using spectrophotometric titration (n=3).

Polymer	pKa of Ibuprofen (\pm std dev)				
	10:1 Ibuprofen: Polymer	1:1 Ibuprofen: Polymer	1:10 Ibuprofen: Polymer	1:50 Ibuprofen: Polymer	1:100 Ibuprofen: Polymer
-	4.26 \pm 0.005				
HPMC	*	4.26 \pm 0.004	4.24 \pm 0.005	4.19 \pm 0.002	4.15 \pm 0.004
PVP- VA64	*	4.26 \pm 0.004	4.27 \pm 0.008	4.28 \pm 0.001	4.30 \pm 0.006
MC	*	4.25 \pm 0.002	4.24 \pm 0.001		**
HPC	*	4.25 \pm 0.011	4.25 \pm 0.001		4.25 \pm 0.012
HPC-SL	*	4.26 \pm 0.007	4.25 \pm 0.000		4.24 \pm 0.010
Soluplus	4.22 \pm 0.006	4.00 \pm 0.007	4.38 \pm 0.002		**
Plasdone K12	*	4.26 \pm 0.003	4.26 \pm 0.005	4.28 \pm 0.002	4.30 \pm 0.002
Kollidon 25	*	4.26 \pm 0.002	4.26 \pm 0.014		4.29 \pm 0.007 (n=2)

* No shift in pKa at 1:1 Ibuprofen:Polymer, so 10:1 ratio not evaluated

** Polymer did not have sufficient solubility in water to evaluate at 1:100
Ibuprofen:Polymer